A NOVEL ROLE OF INTRACELLULAR TRIACYLGLYCEROL IN LIFESPAN REGULATION IN *SACCHAROMYCES CEREVISIAE*

By

Witawas Handee

A DISSERTATION

Submitted to
Michigan State University
in partial fulfillment of the requirements
for the degree of

Cell and Molecular Biology — Doctor of Philosophy

2016

ABSTRACT

A NOVEL ROLE OF INTRACELLULAR TRIACYLGLYCEROL IN LIFESPAN REGULATION IN *SACCHAROMYCES CEREVISIAE*

By

Witawas Handee

Triacylglycerol (TAG) is one of the fundamental molecules of life that exists in all living organisms. TAG is a non-polar lipid which has a role in controlling cellular energy stockpiles, lipid homeostasis, and cellular signaling. Conventional thought holds that cells accumulate TAG only when they consume excess energy, but a growing body of research reveals that TAG accumulation also takes place when cells are exposed to stresses. This suggests a potential life-preserving role for TAG. Our studies have discovered that high accumulation of intracellular TAG in budding yeast, *S. cerevisiae*, correlates with extended chronological lifespan. In general, wild yeast exhibit larger volumes of TAG and significantly longer lifespans than laboratory yeast. Additionally, increasing intracellular TAG levels in laboratory strains by either abolishing TAG lipases or enhancing TAG biosynthesis results in lifespan extension, whereas blocking TAG production leads to premature aging.

The TAG-associated lifespan mechanism is unlikely dependent on several well-characterized longevity pathways such as the Target-of-Rapamysin (TOR) and the RAS/PKA pathways. While TAG accumulation does not protect cells from stresses such as UV light, osmolarity, and acidity, our data suggest that high-TAG yeast may benefit from

decreased reactive oxygen species (ROS) or increased resistance to oxidative damages. In order to quantitatively measure ROS level in yeast cells, we have developed a normalization technique that is applicable to aging studies via using the fluorescent probe, 2',7' -dichlorofluorescein diacetate. The results demonstrate that yeast with high TAG abundance display lower intracellular ROS than that of wild-type yeast. On the other hand, yeast with low TAG exhibit significantly increased ROS and oxidative damages. These results support the mitochondrial free radical theory of aging which suggests that longevity can be extended by reducing cell injury from ROS. Subsequently, we offer the radical sink hypothesis proposing a TAG-mediated longevity mechanism by which TAG can intercept ROS before they impair other vital macromolecules and then safely transfer to lipid droplets.

Because TAG metabolism and most lifespan regulations are highly conserved from yeast to human, it is possible that this lifespan regulation can universally apply to other organisms. It is important to note that these results are consistent with an observation in modern societies called obesity paradox, a phenomenon by which overweight individuals benefit from lower overall mortality rate than normal or underweight people. Our findings thus demonstrate an overlooked function of TAG that could potentially readjust future healthcare guidelines in order to increase greater a healthy life of the advanced age.

ACKNOWLEDGEMENTS

This dissertation could not have been completed without substantial support from many individuals, to whom I take this opportunity to express my sincere gratitude. First, I would like to show my greatest appreciation to my advisor, Professor Min-Hao Kuo. He provided constant motivation, guidelines, and insight to help me solve the countless problems encountered during the study. I cannot say thank you enough for his assistance. I am also very grateful for the enormous support of my research committee members: Dr. Barbara Atshaves, Dr. Daniel Jones, Dr. Karl Olson, and Dr. Kyle Miller. Their suggestions were extremely helpful and supportive. I thank Xiaobo Li, who originated this project 7 years ago; without his brilliant science inspection and extensive work, this dissertation could not have materialized. I also gratefully thank Kevin Hall for his contributions in allowing replicative lifespan analyses become achievable.

I would like to express my appreciation to the advisors who gave me use of the instruments that made this research possible: Dr. Christoph Benning for the gas spectrometers, and Dr. Barry Williams for the micro-manipulator. Many thanks for technical assistance go to Rebecca Roston, Neil Bowlby, Astrid Vieler, Barbara Sears, Bencheng Liu, Jaruswan Warakanont, and Zhiying You. Thank you to all undergraduates who participated in this project: Pan Li, Hao Nguyen, Eve Gardner, Jan Stoltin, and Jaikishan Prasad. A special thank you goes to current Kuo's lab members who greatly

support me inside and outside the workplace: Christopher Buehl, Mengyu Liu, and especially Xiexiong Deng for helping construct yeast strains in the tough time.

In general, I want to further thank my marvelous program, Cell and Molecular Biology, extensively to Dr. Susan Conrad and Becky Mansel; moreover, Biochemistry and Molecular biology department where I mostly conduct research; other labs, departments, and personnel at Michigan State University that I cannot all mention; and lastly, my kind sponsorship, Development and Promotion of Science and Technology, Royal Thai Government that support the stipend during the study. Finally, I want to thank my life companion, Jeff MacGuinness, family, and friends, who always provide encouragement, consolation, love, and big feasts.

TABLE OF CONTENTS

LIST OF TABLES

LIST OF FIGURES

CHAPTER I:

Literature reviews

Aging studies in yeast

Over several decades, improvements in agriculture, food distribution, public sanitation, healthcare, health technologies and other factors have dramatically increased the average lifespan of much of the world's population. Demographically, the elderly constitute a much larger group than ever before, both in number and as a proportion of the population as a whole. This longevity comes at a price, however. Aging is the single most important contributing factor for many medical conditions, including cardiovascular diseases and cancer; these conditions create tremendous social and economic burdens worldwide (Nations 2012). It is no surprise, then, that research into aging has become a fast-developing area in biomedical research in recent decades. An understanding of the mechanisms of aging at the cellular and molecular levels may bring about remedies that improve the quality of life for the elderly.

On a cellular level, aging is a complex process which is predominantly influenced by genetic and environment factors, and is manifested by the chronological decay of cellular functions (Smith et al. 2015). Even though the outcomes of aging are distinctly visible, the underlying mechanistic causes are much more difficult to identify. Surprisingly, aging research in one of the simplest eukaryotic systems, the budding yeast *Saccharomyces cerevisiae*, has achieved spectacular successes in the identification of the conserved molecular mechanisms of aging. Yeast and mammals share highly conserved molecular and biochemical pathways; this fact both justifies and recommends the use of *S. cerevisiae* as a model organism in aging studies for several reasons. Budding yeast

have short doubling time, a small and fully-sequenced genome, and the capability to reproduce in both diploid and haploid cell types (Goffeau et al. 1996; Dickinson & Schweizer 2004). In addition, gene recombination and complementation techniques can be applied to yeast with high efficiency and precision, which greatly supports the use of reverse genetics studies in order to screen for genes related to lifespan regulation. For these reasons, yeast first became an aging model in 1959 (Mortimer & Johnson 1959), and subsequent research successfully revealed the first yeast longevity gene in 1994 (D'mello et al. 1994). At present, more than 238 genes have been identified as potential longevity factors (McCormick et al. 2015). Clearly, outcomes from aging studies in yeast can facilitate our understanding of human aging.

The lifespan of budding yeast consists of two distinct modes that are results of the cellular growth status: the logarithmic phase of rapid growth and replication, and the stationary phase where cells maintain a mitotically resting but metabolically active state (Werner-Washburne et al. 1996). These two growth phases give rise to two cognate paradigms of aging, replicative lifespan (RLS) and chronological lifespan (CLS). RLS refers to the number of times that a given yeast cell can divide (Mortimer & Johnson 1959). This model of aging derives from the fact that a yeast cell can only produce a finite number of progeny before it enters a post-replicative state when cell division is discontinued (Kaeberlein 2010). When a yeast cell divides, the daughter cells usually do not receive maternal senescence factors such as damaged proteins, toxic materials, and extrachromosomal ribosomal DNA circles (ERCs; Sinclair & Guarente 1997; Klinger et al.

2010; Aguilaniu et al. 2003; Eldakak et al. 2010). In the RLS paradigm, the accumulation of such subcellular damages impairs the ability of the mother cells to divide, resulting in replicative aging. When the cumulative damage accrued by the mother cells becomes too great, cell division ceases.

S. cerevisiae reproduces via asymmetrical budding. This facilitates RLS measurement, because it is quite practical for researchers to identify smaller daughter cells and remove them from their mother via a microscopic needle. RLS varies depending on the strain background, but typically falls around 20-30 daughter cells produced by a mother cell (Mortimer & Johnson 1959). It is not intuitive that the RLS lifespan paradigm compares with that of multicellular organisms; however, yeast RLS research has uncovered a number of conserved aging pathways shared by other eukaryotes. It is demonstrated that the RLS model has a high degree of similarity with the aging paradigms in human cell cultures (Hayflick & Moorhead 1961) and human stem cells (Rando 2006). In fact, this asymmetrical fission surprisingly occurs in almost every living organism, even though the morphology of cell division appears to be equal (Barker & Walmsley 1999; Nystrom 2007).

When cell division ceases, yeast cells undergo a shift into a mitotically resting but metabolically active phase. The chronological lifespan (CLS) paradigm provides a quantitative measurement of aging in post-mitotic cells. CLS is defined as a ratio of viable cells from a stationary phase population displayed as a function of time (Longo &

Fabrizio 2012). Measurements of CLS begin when yeast cultures enter a state of post-diauxic shift when cells have to rely on mitochondria-driven respiration for metabolism and survival (Fabrizio & Longo 2007). Over time, intracellular oxidative damages and extracellular acid wastes accumulate, leading to cell death (Burtner et al. 2009; Fabrizio & Longo 2008; Rockenfeller & Madeo 2008; Burhans & Weinberger 2009). Cellular aging is manifested by the progressively smaller percentage of viable cells in a population.

CLS is significantly influenced by growth conditions; the well-defined factors that contribute to variations in CLS include the strain background, nutrient sources, medium pH, and the growth temperature (Werner-Washburne et al. 1996; Longo & Fabrizio 2012; Mirisola & Longo 2012; Burtner et al. 2009; Burtner et al. 2011). Typically, in CLS research the synthetic complete (SC) medium with 2% glucose is used as the growth medium (Fabrizio & Longo 2007).

Technically, there are several ways to quantify yeast CLS. Traditional measurement of CLS tests cell viability at different time points by spreading a known number of cells taken out from stationary phase cultures onto a nutrient-rich YPD plate. The colony forming unit (CFU) change over time is the criterion for CLS (Fabrizio & Longo 2007). This method can be simplified by spotting a small volume of serially diluted cells on the YPD instead of plating cells. This 'spot assay' saves operation time and materials and also provides quantitative comparison of multiple strains at the same time (Matecic et al. 2010; Postnikoff & Harkness 2014). Recently, a high-throughput

"outgrowth" technique has been developed by the Kaeberlein group. The outgrowth method measures the time it takes for a fixed number of stationary cells to reach a selected cell density in fresh, YPD medium (Murakami & Kaeberlein 2009). This method is conducted in a 96-well plate in a "growth curve" machine that measures cell density changes in real time. The time for each culture to reach the set density is inversely proportional to the number of viable cells in the initial inoculum. Cell viability, i.e., the basis for measuring CLS aging, can thus be derived by simple calculation. It is uncommon to measure CLS to the point where the viability of a culture drops to zero. This is due to the occasional appearances of adaptive regrowth (or 'gasping effect') by which cell division is reactivated when cell survival falls below 1% (Zambrano & Kolter 1996; Fabrizio et al. 2004). Therefore, yeast CLS data are often presented in terms of time points at which cell viability reaches a certain level. Nevertheless, this model of aging retains a strong resemblance to cells in mammalian post-mitotic tissues.

Triacylglycerol functions more than storing surplus energy

Triacylglycerol (TAG) is a ubiquitous storage lipid found in all life kingdoms including budding yeast. TAG is composed of three fatty acids (FA) esterified to a glycerol molecule (Figure 1.1) (Daum et al. 2007). This structure packs the highest density of chemical energy among major biomolecules, making TAG a significant source of stored energy. Even though TAG is extremely hydrophobic because it consists nearly only of hydrocarbon chains, it lacks a polar head group to be part of the biological

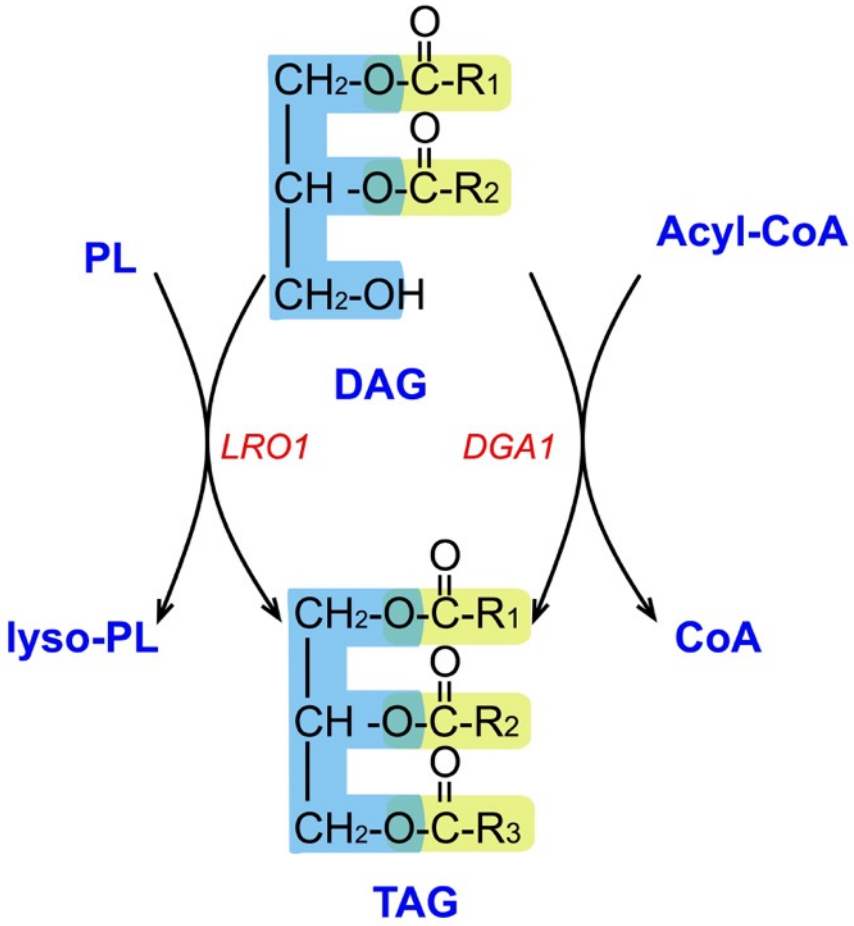

Figure 1.1 Structure of TAG. A TAG molecule contains a glycerol backbone with three esterified acyl chains. TAG is assemble from DAG (diacylglycerol) which receives an acyl group from acyl-CoA or PL (phospholipids)

membranes (Daum et al. 1998; Klug & Daum 2014). Instead, TAG is gathered and densely packed inside a unique monolayer organelle called lipid droplets (LD) or oil particles. Along with TAG, another common neutral lipid found in LD is steryl ester (STE) (Daum et al. 1998; Mullner & Daum 2004; Klug & Daum 2014).

TAG is best-known for its function as a surplus energy supply. Interestingly, TAG accumulation is not a response of surplus nutrients, but rather of different cellular stresses. For instance, research that restricted various nutrients such as nitrogen and phosphorus caused the model microalgae *Chlamydomonas reinhardtii* to increase levels of TAG (Li et al. 2012; Cakmak et al 2014). Additional molecular roles of TAG have been reported by numerous studies over the years, including the control of lipid homeostasis, prevention of fatty acid-induced cytotoxicity, and buffering against various cellular stresses (Murphy 2012). Despite the diverse functions of TAG, its metabolism is highly conserved in eukaryotes ranging from yeast to humans (Murphy 2012), which suggests an essential role of TAG that was acquired through millennia of evolution.

TAG biosynthesis

TAG biosynthesis in budding yeast begins with the formation of its precursors, phosphatidic acid (PA) and diacylglycerol (DAG) (Sorger & Daum 2003). The *de novo* synthesis of PA occurs through either the acylation of glycerol-3-phosphate (G3P) by G3P acyltransferase, or via a series of acylation and reduction reactions of dihydroxyacetone phosphate (DHAP) by DHAP acyltransferase and acyl-DHAP reductase (Figure 1.2) (Klug & Daum 2014). Both reactions produce lysophosphatidic acid (LPA) which is further acylated at the sn-2 position by 1-acyl-G-3-P acyltransferase, yielding a PA molecule (Daum et al. 2007). Aside from the *de novo* synthesis, PA alternatively can be derived from two bypass systems: the hydrolysis of glycerophospholipids by phospholipase D (McDermott et al. 2004), or via DAG phosphorylation by a DAG kinase (Han et al. 2008).

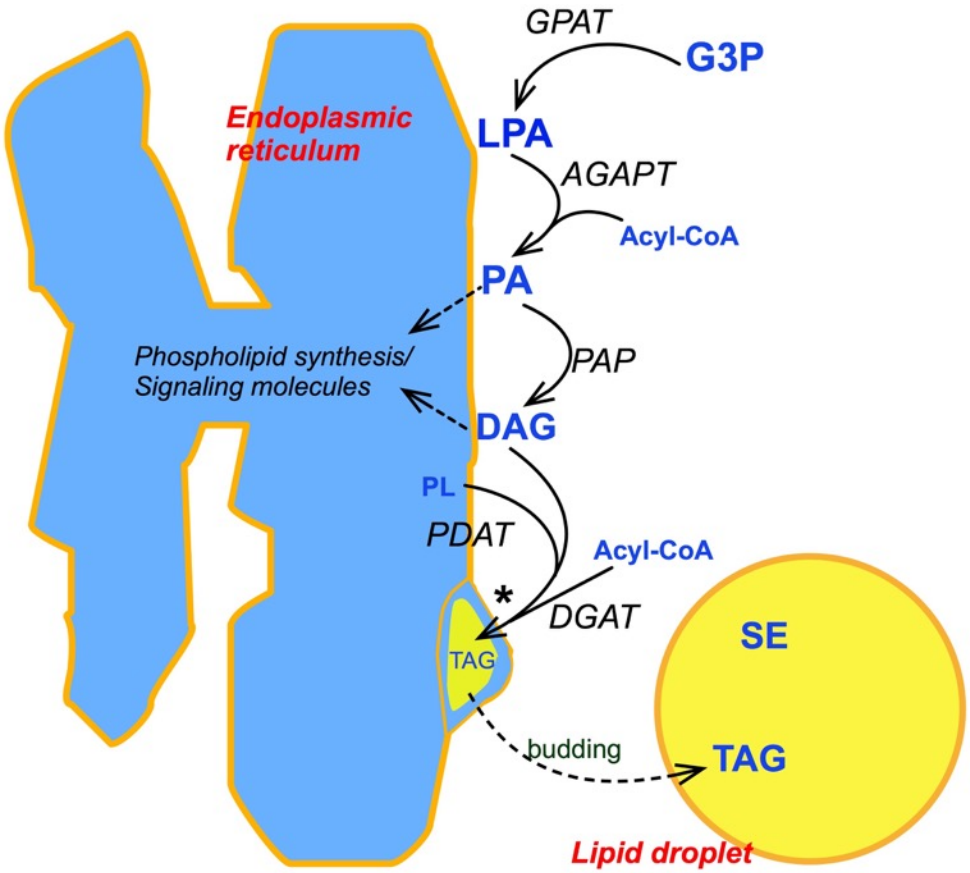

Figure 1.2 TAG biosynthesis pathway. The establishment of TAG involves multiple acylation enzymes located on the ER membrane. TAG and in some organisms, together with steryl esters (SE) are stored in lipid droplets. Abbreviations for metabolites: DAG, diacylglycerol; G3P, glycerol-3-phosphate; LPA, lysophosphatidic acid; PA, phosphatidic acid; PL, phospholipids; SE, steryl ester; TAG, triacylglycerol. Abbreviations for enzymes: AGPAT, 1-acylglycerol-3-phosphate acyltransferase; DGAT, acyl CoA:diacylglycerol acyltransferase; GPAT, glycerol-3-phosphate acyltransferase; PDAT, phospholipid:diacylglycerol acyltransferase; PAP, phosphatidic acid phosphatase.

PA serves as the important divergent metabolite in *de novo* pathways of various lipid biosyntheses such as phospholipids, sphingolipids, and TAG. For TAG formation, the phosphate ester of PA is first hydrolyzed to generate DAG by phosphatidate phosphatases (PAP; Pah1 in *S. cerevisiae*). This is one of the crucial regulatory steps. Disruptions of Pah1 cause direct effects and reduce DAG and TAG levels (Oshiro et al. 2003). The *PAH1*-null strain (*pah1*Δ) does not show logarithmic growth defects under normal conditions, but is unable to use non-fermentable carbon sources such as glycerol and is sensitive to high temperature (Han et al. 2008), suggesting that the PAP pathway has a function beyond TAG biosynthesis. Indeed, the *pah1*Δ mutant exhibits higher levels of radical species and relatively shortened chronological lifespan because the lipid flux cannot go to TAG so it diverts to make more phospholipids, causing membrane disruption (Park et al. 2015).

The last stage of TAG biosynthesis involves the transfer of an acyl group to the sn-3 position of DAG. In budding yeast, the two key enzymes for this reaction are Dga1p and Lro1p, homologous to the mammalian DGAT2 (diacylglycerol acyltransferase 2) and LCAT (lecithin cholesteryl acyltransferase) families, respectively (Mullner & Daum 2004). Even though both Dga1p and Lro1p have acyltransferase activity, they operate with different substrates and types of chemical reaction. Dga1p assembles TAG by using acyl-CoA as the substrate in an acyl-CoA dependent acylation reaction (Sorger & Daum 2002). Conversely, Lro1p performs acyl-CoA independent esterification by transferring an acyl group from glycerophospholipids, preferably phosphatidylcholine (PC) and

phosphatidylethanolamine (PE) (Oelkers et al. 2000) to DAG, resulting TAG and a lyso-phospholipid (Figure 1.1).

Dga1p and Lro1p have complementary functions in TAG formation, but the contribution of each individual enzyme is not well defined. A single deletion of either Dga1 or Lro1 decreases TAG abundance by only 20-30% (Sorger & Daum 2002; Dahlqvist et al. 2000). However, in *dga1*Δ *lro1*Δ double mutant cells, 95% of TAG accumulation is depleted (Sorger & Daum 2002). Different yeast strains growing in different environments demonstrate varying levels of TAG accumulation as well as variations in the relative contribution of these two acyltransferases (Sorger & Daum 2002; Sandager et al. 2002). Nevertheless, the cell's life phase appears to be the most influential factor in defining acyltransferase contribution to TAG biosynthesis (Oelkers et al. 2000). The *lro1*Δ mutant has significantly reduced TAG production in logarithmic phase but only minor reduction in stationary phase (Oelkers et al. 2000; Sandager et al. 2002). *DGA1*-null cells showed approximately 50% reduction of TAG accumulation during stationary phase, but less than 25% reduction during the logarithmic phase (Oelkers et al. 2000). Furthermore, transcriptional expression of *DGA1* was up-regulated in diauxic shift and stationary phase relative to that of *LRO1* (Gasch et al. 2000). These studies indicate that Dga1p plays the principal role of TAG production in stationary phase while Lro1p is more active at the logarithmic phase.

While *DGA1* and *LRO1* are responsible the major TAG synthesis, it is suspected that TAG could be derived from a third, yet to be defined pathway, which explains how 5% of TAG remained in *dga1*Δ *lro1*Δ mutants (Sorger & Daum 2003). There are two proposed unconventional routes of TAG biosynthesis. Several reports demonstrate that *ARE1* and *ARE2*, the *S. cerevisiae* STE synthesis genes (related to ACAT, cholesterol acyltransferase), could participate in TAG production when *DGA1* and *LRO1* are not functional (Oelkers et al. 2000; Sandager et al. 2002). However, the contribution of Are1/2 enzymes in TAG production remains unclear (Sorger & Daum 2003). Another proposed pathway may involve a direct acylation of free fatty acids (FFA) into DAG via a phospholipase A2-dependent deacylation-reacylation reaction (Sorger & Daum 2002; Wagner & Paltauf 1994). However, such a gene in yeast, if exists, remains elusive.

It should be noted that TAG accumulation appears to be non-essential for yeast vegetative growth (Sandager et al. 2002). The quadruple deletion of *DGA1*, *LRO1*, *ARE1*, and *ARE2* resulted in normal-growing yeast with complete ablation of neutral lipids and lipid droplets. However, the mutant is highly sensitive to exogenous unsaturated FA which causes an imbalance in membrane proliferation and leads to premature loss of cell viability (Petschnigg et al. 2009). This phenomenon is widely known as lipotoxicity, a condition by which FFA induces cell stress, unfolded protein response (UPR), intracellular reactive oxygen species (ROS), and cell apoptosis (Eisenberg & Büttner 2013; Garbarino et al. 2009).

TAG hydrolysis

TAG breaks down into fatty acids and DAG; the latter can be further hydrolyzed into monoacylglycerol and glycerol, and more fatty acids. Fatty acids mobilized from TAG are materials for ß-oxidation, whereas DAG, if not further hydrolyzed, can be a precursor for phospholipid biosynthesis, and other signaling molecules (Figure 1.3) (Sorger & Daum 2003).

TAG hydrolysis is catalyzed by lipases (Zimmermann et al. 2004). Three well-known TAG lipases in *S. cerevisiae* are Tgl3p, Tgl4p, and Tgl5p (Kurat et al. 2006; Athenstaedt & Daum 2003; Athenstaedt & Daum 2005). These lipases contain the consensus sequence GXSXG for serine esterase and α/ß hydrolase fold, which is commonly found in proteins with lipolytic activity (Athenstaedt & Daum 2003). Tgl3p is considered the main TAG lipase with low FA specificity hydrolyzing all kinds of incorporated FA in TAG molecules. Tgl4p also has a wide range of substrates but works better with TAG that contains myristic (C14:0) and palmitic acid (C18:0), while Tgl5p prefers working with hexacosanoic acid (C26:0) (Athenstaedt & Daum 2005). That different TAG lipases prefer slightly altered TAG substrates suggests that FFA is produced in a controlled manner by the specificity of TAG breakdown enzymes (Kurat et al. 2006).

It should be noted that many lipases display more than a lipid hydrolytic function. Tgl4p exhibits an additional role in cell cycle control during the G1-to-S phase via Cdk1-

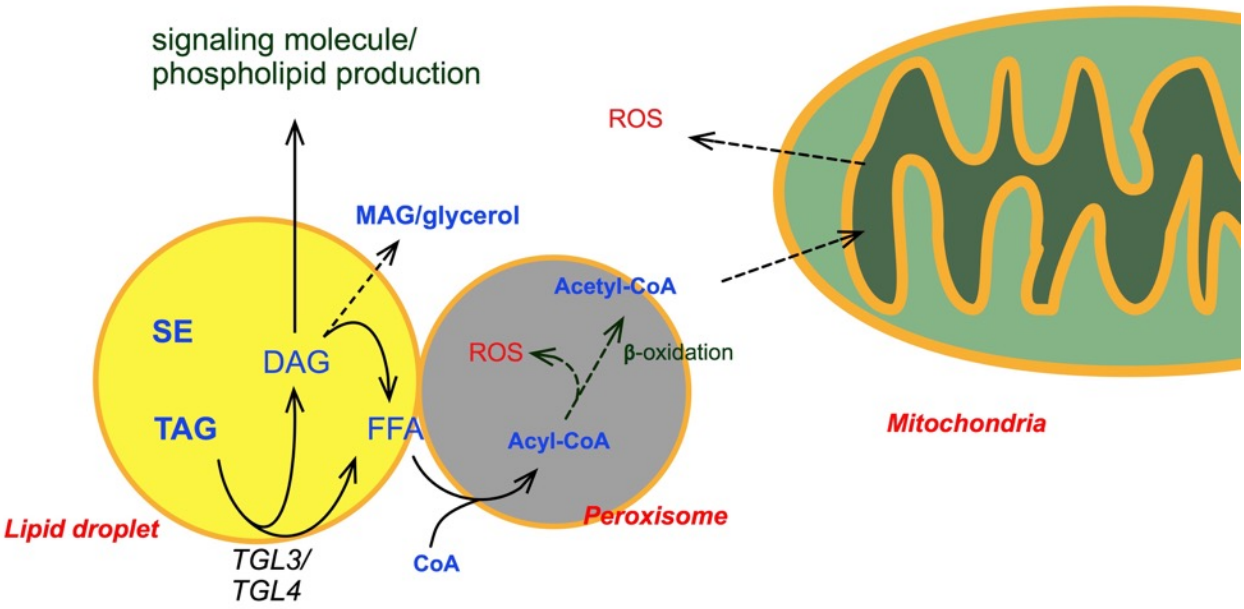

Figure 1.3 TAG hydrolysis pathway. TAG is remobilized via lipases (Tgl3 and Tgl4 in budding yeast) leading to DAG (diacylglycerol) and FFA (free fatty acid). DAG can get further hydrolyzed to yield MAG (monoacylglycerol) or incorporate into phospholipid productions. Cells can breakdown FFA through the ß-oxidation in peroxisome to produce acetyl-CoA for cellular respiration. These processes are known to produce ROS (reactive oxygen species) as the byproduct.

dependent phosphorylation pathway (Zimmermann et al. 2004). Failure to phosphorylate Tgl4p results in delayed bud development and cell-cycle progression (Kurat et al. 2009). Tgl3p and Tgl5p also contain the H-(X)4-D acyltransferase motif which is involved in acylation of lysophosphatidylethanolamine and lysophosphatidic acid, respectively (Rajakumari & Daum 2010a). The acylation function of Tgl3p and Tgl5p appears to be activated when cells are in the lag phase or when commit ted to sporulation (Rajakumari & Daum 2010a), which suggests that the phospholipid acyltransferase activities of Tgl3p and Tgl5p work independently from the TAG lipase

activity. Single, double, and triple deletion of *TGL3*, *TGL4*, or *TGL5* did not display major growth or sporulation defects (Athenstaedt & Daum 2005; Kurat et al. 2009; Rajakumari & Daum 2010a; Rajakumari & Daum 2010b). This indicates that TAG lipases as well as TAG accumulation were non-essential under normal, laboratory conditions. Intriguingly, significant TAG accumulation is seen in *tgl3*Δ and *tgl4*Δ strains; the *tgl5*Δ cells appear to maintain a normal level of TAG (Rajakumari & Daum 2010a; Rajakumari & Daum 2010b). Recently, additional TAG lipases *AYR1* and *LPX1* have been shown to have the TAG hydrolytic activity but with significantly less robustness (Ploier et al. 2013). Taken together, the existence of various TAG lipases with slightly different functions and substrate specificities suggests that there is a regulatory approach by which cells can control activities of TAG hydrolysis in response to different cell conditions. However, such regulation remains poorly understood and requires further elucidation.

Interaction of organelles in TAG metabolism

TAG metabolism involves the interplay of diverse enzymes localized in different organelles such as the endoplasmic reticulum (ER), lipid droplet (LD), mitochondria, peroxisome, vacuole, cytoplasm, and plasma membrane (Figure 1.4) (Rajakumari et al. 2008; Grillitsch et al. 2011; Huh et al. 2003). During TAG construction, the intermediates (i.e., G3P, PA, and DAG) progressively increase in hydrophobicity which determines the sub-cellular compartments where they are found, ranging from cytosol (high hydrophilicity) to the hydrophobic core of LD (Sorger & Daum 2003). Intracellular movements are dictated by the locations of the responsible enzymes which are

predominantly on the ER membrane (Rajakumari et al. 2008). For example, PA is dephosphorylated at the ER surface, releasing DAG to the cytosol. DAG acylation yields TAG, a reaction taking place in between the two layers of phospholipids of the ER membrane in order to avoid contact with solution. Localized accumulation of TAG in the inter-leaflet space of the ER membrane eventually causes the bulging and budding of lipid droplets from ER (Tobias & Walther 2012). On the other hand, the underlying mechanism driving LD segregation from ER is still obscure. Furthermore, proteomics studies of LD uncovered unexpected proteins for LD formation and targeting, as well as TAG and STE biosynthesis (Binns et al. 2006; Natter et al. 2005; Huh et al. 2003; Athenstaedt et al. 1999; Sorger & Daum 2002). These unexpected LD-associated proteins appear to support the notion that LD can grow in size and number, in a way that is similar to other organelles. However, the true functions of most LD proteins remain to be delineated (Tobias & Walther 2012; Thiam et al. 2013).

Many proteins involved in the metabolism of neutral lipids (i.e., TAG and SE) share common organellar locations such as ER and LD (Grillitsch et al. 2011). In budding yeast, TAG anabolic enzymes such as Pah1p, Dga1p, and Lro1p are located in the cytoplasm or ER (Dahlqvist et al. 2000; Oelkers et al. 2000; Kohlwein et al. 2013; Sorger & Daum 2002). Changing locations of these proteins sometimes serves as a mechanistic control for the protein activity. For instance, Pah1p can change its sub-cellular localization from cytosol to ER membrane depending on its phosphorylation states. The phosphorylated Pah1p is inactive and remains in cytosol, while the

unphosphorylated proteins translocate to ER membrane and become active (Choi et al. 2011; Adeyo et al. 2011; Han et al. 2006). The Pah1p phosphorylation thus functions as a regulatory step during TAG biosynthesis (Carman & Henry 2007).

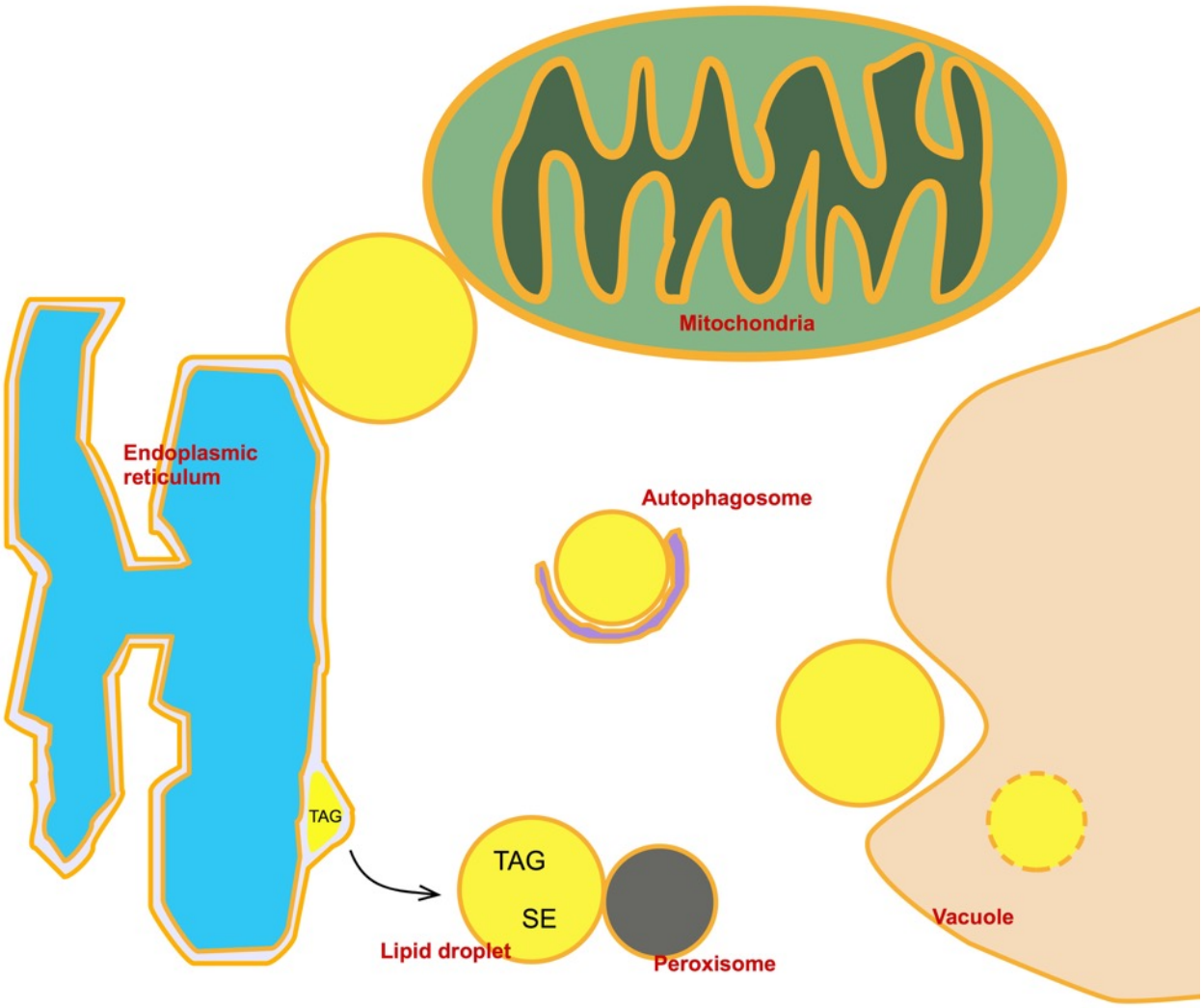

Figure 1.4 TAG and LD metabolisms associate with various organelles. LD can interact with many other organelles, such as endoplasmic reticulum (ER), mitochondria, peroxisomes and autophagosomes.

The subsequent DAG acylation reaction takes place in the ER membrane where both Dga1p and Lro1p are located. While Lro1p can be found only on the ER membrane, Dga1p can co-localize on both ER and LD surfaces (Natter et al. 2005; Grillitsch et al. 2011). It is proposed that Dga1p located on the LD membrane may provide an opportunity for LD to grow in the bigger size after it is budded from the ER. Nevertheless, conventional theory suggests that the majority of TAG is synthesized by Dga1p and Lro1p, and accumulated between two phospholipid layers of ER membrane and subsequently developed into a LD in the cytoplasm (Thiam et al. 2013; Wilfling et al. 2013; Robenek et al. 2005). One apparent issue regarding this observation is how such membrane-bound proteins maintain their functions at the different locations, specifically, when LD has only a single layer of phospholipids unlike the others (Zinser et al. 1991; Sorger & Daum 2002). The predicted protein topology indicates that Dga1p has a hairpin structure by which two transmembrane domains are inserted into the membrane leaving N- and C-terminal portions in the cytoplasm (Ingelmo-Torres et al. 2009; Stone et al. 2006; Abell et al. 2004). Interestingly, Dga1p from isolated microsomes and LD retains normal enzymatic activity, suggesting that the protein structures and functions are maintained after the migration from ER (which is present in the microsome fraction) to LD (Oelkers et al. 2000; Sorger & Daum 2002). Recent evidence indicates that after budding, LD continues to have close proximity to the parental ER (Wolinski et al. 2011; Knoblach & Rachubinski 2015). Furthermore, proteins on LD shuttle back to the ER and vice versa (Jacquier et al. 2011). This finding suggests that LD and ER can exchange some of their membrane components even though they are

physically separated. Nevertheless, many related questions such as how LD and ER interact or how ER proteins are targeted to LD are still poorly understood.

Not all of the TAG-mobilized enzymes have the same shape and activity when they translocate. For example, Tgl3p is predominantly located on the LD surface, but also can be found on the ER, usually when cells are unable to form a LD. The Tgl3p that is retained on the ER membrane presumably serves as a waiting dock before LD formation (Schmidt et al. 2013). However, it displays much shorter half-life and lacks lipase activity (Schmidt et al. 2013). This is because the C-terminus of Tgl3p which is critical for protein stability and function normally faces the hydrophobic core in LD, but on the ER, it is exposed to the cytosol (Koch et al. 2014). This finding indicates that during the process of LD budding, ER-associated Tgl3p must be modified in shape so that the C-terminal can move from cytosol into the hydrophobic core. It is unclear how a protein can drastically change the conformation from such a hydrophilic environment to the very opposite. Overall, it is undeniable that enzyme compartmentalization plays a critical role in regulation of TAG metabolism.

Even though LD stores predominantly TAG, proteins coating the LD surface are not solely devoted to TAG metabolism, but rather are highly diversified (Gao & Goodman, 2015). The proteomics of lipid droplets demonstrate a variety of protein trafficking that is conserved from bacteria to human (Yang et al. 2012; Ding at al. 2012; Low et al. 2010). In mammals, a number of SNARE proteins are discovered such as

perilipin protein that is involved in the action of the hormone-sensitive TAG lipase, and Rab18 that mediates the interaction between lipid droplets and endoplasmic reticulum (ER). In yeast, the lipin1 protein, a homologue of seipin in human has been characterized recently (Szymanski et al. 2007; Wolinski et al. 2011). The mutation of yeast seipin (Fld1p) demolishes the ability to control LD fusion and TAG hydrolysis leading to supersized LD (Fei et al. 2008). Even though the mechanism of Fld1p is not well characterized, the seipin-mutating yeast has become an excellent model for studying a human disorder, lipodystrophy syndrome, by which subcutaneous adipose tissues progressively lose the ability to synthesize and redistribute TAG (Wolinski et al. 2011).

LD also have close contact with mitochondria as observed in adipocytes (Novikoff et al. 1980; Blanchette-Mackie & Scow 1983), hepatocytes (Kalashnikova & Fadeeva 2006), and skeleton myocytes (Shaw et al. 2008). The synaptosome associated protein 23 (SNAP23), a member of SNARE protein family, was discovered as a mediator between LD and mitochondria in human muscle cells (Jägerström et al. 2009; Strauss et al. 2015). How these two compartments interact is unclear, but recent evidence suggests that a bidirectional transport channel may be formed, allowing free fatty acids, hydrolyzed from TAG in LD, to quickly transport to mitochondria for ß-oxidation (Rambold et al. 2015). Likewise, phosphatidylcholine synthesized in mitochondria can move to LD, serving as a phospholipid precursor for the LD growth (Horl et al. 2011; Bartz et al. 2007; Barbosa et al. 2015). In budding yeast, ß-oxidation occurs in the peroxisome instead of in the mitochondria (Binns at al. 2006), but shuttle mechanism for

lipid intermediates is also observed. A LD protein called Erg6, which is the sterol Δ^{24}-methyltransferase functioning in ergosterol biosynthesis, can mediate the interaction between LD and mitochondria (Pu at al. 2011; Gaber et al. 1989). In addition, Erg6 protein is physically associated with many lipid metabolism proteins in the three-way connection among LD, mitochondria, and peroxisome (Pu at al. 2011; Binns et al. 2006). The examples of these proteins are *Tgl3/4* (TAG hydrolysis), *Mcr1* (ergosterol synthesis), *Ayr1* (PA synthesis), and *Pex11* (FFA oxidation) (Pu at al. 2011). These findings indicate that LD is the central organelle in the regulation of global lipid homeostasis. The control of TAG which is the major component of LD is therefore crucial for healthy cells.

Research Interests and significance

Modern omics studies reveal that a cell's ability to mitigate or delay the effects of aging relies on effective control of energy flux. Many metabolites such as amino acids and carbon sources have been shown to be associated with lifespan control. Little is known, however, about how lipid homeostasis relates to lifespan regulation.

TAG is the ubiquitous neutral lipid found in all living organisms. Conventional thought has it that TAG is synthesized only when cellular energy is oversupplied. Many recent studies suggest a more complex paradigm, however. These studies reveal that TAG synthesis may in fact be activated under conditions of nutrient deprivation and other cellular stress. While the benefit of accumulated TAG in these conditions is

unclear, these findings strongly imply a role in the lifespan control of cells growing in the post-mitotic phase.

This thesis aims to elucidate the energy-independent role of TAG related to lifespan regulation of *S. cervisiae*. In chapter II, a novel function of TAG in the regulation of yeast chronological lifespan is demonstrated. The underlying mechanism of this function operates via a pathway that is independent of other well-known aging determinants such as dietary restriction (DR) and the rapamycin (TOR)/Ras2 pathway. Data suggest that the cytoprotective action of TAG is associated with decreased levels of reactive oxygen species. This leads to the introduction of the Radical-Sink hypothesis in Chapter III, which proposes that TAG molecules prevent oxidative damage to cells by depleting free radical species. Chapter IV discusses the applications of the Radical-Sink model of intracellular TAG to health care, and its potential to decrease age-related diseases, prolong lifespan, and increase functional ability in those of advanced age.

CHAPTER II:

An Energy-Independent Pro-longevity Function of Triacylglycerol in Yeast[1]

[1] This research was published in: Handee, W., Li, X., Hall, K. W., Deng, X., Li, P., Benning, C., Williams, B. L., Kuo, M. K. (2016). An Energy-Independent Pro-longevity Function of Triacylglycerol in Yeast. *PLoS Genetics*, *12*(2), e1005878. I contributed to the data shown in all of the figures, except Figure 2.3B is from Xiaobo Li.

Abstract

Intracellular triacylglycerol (TAG) is a ubiquitous energy storage lipid also involved in lipid homeostasis and signaling. Comparatively, little is known about TAG's role in other cellular functions. Here we show a pro-longevity function of TAG in the budding yeast *Saccharomyces cerevisiae*. In yeast strains derived from natural and laboratory environments a correlation between high levels of TAG and longer chronological lifespan was observed. Increased TAG abundance through the deletion of TAG lipases prolonged chronological lifespan of laboratory strains, while diminishing TAG biosynthesis shortened lifespan without apparently affecting vegetative growth. TAG-mediated lifespan extension was independent of several other known stress response factors involved in chronological aging. Because both lifespan regulation and TAG metabolism are conserved, this cellular pro-longevity function of TAG may extend to other organisms.

Author summary

Triacylglycerol (TAG) is a ubiquitous lipid species well-known for its roles in storing surplus energy, providing insulation, and maintaining cellular lipid homeostasis. Here we present evidence for a novel pro-longevity function of TAG in the budding yeast, a model organism for aging research. Yeast cells that are genetically engineered to store more TAG live significantly longer without suffering obvious growth defects, whereas those lean cells that are depleted of TAG die early. Yeast strains isolated from the wild in

general contain more fat and also display longer lifespan. One of the approaches taken here to force the increase of intracellular TAG is to delete lipases responsible for lipid hydrolysis. Energy extraction from TAG thus is unlikely an underlying cause of the observed lifespan extension. Our results are reminiscent of certain animal studies linking higher body fat to longer lifespan. Potential mechanisms for the connection of TAG and yeast lifespan regulation are discussed.

Introduction

Lipid is essential for all life forms on earth. Polar lipids, most notably phospholipids, are the primary components of biological membranes, whereas neutral lipids such as triacylglycerols (TAG; or triglycerides, TG), are long believed to store excessive energy and to provide thermal and physical insulation for animals. By esterifying three molecules of fatty acids to the glycerol backbone, TAG packs the highest density of chemical energy among major biomolecules, consistent with a role in storing surplus energy. In addition, TAG metabolism is linked to the overall lipid homeostasis in cells and the organism (Murphy 2012). This is commonly achieved via diacylglycerol, DAG, which is a shared precursor for TAG and phospholipids biosynthesis. Interestingly, in many organisms, TAG accumulation is not a response of surplus nutrients, but of different stresses. For example, starvation for nitrogen, phosphorus, or sulfur causes a model photosynthetic microalga *Chlamydomonas reinhardtii* to accumulate TAG (Li et al. 2012; Çakmak et al. 2014). Even the oleaginous marine alga *Nannochloropsis* species

increase the TAG content by 50% when starved of nitrogen, and to a lesser extent when stressed by high light and salinity (Pal et al. 2011). In animals, mild (5%) calorie restriction administered to laboratory mice shifted the relative abundance of fat and muscle by increasing the fat mass by 68%, and reducing the lean mass by 12%, with total bodyweight remained unchanged (Li et al. 2009). In budding yeast *Saccharomyces cerevisiae*, a minimal amount of TAG is synthesized by vegetatively growing cells. When glucose becomes limited and that cells enter the stationary phase, TAG synthesis rises sharply (Taylor & Parks 1979). One apparent reason for these organisms to maintain a larger storage of TAG under stress is to cope with the uncertainties of the environments. By storing chemical energy and materials for membrane lipid biosynthesis, TAG helps the underlying cells quickly resume robust metabolism and growth when conditions improve. On the other hand, whether the existence of TAG in cells affords other benefits for survival through the environmental stress remains an unaddressed question.

TAG is composed of a glycerol backbone esterified to three fatty acids by acyl coenzyme A:diacylglycerol acyltransferases, DGATs, and phospholipid:diacylglycerol acyltransferases, PDATs. In budding yeast, Dga1p and Lro1p are the major DGAT and PDAT, respectively (Daum et al. 2007). Of these two, Lro1p appears to be responsible for TAG synthesis in vegetatively growing cells, whereas Dga1p contributes more significantly to the post-diauxic shift accumulation of TAG (Oelkers et al. 2000; Oelkers 2001; Sandager et al. 2002). In addition to TAG, fatty acids can be esterified to sterols to form steryl esters (SE), another class of storage neutral lipids (Sandager et al. 2002).

The two major enzymes responsible for SE biosynthesis are Are1p and Are2p (Sandager et al. 2002). In contrast to the stark differentiation of TAG abundance in log and stationary phase cells, SEs are maintained at a constant level at different phases of the growth curve (Fenner & Parks 1989), suggesting a function unique to TAG in the stationary phase. Intriguingly, deleting the four major neutral lipid biosynthetic genes (*DGA1, LRO1, ARE1, ARE2*), while causing yeast cells to lose practically all storage neutral lipids, does not result in significant deleterious effects in vegetatively growing cells (Sandager et al. 2002). However, these lean cells are hypersensitive to exogenous fatty acids and die with a phenotype of membrane over-proliferation (Petschnigg et al. 2009), indicating that maintaining the capacity of incorporating excessive free fatty acids in the form of TAG or SE affords an important means to prevent lipotoxicity of free fatty acids. Accumulation of TAG and SE in the ER membrane causes expansion of the membrane, which eventually buds out to form lipid droplets (LD), a dynamic phospholipid monolayered organelle that has gained increasing research interests (Welte 2015; Radulovic et al. 2013). A variety of proteins have been found associated with LD, including multiple TAG and SE hydrolases and signaling proteins that together play important roles in lipid homeostasis (Hodges & Wu 2010). The yeast *TGL3* and *TGL4* genes encode the two major TAG lipases in yeast; additional lipases Tgl5p, Ayr1p and Lpx1p appear to be less robust enzymatically (Ploier et al. 2013). Tgl4p, which is thought to be the functional orthologue of the mammalian ATGL (Zimmermann et al. 2004; Athenstaedt & Daum 2005), has been shown to be regulated by Cdk1-mediated phosphorylation in G1-to-S transition of dividing cells (Kurat et al. 2009). Blocking this

phosphorylation event delays bud emergence. Deleting either or both major TAG lipases causes accumulation of TAG in stationary phase cells without a clear growth defect (Athenstaedt & Daum 2005). Similar to TAG, SE can be broken down by functionally redundant lipases Tgl1p, Yeh1p, and Yeh2p (Köffel et al. 2005; Köffel & Schneiter 2006). SE lipase triple knockout cells, aside from possessing a significantly larger pool of SE, are phenotypically indistinguishable from the wildtype counterpart (Köffel et al. 2005). Together, these studies demonstrated clearly that yeast cells have the capacity of metabolizing neutral storage lipids. However, these lipids are not essential for cellular viability.

Budding yeast has been a model for two modes of aging (Kaeberlein 2010; Longo et al. 2012), chronological lifespan (CLS) and replicative lifespan (RLS). CLS refers to the overall viability of stationary-phase cells over time. RLS examines the number of daughters that each mother cell can produce before ceasing division. These two modes simulate, respectively, the senescence of post-mitotic (e.g., muscles and neurons) and stem cells in metazoans. Chronological aging in yeast has been linked closely to the nutrient status. When glucose is depleted, yeast cells exit from the log phase to enter diauxic shift, then into the stationary phase, a mitotically inactive yet metabolically active state (Herman 2002). The population viability is maintained in cells that enter the quiescent state (Allen et al. 2006; Werner-Washburne et al. 2012). However, over time, the number of viable quiescent cells diminishes as well, resulting in a progressive

increase of population mortality, a condition similar to metazoans including humans (Kaeberlein 2010). While there are yeast-specific chronological senescence and longevity factors (e.g., acetic acid and glycerol, respectively) (Burtner et al. 2009; Wei et al. 2009), a number of pathways are conserved (Kaeberlein 2010; Longo et al. 2012). Some of the most notable pro-aging pathways include the Target Of Rapamycin (TOR)/S6 kinase (Sch9p in yeast) (Fabrizio et al. 2001) and the Ras/adenylate cyclase/PKA pathways (Longo 1999). Intriguingly, these pathways control both CLS and RLS (Longo et al. 2012). These two pathways are activated in response to the intake of selective nutrients, and are suppressed by caloric restriction, consistent with many reports that different organisms extend their lifespan when subjected to calorie restriction (Sinclair 2005; Mirisola et al. 2014). Other pro-aging factors include oxidative stresses (Longo et al. 1996), mitochondrial dysfunction (Bonawitz et al. 2006; Schroeder & Shadel 2014), defective autophagy (Carmona-Gutierrez et al. 2010), DNA damages and replication stresses (Weinberger et al. 2007), and metabolic alterations (Goldberg et al. 2009). Yeast genome-wide studies have identified a variety of gene mutations that extend chronological lifespan (Smith et al. 2008; Powers et al. 2006; Matecic et al. 2010; Burtner et al. 2011). Many of these genes are involved in the metabolism of amino acids, nucleotides, or alternative carbon source, further underscoring the important roles played by metabolites in the control of lifespan. However, despite these relatively unbiased screens, very little is known regarding the role of lipids in the control of CLS. Here we present evidence for a novel energy usage-independent, anti-senescence function of TAG in yeast.

Results

TAG extends chronological lifespan

Budding yeast is an excellent model for elucidating gene functions, biochemical pathways, stress responses, and aging. Natural variations among yeast strains, including traits altered during laboratory domestication may help uncover the relationships between genotype and phenotype (Liti & Louis 2012; Kvitek et al. 2008). We speculated that phenotypic differences between laboratory and wild isolates could reveal important biological information, including the relationship between lipid and aging. To this end, we first examined the growth curves, under standard laboratory growth conditions, of eight wild strains isolated from diverse natural environments and three laboratory strains. These wild strains were *ho*$^{-}$ (i.e., unable to switch mating type) haploid segregants of isolates from vineyards, oak exudates, and clinical samples. The three laboratory strains were yMK839, a derivative of EG123 (Siliciano & Tatchell 1984), W303, and BY4742. Figure 2.1A shows that, in general, wild strains had a shorter lag phase and faster growth rate in log phase than laboratory strains (doubling time in YPD: lab, 94 ± 2 min; wild, 80 ± 3 min). In addition, the cell density at saturation, i.e., stationary phase, was also higher for the wild strains. The ability to accumulate higher cell density in spent medium indicated that these wild strains may have adapted more effectively to nutrient limitations in a harsh environment, and, if true, further suggested that such cells might survive better through stationary phase than their domesticated counterparts. To test this hypothesis, we measured the percent of cells able to re-enter vegetative growth from revival of the saturated cultures over a period of one month,

using the quantitative "outgrowth" approach developed by Kaeberlein and colleagues (Murakami et al. 2008). The survival plot in Figure 2.1B demonstrates higher viability of

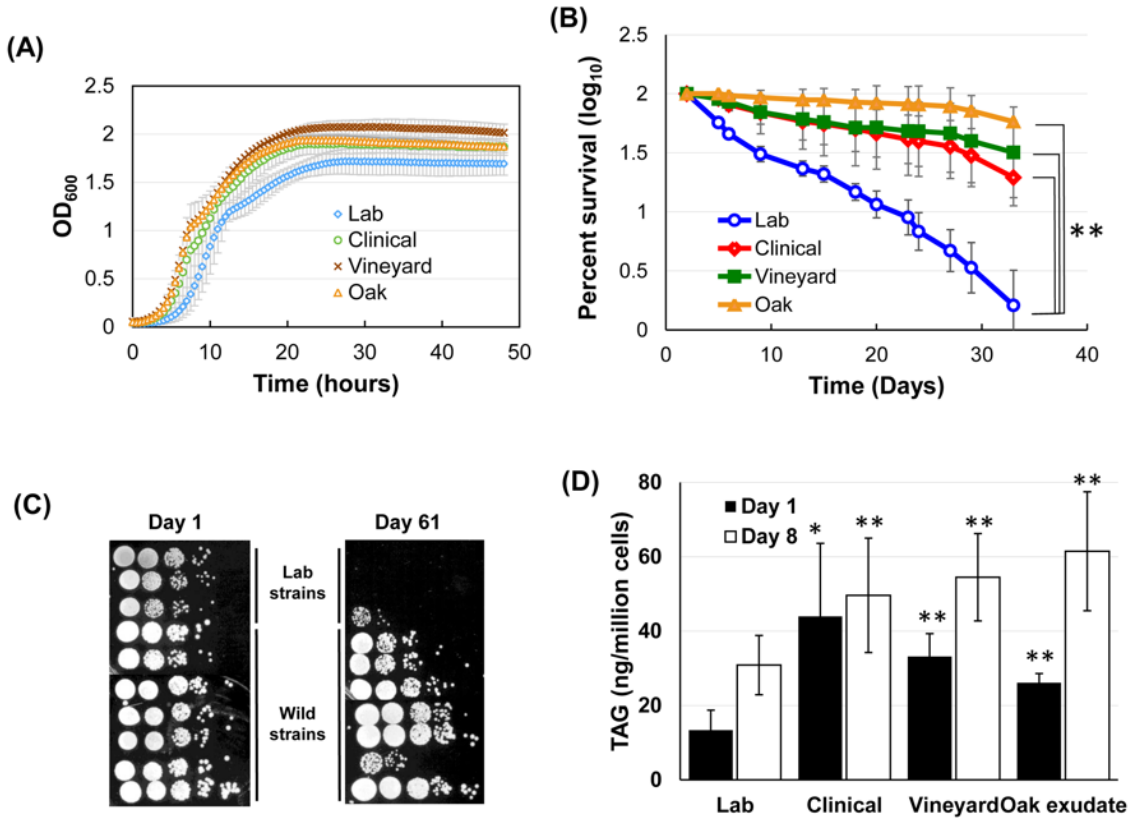

Figure 2.1 Wild yeast strains from different origins accumulate higher levels of triacylglycerol (TAG) and exhibit longer chronological lifespan. (A) Growth curves of wild strains isolated from oak exudates, vineyards, and clinical samples vs. three laboratory strains. Cells were grown in YPD at 30° in a 96-well plate. Each curve represents the average of growth of 2 to 4 strains in the category. Shown are representative results from two biological replicates. (B) Chronological lifespan in SC medium was measured by the "outgrowth" approach. (C) Chronological lifespan examined by spot assays. Viability of cultures was assayed every 3 to 5 days for two months. Only day 1 (all strains showed close to 100% viability) and day 61 images are shown. Cultures were 10-fold serially diluted in water before inoculation. (D) Quantification of triacylglycerol of cells harvested from day 1 and day 8 post-saturation YPD cultures.

wild strains. In a separate “spot assay”, cells cultivated for 61 days were serially diluted and spotted to a fresh solid medium. Two of the three laboratory strains fell below the detection limit of this assay, whereas the majority of the wild strains were capable of forming new colonies, indicating higher survival rates (Figure 2.1C).

Figures 2.1A-C suggest that the laboratory domestication of *S. cerevisiae* might have artificially selected for certain physiology features leading to distinct phenotypes in the stationary phase (Gray et al. 2004). Microscopic inspection of 5-day old stationary phase cells revealed more abundant cytoplasmic granules stainable by the neutral lipid dye Nile red in wild strains (Figure 2.2). These Nile red stained lipid droplets are organelles that store neutral lipids, i.e., triacylglycerol and steryl esters (Radulovic et al. 2013). Whereas the SE level stays constant through the growth curve (Fenner & Parks 1989), TAG abundance rises sharply when cells enter the stationary phase (Taylor & Parks 1979). TAG thus seemed to be a plausible causal link to the observed difference in survival following saturation. To test this hypothesis, we first quantified cellular TAG abundance of day-1 and day-8 post-saturation cultures. Consistent with the microscopic observations, the wild strains contained higher levels of TAG at both time points (Figure 2.1D), providing a positive correlation between TAG abundance and survival.

The differential age-dependent survival shown above is equivalent to yeast chronological lifespan (Mortimer & Johnson 1959; Fabrizio & Longo 2003), suggesting that TAG may have a role in maintaining or even extending chronological lifespan. To

understand the causal relationship between TAG metabolism and chronological lifespan, we turned to a laboratory strain (yMK839) for genetic manipulation and phenotypic assessment.

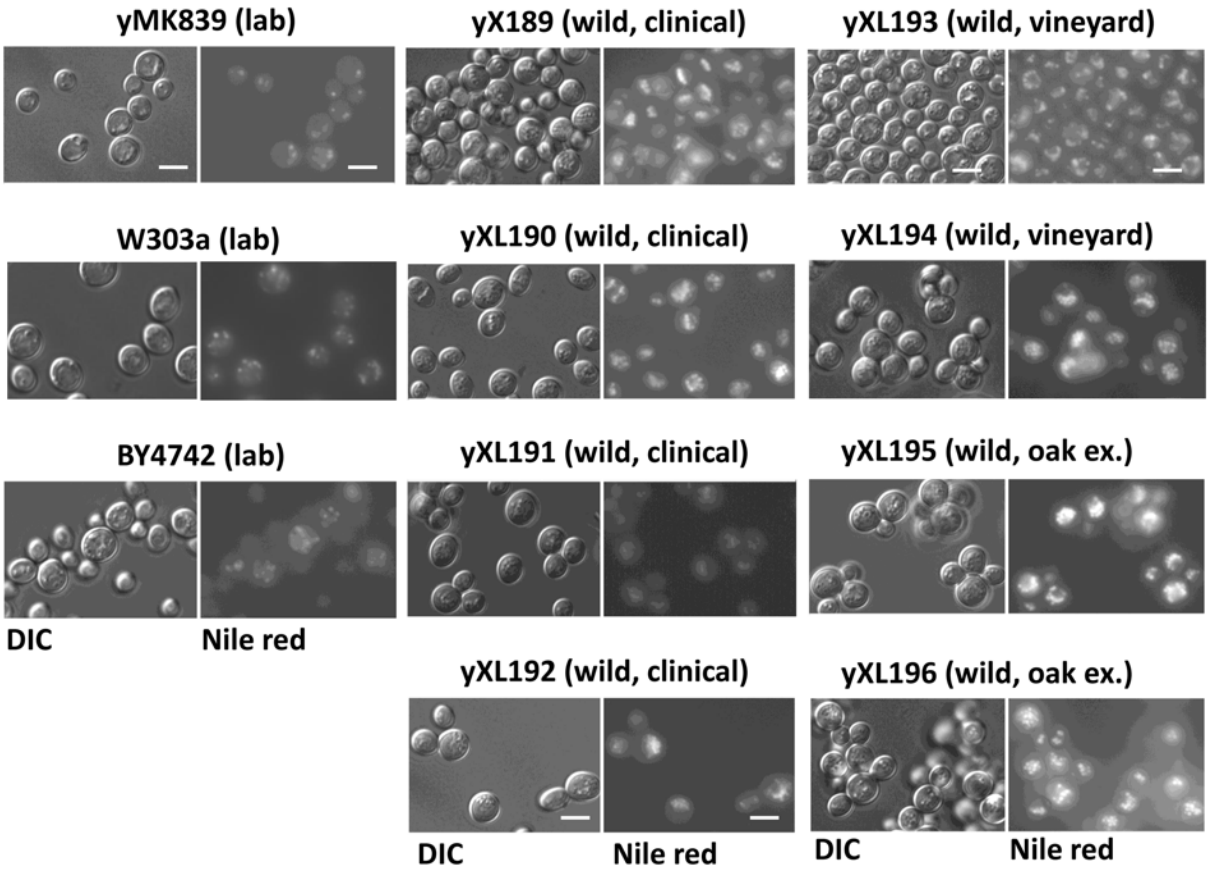

Figure 2.2 Wild yeast accumulate higher TAG. Lab and wild yeast strains used in this work were examined by microscopy. 5-day old stationary phase cultures were harvested for neutral lipid staining with Nile red. DIC (differential interference contrast) and fluorescence microscopy were done using an Olympus BX51 station equipped with a Exfo X-cite 120 UV light fixture and a DP30-BW CCD camera. Fluorescence micrographs were taken with a fixed, 2-second exposure to aid comparison of the fluorescence intensity. Scale bars: 5 μm. All pictures were re-sized identically for presentation.

In yeast, Dga1p and Lro1p are the major TAG biosynthetic enzymes (Figure 2.3A). The aliphatic chain of each constituent fatty acid contains chemical energy that can be converted to metabolically useful energy by a series of β-oxidation reactions taking place in peroxisomes, following lipolysis by lipases Tgl3p and Tgl4p (Athenstaedt & Daum 2005; Athenstaedt & Daum 2003; Kurat et al. 2006). To test whether the increased TAG storage prolongs chronological lifespan, we deleted *TGL3* and *TGL4*, which caused TAG accumulation while blocking energy extraction from this lipid species. Consistent with published results (Athenstaedt & Daum 2005; Kurat et al. 2006), the TAG level was elevated in *tgl3*Δ , *tgl4*Δ , and *tgl3*Δ *tgl4*Δ strains at stationary phase (Figure 2.4). Importantly, all three TAG-rich strains showed extension of chronological lifespan (Figures 2.3B, and 2.5 rows 2 to 4). These results indicate that the storage of TAG, but not its hydrolysis as a prerequisite for energy conversion or other cellular uses, is associated with improved viability in stationary phase. Intriguingly, deleting the TAG lipase did not cause discernible defects in doubling time (Figure 2.3E), mating efficiency of haploid cells, or sporulation of homozygous *tgl3*Δ */tgl3*Δ cells (Figure 2.6). Because deleting either or both TAG lipase genes resulted in similar phenotypes with respect to TAG accumulation and lifespan extension (Figure 2.3B), the *tgl3*Δ strain is representatively shown in further experiments below.

Blocking TAG hydrolysis also diminishes downstream reactions, including peroxisomal β-oxidation that produces H_2O_2 that may cause oxidative stresses and cell death (Kumar et al. 2014). If a reduction of lipolysis-associated H_2O_2 production was

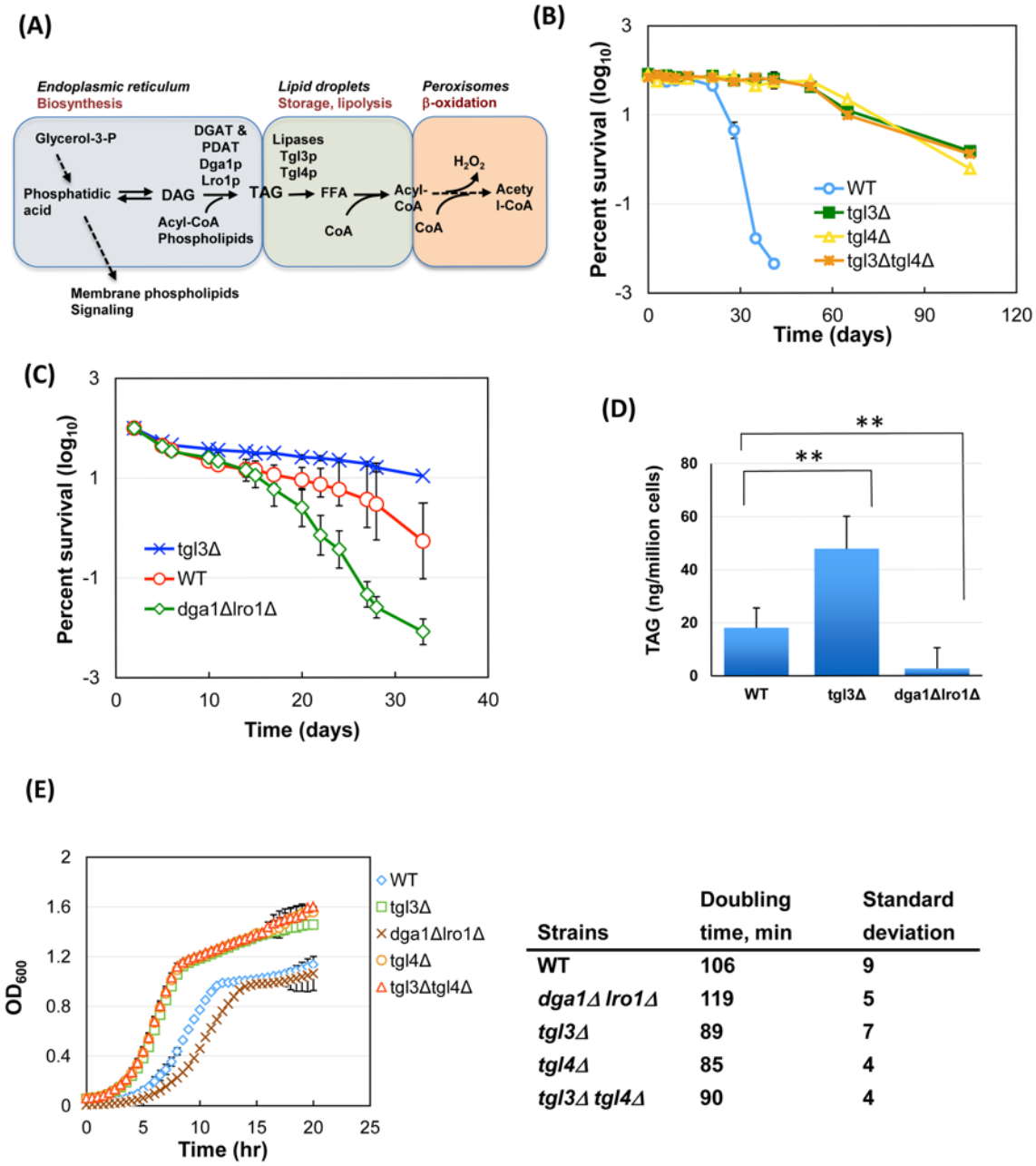

Strains	Doubling time, min	Standard deviation
WT	**106**	**9**
dga1Δ lro1Δ	**119**	**5**
tgl3Δ	**89**	**7**
tgl4Δ	**85**	**4**
tgl3Δ tgl4Δ	**90**	**4**

Figure 2.3 Elevated intracellular TAG level promotes longevity during chronological aging, whereas TAG depletion shortens lifespan. (A) Abbreviated view of TAG metabolism in yeast. (B) A laboratory strain yMK839 and its single and double lipase knockout derivatives were grown deeply into stationary phase in SC medium. At different time points, cells were spread to fresh YPD plates to quantify the colony forming units, expressed as percent survival. The plot was from two

Figure 2.3 (cont'd)

biological replicates of each strain. (C) Deleting *DGA1* and *LRO1* causes early death in stationary phase. Shown are averages of five biological repeats by the outgrowth approach. ** $p < 0.01$. Note the difference in time scale between panel B and panel C. Also, the two different assays for chronological lifespan quantification, i.e., colony forming units and outgrowth method, might give rise to differences in the absolute numbers of percent survival. The former did not differentiate colony size variations, whereas the latter outgrowth assay, which relied on the population growth rate, would be impacted by differences in doubling time and in the time when a cell exited the lag phase. (D) Quantification of intracellular TAG from day-8 post-saturation cultures in SC medium. (E) Growth comparison of yMK839 and its TAG-rich and -depleted derivatives. Growth curves were obtained as in Figure 2.1A.

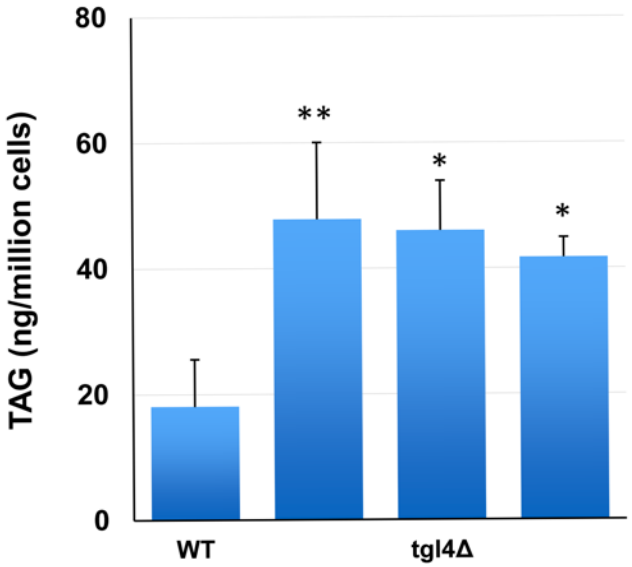

Figure 2.4 Deleting either or both TAG lipase genes resulted in similar upregulation of TAG in yeast. Total TAG, expressed as percentage of total cellular lipids, of wildtype, *tgl3*Δ , *tgl4*Δ , and *tgl3*Δ *tgl4*Δ strains were isolated and quantified by gas chromatography. Cells were from 3-day old YPD cultures. *, P<0.05; **, P<0.01

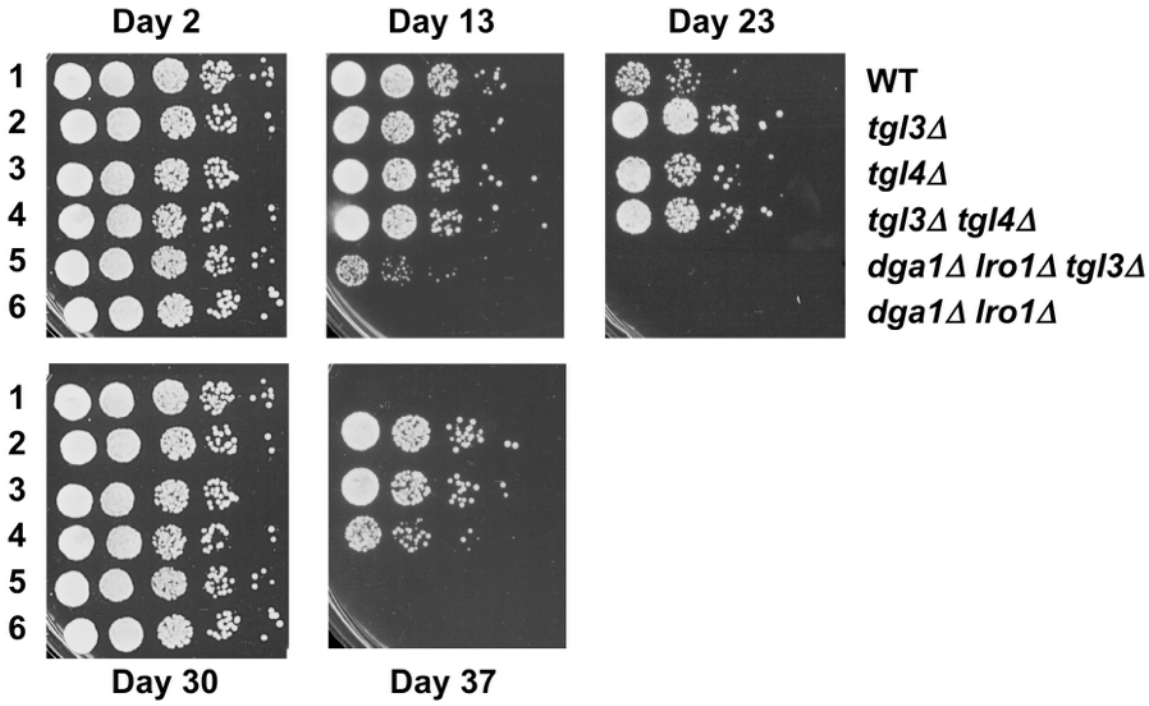

Figure 2.5 Deleting *TGL3* does not rescue the early death phenotype of the *dga1*Δ *lro1*Δ lean cells. The indicated strains (on the right) were grown in SC with 2% glucose and sampled at the indicated time for semi-quantitative comparison of colony forming units. 10-fold serially diluted cell suspension was spotted to YPD.

solely responsible for the observed viability retention, deleting the two major TAG biosynthetic acyltransferases, Dga1p and Lro1p, would prevent TAG synthesis and the subsequent β-oxidation (Figure 2.3A), and a similar beneficial effect on longevity would result as well. However, phenotypic analysis of the *dga1*Δ *lro1*Δ strain revealed the opposite. Deleting the two TAG biosynthetic acyltransferases caused a reduction of chronological lifespan (Figure 2.3C, and Figure 2.5, row 6) and nearly eliminated cellular TAG (Figure 2.3D). The log phase growth rate also was reduced by the double

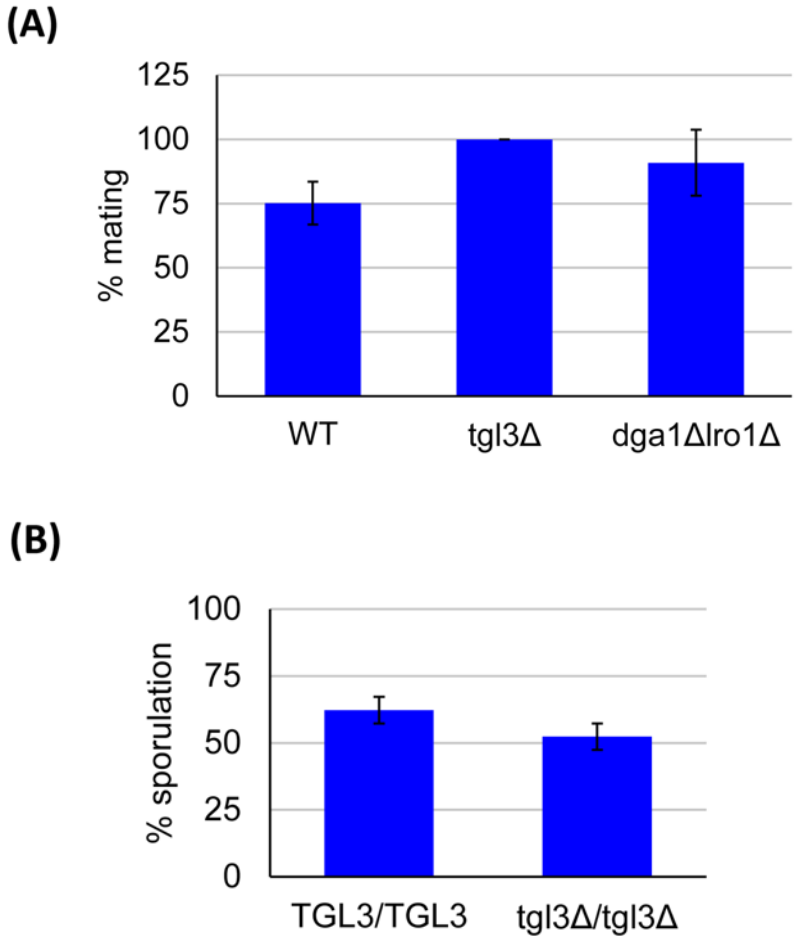

Figure 2.6 TAG accumulation does not affect mating efficiency, sporulation, or medium acidification. (A) Haploid strains, as indicated, were tested for their mating efficiency with a tester strain. (B) TGL3 +/+ and -/- diploid strains were subjected to sporulation. 3 days after transferring cells to the sporulation medium, cells were examined under a microscope to quantify for the number of tetrads.

deletion by approximately 12% (Figure 2.3E), which likely resulted from a defect in maintaining the cell's replicative potential (see Figure 2.7 and below). This shortened chronological lifespan could not be rescued by deleting *TGL3* (Figure 2.5, row 5), underscoring the necessity of keeping the physical presence of TAG to maintain cellular viability during stationary phase.

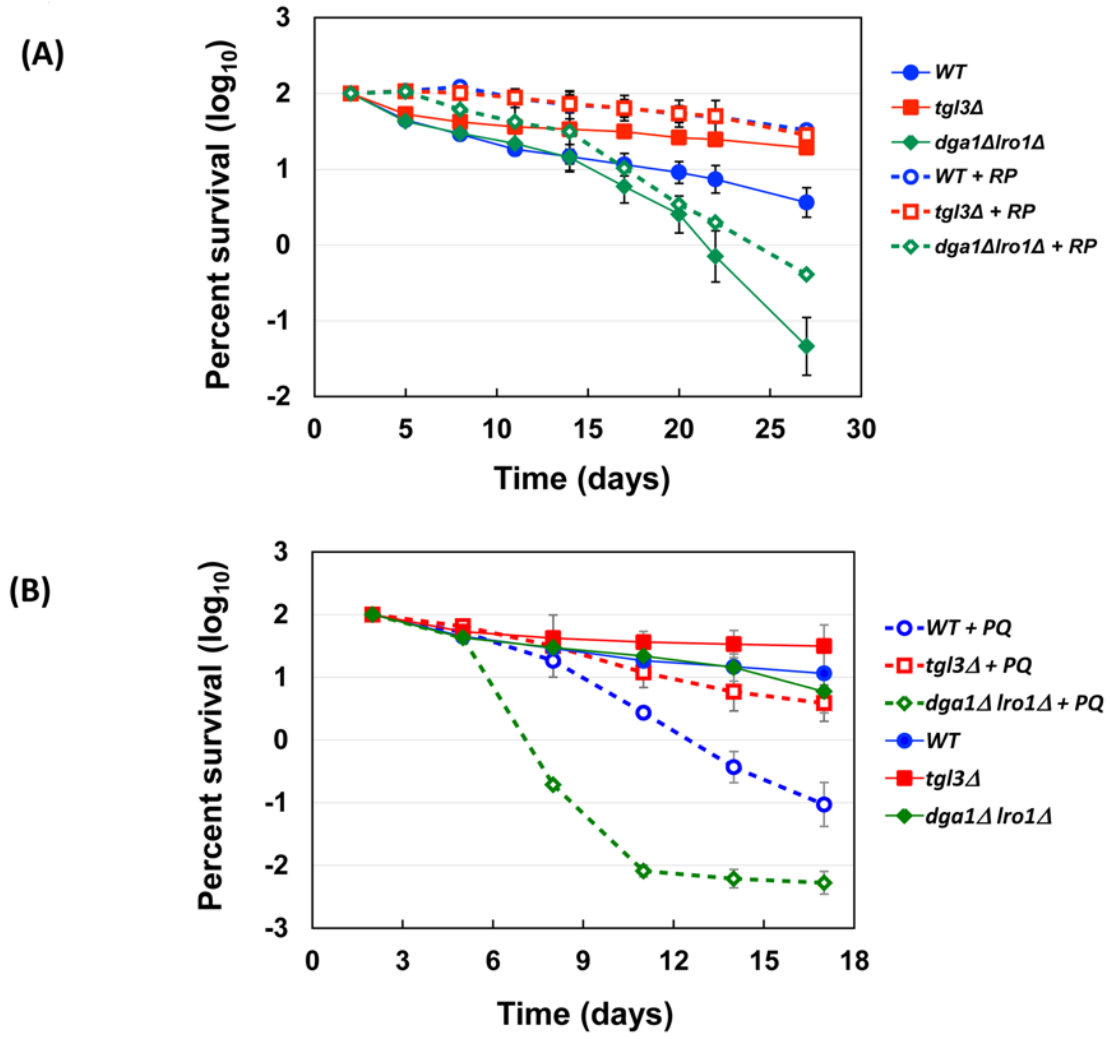

Figure 2.7 Rapamycin and paraquat respectively extends and shortens lifespan of the three core strains. 10 nM of Rapamycin (RP, panel A) and 10 μM of paraquat (PQ, panel B) were included in SC medium to assess the effects on the lifespan. Other parameters were identical to experiments shown in Figure 2.3C.

To further confirm the pro-longevity role of TAG, we overexpressed a TAG biosynthetic enzyme Dga1p (Oelkers et al. 2001) by introducing a multi-copy plasmid bearing *DGA1* under the control of the native *DGA1* promoter or a constitutive *ADH1*

promoter to *TGL3*$^{+}$ and *tgl3*Δ strains. Cells from day-8 post-saturation cultures were processed for lipid extraction and TAG quantification. Data in Figure 2.8A confirmed the increased TAG content by Dga1p overproduction. The wildtype cells with a higher level of TAG exhibited longer lifespan (Figure 2.8B), strongly suggesting that TAG plays a causal role in preserving cellular viability during chronological senescence. Intriguingly, while Dga1p overexpression also raised the TAG content in *tgl3*Δ cells, the lifespan

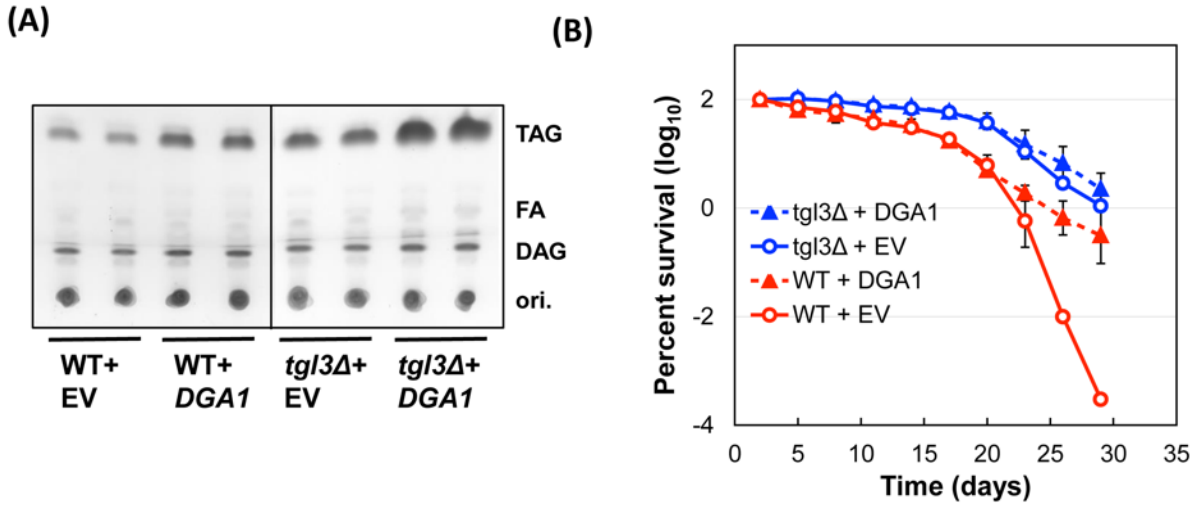

Figure 2.8 Overproducing Dga1p increases TAG abundance and extends chronological lifespan. (A) Thin-layer chromatography of neutral lipids from eight-day old stationary phase cultures bearing either the empty vector (EV) or one that expresses Dga1p. DAG, diacylglycerol; FA, free fatty acids; ori., origins for chromatography. The two EV lanes in panel A are biological duplicates; each of the two *DGA1* lanes represents the two different constructs with *DGA1* or *ADH1* promoter driving the recombinant gene expression. (B) Survival curves. These are averages of four *DGA1* overexpression isolates (two of each plasmid transformants), and two vector control duplicates. To accommodate the use of episomal plamids, yeast cells were grown in SC-uracil medium, which, compared with the use of synthetic complete medium seen in Figures 2.1 and 2.3, likely caused slightly faster viability loss of all strains analyzed.

extension was relatively minor in this already long-living background. This observation indicates a limit of lifespan extension by TAG. Taking together the data in Figures 2.1, 2.3, and 2.8, we conclude that intracellular triacylglycerol is essential for the maintenance of chronological lifespan, and that forcing the accumulation of TAG by either blocking its hydrolysis or increasing its biosynthesis, can extend lifespan.

TAG promotes longevity independently of other lifespan control pathways

The yeast chronological lifespan is regulated by common as well as yeast-specific factors. Rapamycin and paraquat extends and shortens lifespan, respectively (Powers et al. 2006; Loewith & Hall 2011). Caloric restriction, e.g., reducing the initial glucose concentration from 2% to 0.5% or lower in the medium, promotes longevity, whereas excessive glucose (e.g., 10%) shortens it. More specific to yeast is medium acidification from fermentation that causes senescence, an aging mechanism that can be antagonized by using a buffered, neutral pH medium (Burtner et al. 2009; Mirisola & Longo 2012; Burhans & Weinberger 2009). We examined the relationship between TAG and these lifespan regulators, and found that the lifespan-extending regimes of caloric restriction (0.05% glucose), medium neutralization (pH6 with citrate phosphate), and high osmolarity (8% sorbitol) all delayed senescence for both the yMK839 wildtype and its TAG-depleted derivative (Figures 2.9A and 2.9B), with the latter still exhibiting shorter lifespan. The exceptionally long lifespan of *tgl3*Δ cells prohibited us from quantitatively assessing the effect of these lifespan extending treatments. 10% glucose caused all three strains to die early, yet the lipase-null cells remained to be the longest-living strain,

suggesting strongly that CLS regulation by the abundance of TAG operates in a novel pathway. The observation that medium neutralization effectively extended the lifespan of *dga1*Δ *lro1*Δ and wildtype cells (Figure 2.9A fourth column from left) could be interpreted as that differences in medium acidification underlay the observed differential lifespan. However, direct measurement of the medium pH of the three normal, lean, and fat strains for more than 10 days (Figure 2.10A), or of 4-day old cultures of the three lab strains and 8 wild strains (Figure 2.10B) revealed statistically indistinguishable degrees of medium acidification. These data therefore ruled out that changes in the TAG level would alter the acidity of the medium and, consequently, the lifespan of cells. Together, Figures 2.9 and 2.10 demonstrate that the chronological lifespan can be controlled by the abundance of intracellular TAG in a mechanism that is independent of pathways involving glucose, medium pH and osmolarity.

Rapamycin and paraquat are two potent extragenic lifespan modulators for many species (Sinclair 2005; Powers et al. 2006). When treated with these two compounds, all three core strains responded similarly. That is, rapamycin extended, whereas paraquat shortened the lifespan of all three (Figure 2.7). When several highly conserved lifespan control genes *TOR1*, *RAS2*, and *SOD2* were deleted from the three core strains, we observed differential responses (Figure 2.11). From the time for each strain to drop to 10%, 1%, and 0.1% viability (Table 2.1), it is clear that deleting *TOR1* made the wildtype strain live longer, in agreement with previous findings (Wei et al. 2009). Intriguingly, despite that rapamycin (10 nM) treatment prolonged cellular survival (Figure 2.7A),

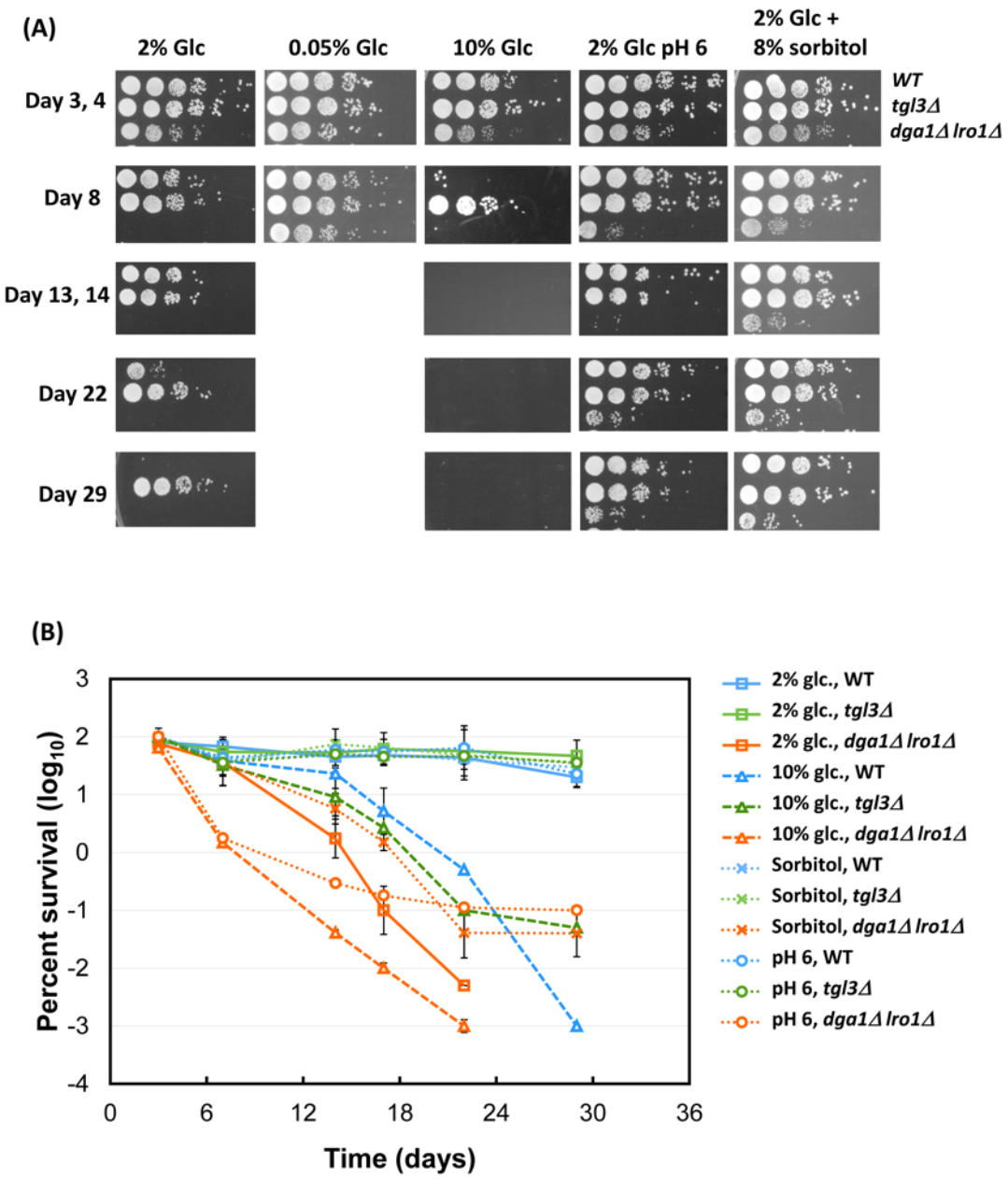

Figure 2.9 TAG-medicated lifespan control is independent of several yeast-specific and common lifespan regulatory regimes. (A) Semi-quantitative comparison of lifespan of the three "core" strains used in this study: wildtype (WT), TAG lipase knockout (*tgl3*Δ), and TAG synthesis deficient mutant (*dga1*Δ *lro1*Δ) under different growth conditions. Glc, glucose; the medium neutralization experiment (fourth column from left) was done with SC medium supplemented with 64.2 mM Na_2HPO_4 and citric acid to stabilize the pH at 6.0. Shown are representative results of 2 or 3 biological repeats. (B) Quantitation of the spot assay results. All data were from three biological duplicates.

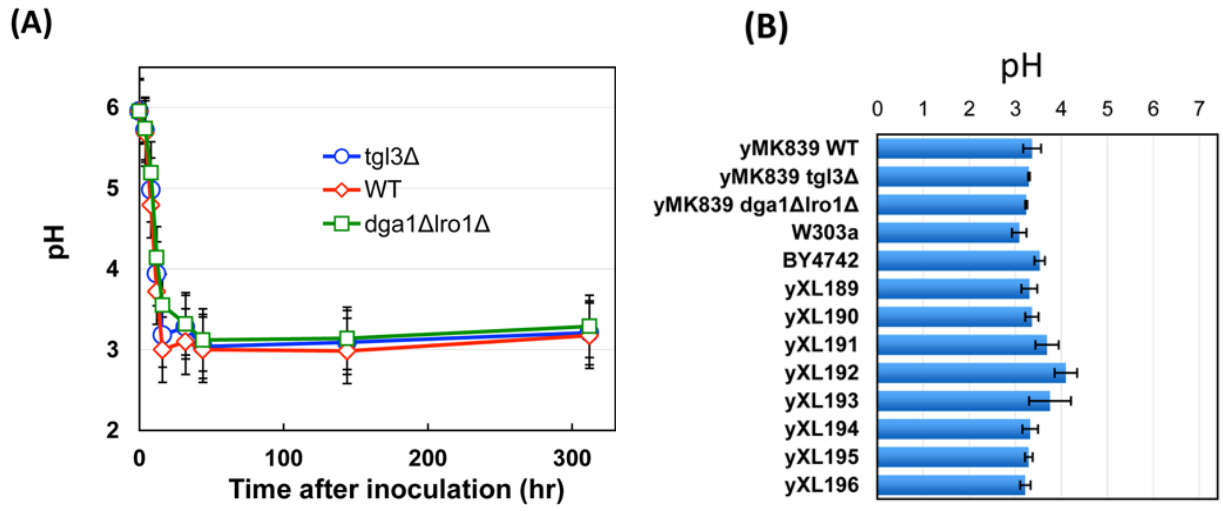

Figure 2.10 Culture medium pH changes are comparable among strains with different chronological lifespan. The pH changes of YPD cultures were monitored for 312 hours after inoculating overnight cultures to fresh medium (Panel A). In a second set of experiments (Panel B) the medium pH was measured from 4-day old YPD cultures of the indicated lab and wild strains. n ≥ 3.

deleting the entire Target of Rapamycin *TOR1* gene actually shortened the lifespan of both the fat, *tgl3*Δ cells and the lean, *dga1*Δ *lro1*Δ cells (Figure 2.11 and Table 2.1). Because these lipase- and DGAT-deficient strains were unable to extract energy from TAG metabolism, we suspect that *tor1*Δ cells survived at least partly on the energy stored in TAG. Lacking either *TGL3* or *DGA1* and *LRO1* resulted in the loss of viability during chronological aging. In contrast to the differential effects *TOR1* deletion, knocking out *RAS2* or *SOD2* shortened lifespan of all three parental strains (crosses and open squares, Figure 2.11). *RAS2* in the RAS/cAMP/PKA pathway is involved in stress response and lifespan control (Longo 2004). Deleting *RAS2* has been shown to preserve chronological

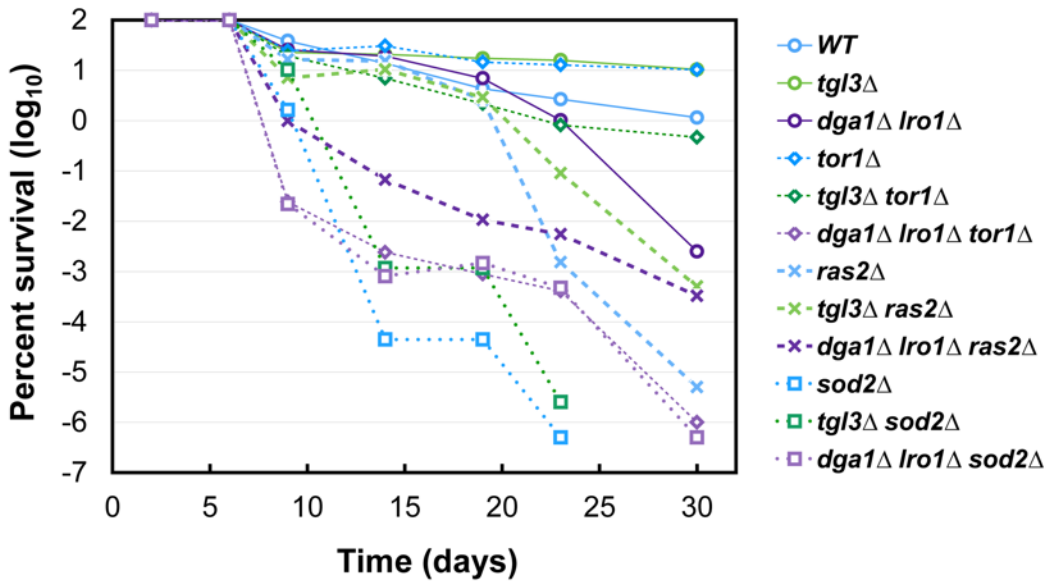

Figure 2.11 TAG controls chronological lifespan independently of conserved pathways. *TOR1*, *RAS2*, and *SOD2* were deleted from the three core strains with a normal, higher, and lower TAG content. The resultant strains were grown for outgrowth assays to compare their CLS with the corresponding parental strains. Representative plot of one of three biological duplicate outgrowth experiments.

Table 2.1 Quantitative analysis of lifespan from the outgrowth data seen in Figure 2.11.

	Survival	Days	Relative change
		wt	
WT	10%	15.25±0.35	0
	1%	29.5±0.71	0
	0.1%	> 30	0
tgl3Δ	10%	23±9.90	0
	1%	> 30	0
	0.1%	> 30	0

Table 2.1 (cont'd)

	Survival	Days	Relative change
dga1Δ lro1Δ	10%	14.25±3.89	0
	1%	20±4.24	0
	0.1%	23.4±3.39	0
		tor1Δ	
WT	10%	30	+14.25
	1%	> 30	-
	0.1%	> 30	-
tgl3Δ	10%	16.0±4.95	-7
	1%	26.0±5.66	-
	0.1%	> 30	-
dga1Δ lro1Δ	10%	6.53±1.62	-7.72
	1%	11.20±3.35	-8.8
	0.1%	16.67±7.59	-6.73
		ras2Δ	
WT	10%	13.50±2.12	-1.75
	1%	19.5	-10
	0.1%	20.8	-
tgl3Δ	10%	14	-9
	1%	20.3	-
	0.1%	23	-
dga1Δ lro1Δ	10%	7.37±2.0	-6.88
	1%	7.90±1.56	-12.1
	0.1%	10.55±3.89	-12.85

Table 2.1 (cont'd)

	Survival	Days	Relative change
		***sod2*Δ**	
WT	10%	6.90±1.27	-8.35
	1%	9.15±0.21	-20.35
	0.1%	10.90±0.85	-
***tgl3*Δ**	10%	7.40±0.57	-15.6
	1%	10.15±0.21	-
	0.1%	12.0±0.71	-
***dga1*Δ*lro1*Δ**	10%	8.70±2.48	-5.55
	1%	10.97±2.84	-9.03
	0.1%	13.17±4.05	-10.23

Table 2.1 The time (in days) it took for each strain to drop to 10%, 1%, and 0.1% viability was calculated (see Materials and Methods) from two or three independent assays, whenever data available. Some thus did not yield a standard deviation. The lifespan changes of the *tor1*Δ , *ras2*Δ , and *sod2*Δ strains were differences (days to reach 10%, 1%, and 0.1% viability) from the corresponding parental strains. Asterisks (*) indicate that at least one of the two strains being compared maintained the viability higher than 1% or 0.1% throughout the duration of the experiments.

lifespan (M. Wei et al. 2009). However, a genome-wide screen showed reduced survival of chronologically aging *ras2*Δ cells (Garay et al. 2014). In our hands, all *ras2*Δ strains died earlier than their corresponding parental strains regardless of the TAG content (Figure 2.11, cross markers, and Table 2.1 summary), suggesting that Ras2p controls the lifespan in a TAG-independent manner. Similarly, deleting *SOD2*, which encodes a

mitochondrial manganese superoxide dismutase that is a key to the defense against reactive oxygen species originated from mitochondria, and to the preservation of full lifespan potential (Unlu & Koc 2007), significantly reduced the life expectancy of all three strains. These observations suggest that Sod2p remained to be a critical vitality enzyme in the long-living *tgl3*Δ cells, and that TAG likely functions independently of Sod2p to protect aged cells.

TAG is required for achieving full replicative potential

Like CLS, replicative lifespan of budding yeast is another model for cellular senescence, which is determined as the number of daughters produced by a mother cell during its lifespan (Mortimer & Johnson 1959). One fundamental difference between chronological and replicative lifespan is that the ability to proliferate is measured from cells sampled from saturation versus logarithmic growth, respectively (Figure 2.12A). Intriguingly, log phase yeast cells, which allocate most fatty acids to phospholipid synthesis to support cell growth and division, store very little TAG (Taylor & Parks 1979). Although TAG is dispensable for cell survival (Sandager et al. 2002) (Figure 2.3), the immediate precursor for TAG, diacylglycerol, also supplies building blocks for phospholipids (Carman & Han 2009). It is possible that changes in the flux of the albeit small amount of TAG in dividing cells may still impact their replicative lifespan by, for example, influencing the metabolism of other lipids derived from DAG.

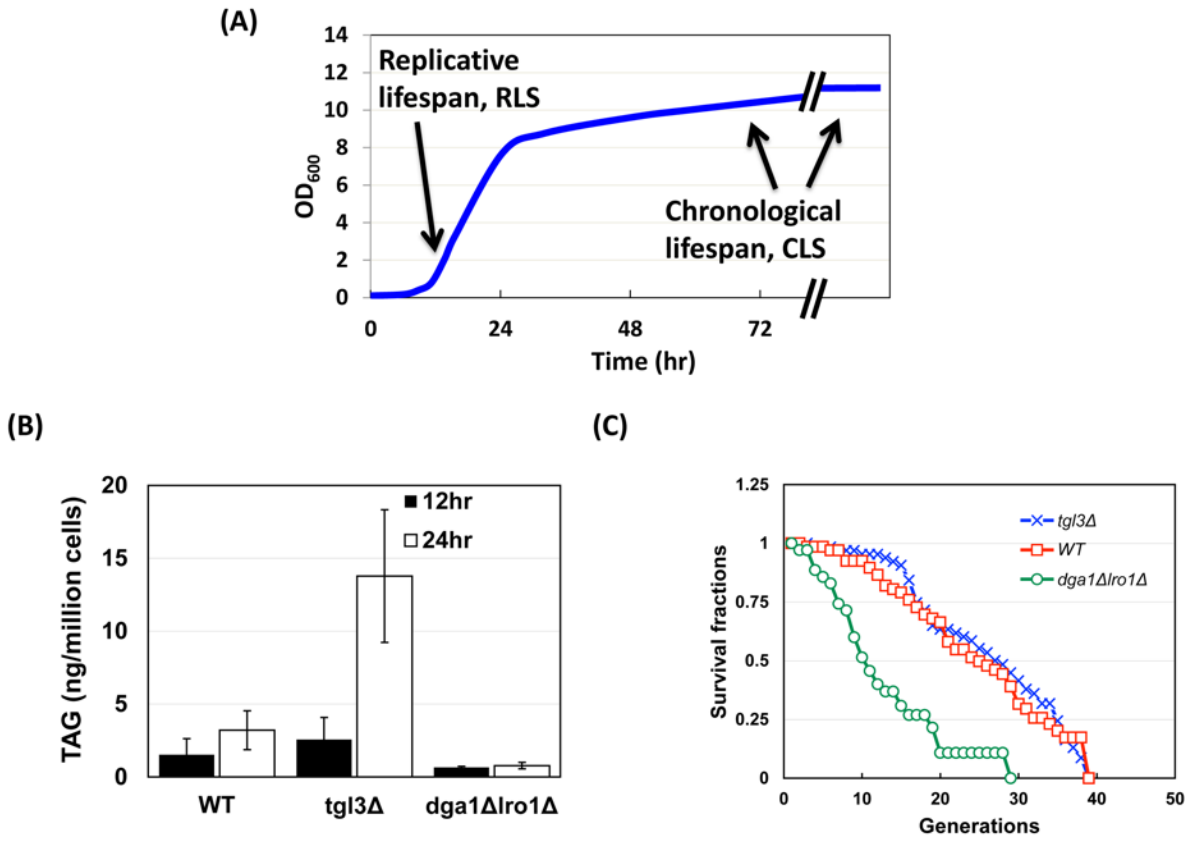

Figure 2.12 Full replicative lifespan requires TAG. (A) Replicative and chronological lifespan examine cells from log and stationary phase, respectively. (B) TAG quantification of strains harvested 12 and 24 hours after inoculation. These cells were at early and late log phase, respectively. The y axis was set at between 0 to 80 ng/million cells to be consistent with other similar Figures and to highlight the low abundance of TAG in log phase cells. (C) 60 to 90 newly divided daughter cells from the indicated strains were compared for their replicative lifespan. Shown are representative results from three biological duplicates. Breslow analysis showed that the RLS of the *dga1*Δ *lro1*Δ cells was significantly different from the other two strains ($p < 0.0001$).

To assess the influence of TAG on replicative lifespan, yMK839 wildtype, *dga1*Δ *lro1*Δ , and *tgl3*Δ strains were subjected to replicative lifespan comparison by the traditional microscopy approach (Longo et al. 2012). Deleting the TAG biosynthetic enzymes further diminished the small TAG pool in log phase cells (12-hour post-

inoculation, black bars, Figure 2.12B). Importantly, both maximum and median replicative lifespan were decreased in cells depleted of TAG (Figure 2.12C). This shortened replicative lifespan likely accounted for the increased population doubling time of *dga1*Δ *lro1*Δ cells (Figure 2.3E). On the other hand, deleting *TGL3* had a minimal effect on the TAG level in early log phase cells (12-hour post-inoculation), and the lifespan of *tgl3*Δ cells also was unchanged (blue cross marker, Figure 2.12C). Together, these data demonstrate that maintaining a certain amount of TAG, or the ability to synthesize TAG, is required to reach full replicative potential. TAG hydrolysis apparently is not essential for replicative lifespan maintenance.

Discussion

Here we present evidence for a novel pro-longevity function of intracellular TAG in yeast. Deleting TAG lipases or overproducing a DGAT increased TAG accumulation and extended chronological lifespan. Deleting the two TAG biosynthetic enzymes practically eliminated TAG and significantly shortened the chronological lifespan, as well as the median and maximum replicative lifespan. The fact that chronological lifespan extension is seen in different lipase knockout (i.e., *tgl3*Δ , *tgl4*Δ , and *tgl3*Δ *tgl4*Δ) and in DGAT overexpression strains argues strongly that the accumulation of TAG was the contributing factor for lifespan extension. This conclusion is consistent with the observation that deleting *TGL3* cannot rescue the early death phenotype of *dga1*Δ *lro1*Δ lean cells (rows 5 and 6, Figure 2.5). Unlike other lifespan extension regimes such as *SCH9* knockout and rapamycin treatment that also retard mitotic growth (Neklesa & Davis 2008; Toda et al.

1988), we have yet to detect obvious growth defects in the three lipase deletion strains. For example, aside from normal, or even faster growth rates (Figure 2.3E), mating and sporulation efficiency of these fat cells was essentially identical to their wildtype mother strain (Figures 2.6A and 2.6B). There were no significant differences in cellular sensitivity to heat (55°C), 260 nm UV, high concentrations of NaCl, or to H_2O_2 (Figure 2.13). It is perceivable that a negative phenotype would be linked to TAG lipase null cells if they were grown without any fatty acid supplement, and with concomitant presence of a fatty acid synthase inhibitor such as cerulenin (Nomura et al. 1972). These cells would suffer from the lack of energy and fatty acid building blocks for growth and division. TAG hydrolysis is thus by and large dispensable as long as fatty acids are available from the environment or can be synthesized by de novo activities. It should be noted that Daum and colleagues reported that *tgl3*$^{-}$ homozygous knockout cells were unable to form spores (Athenstaedt & Daum 2005). Possible causes for this discrepancy may include differences in the genetic background of the strains, and the protocols for sporulation.

Chronological lifespan of *S. cerevisiae* is regulated by both yeast-specific and conserved factors and drugs. Experimental results shown in Figures 2.7 to 2.11 strongly suggest that TAG preserves viability during chronological senescence in a manner that is independent of those factors tested herein, including caloric restriction, high osmolarity, medium pH, rapamycin and paraquat responses, and conserved pathways involving *TOR1*, *RAS2*, and *SOD2* genes. Results from genetic interaction tests also suggest a novel TAG pathway in CLS control. Both fat and lean strains responded similarly to the

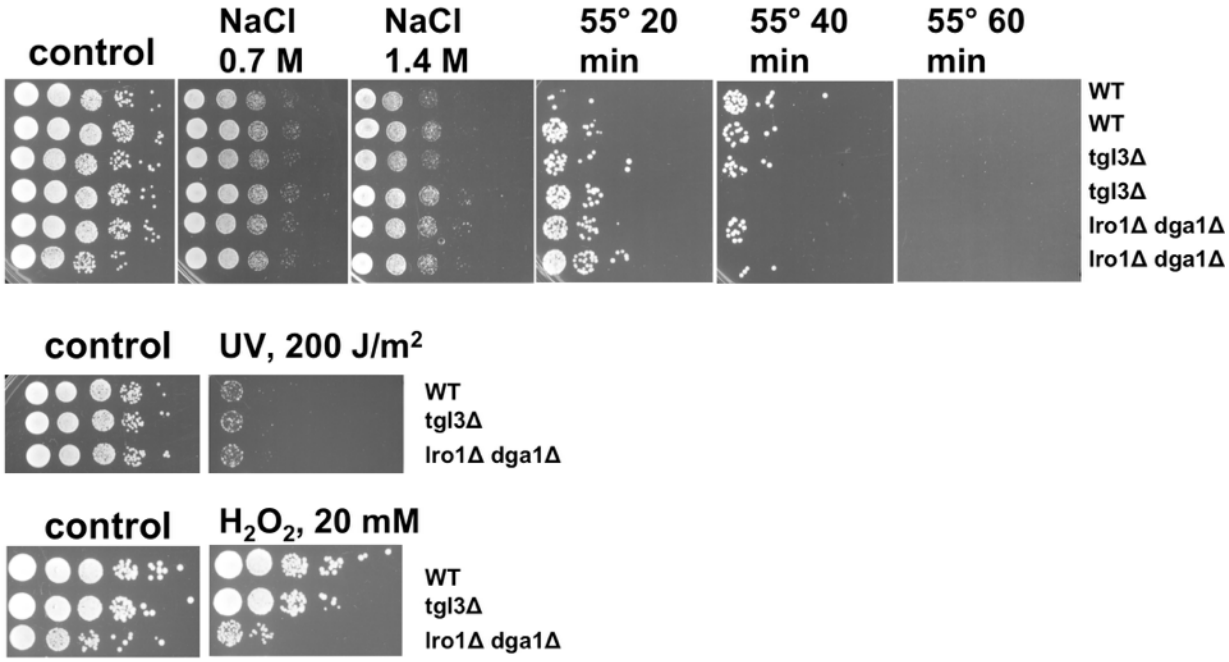

Figure 2.13 TAG-rich and –deficient cells do not exhibit significant differential susceptibility to common stresses. Day 3 early-stationary phase cultures were exposed to the shown stresses before plating to YPD. For the test of salt sensitivity, NaCl (0.7 or 1.4 M) was included in the YPD plate. Heat and H_2O_2 sensitivity were conducted by exposing cell suspension (after water wash for H_2O_2) to the stress before serially diluted for plating. For UV exposure, serially diluted cells were spotted to YPD before UV exposure. The plates were incubated in dark afterwards.

deletion of *TOR1*, *RAS2*, or *SOD2* (Figure 2.11), indicating that changes in TAG metabolism does not affect the function of these conserved CLS regulators. Intriguingly, deleting *TOR1* shortens the lifespan of both lipase-null and DGAT-deficient cells (Figure 2.11) but, as expected, protects those cells possessing the normal TAG metabolic capacity. We suggest that *tor1*Δ cells that survive on the caloric restriction pathway through chronological aging (Longo et al. 2012; Wei et al. 2009) need to tap into the energy depot of TAG. Without TAG biosynthetic enzymes or TAG hydrolytic lipases

perturbs this energy flux, thus resulting in early death of *tor1*Δ cells. In addition to *TOR1* and *RAS2*, we have also combined *tgl3*Δ and *sch9*Δ mutations. Deleting *SCH9*, the ribosome S6 kinase homologue, has been shown to activate the Rim15-Msn2/4 and superoxide dismutase (SOD) stress pathways and prolongs lifespan significantly (Fabrizio et al. 2001; Fabrizio et al. 2003). Our tests of the genetic interaction between *TGL3* and *SCH9* were inconclusive. Independent *tgl3*Δ *sch9*Δ isolates showed mixed results, ranging from longer CLS to synthetic sickness (Figure 2.14). The reason for the stochastic phenotypes is unclear.

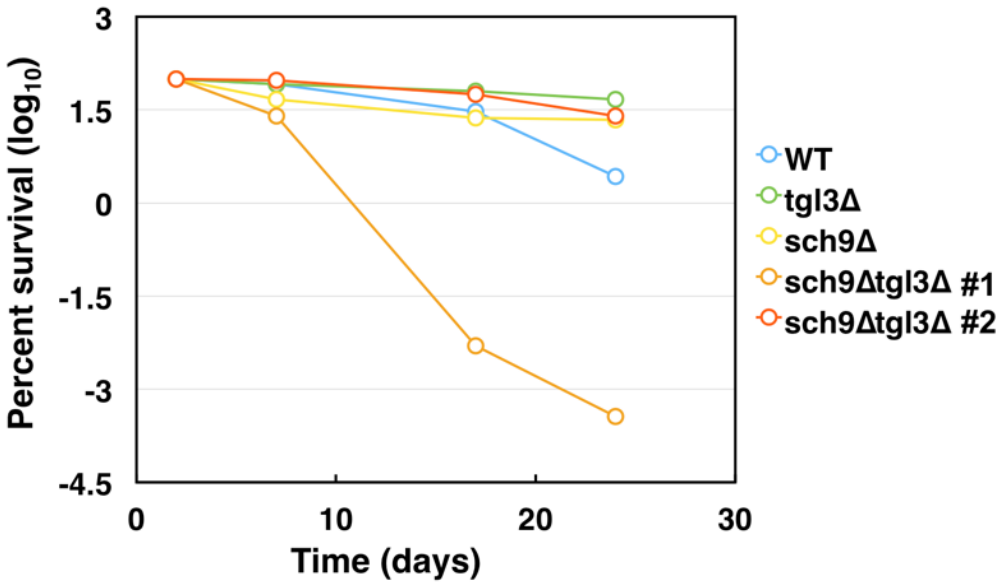

Figure 2.14 Combining *tgl3*Δ and *sch9*Δ null alleles caused stochastic growth defects. *SCH9* was deleted from *TGL3*$^{+}$ and *tgl3*Δ backgrounds for chronological lifespan assessment. Two independent *tgl3*Δ *sch9*Δ transformation colonies were isolated and tested. Both were $\rho+$, but one apparently was synthetic sick while the other exhibited normal growth and extended lifespan. Shown are representative results of two independent *SCH9* knockout attempts.

Taking into account the observations presented above as well as from previous reports, we hypothesize that TAG has a role in stress response that underlies the observed phenotypes in chronological aging. Firstly, TAG accumulates when yeast cells enter stationary phase in which nutrients are becoming progressively limited (Taylor & Parks 1979; Gray et al. 2004). Starvation and stress-induced TAG accumulation appears to be a widespread response in different organisms, including photosynthetic algae (Li et al. 2012; Çakmak et al. 2014; Pal et al. 2011; Vieler et al. 2012) and animals as well (Khatchadourian et al. 2012; Younce & Kolattukudy 2012; Lee et al. 2013). Dietary restriction has been suggested to prolong lifespan by eliciting cellular stress response (Sinclair 2005). Intriguingly, laboratory mice (Li et al. 2009) and developing *Caenorhabditis elegans* (Palgunow et al. 2012) have an increased body fat mass when subjected to dietary restriction. Secondly, wild yeast strains in general exhibit higher TAG content and longer chronological lifespan (Figure 2.1). Food shortage is a common environmental crisis in the wild, but rarely a relevant factor for lab strains. A systematic phenotypic and transcriptomic survey of wild and laboratory strains showed that the latter are less tolerant of many environmental stresses (Kvitek et al. 2008). Certain traits, including stress responses and high levels of TAG, might have lost during the domestication of *S. cerevisiae* in laboratory environments, in which the selection pressure for long-living, stress-tolerant stationary phase cells is low. It seems plausible that besides preserving energy to cope with uncertainties in food supply, the increased fat content in stressed cells may confer an additional, energy-independent function that helps sustain longevity.

The presumptive stress antagonized by TAG in post-mitotic cells remains to be identified. One candidate is fatty acid-solicited lipotoxicity (Schrauwen et al. 2010). Sequestering fatty acids in the form of TAG may prevent lipotoxicity that erodes replicative potential and chronological viability. Disabling TAG biosynthesis results in surplus fatty acids, which may arise from de novo synthesis, uptake from environment, or from lipolysis, that may disrupt membrane lipid homeostasis (Oelkers et al. 2000). Indeed, in an extreme situation where the ability to incorporate fatty acids to TAG and SE is altogether eliminated, yeast cells become hypersensitive to fatty acids and die with membrane hyper-proliferation (Petschnigg et al. 2009). Similarly, the fission yeast *Schizosaccharomyces pombe dga1*$^{+}$ and *plh1*$^{+}$ double knockout cells (equivalent to the *dga1*Δ *lro1*Δ strain of *S. cerevisiae*) also die upon entering stationary phase, and are hypersensitive to exogenous fatty acids during vegetative growth (Zhang et al. 2003). While this lipotoxicity model explains the early death phenotype of *dga1*Δ *lro1*Δ cells, total lipid analysis of our long-living fat cells failed to detect significant changes in free fatty acids or DAG (see, for example, Figure 2.8A). While we cannot rule out the possibility that a small but critical change in certain lipid species contributes more critically to lifespan extension, other hypotheses are worth considering.

One frequently cited cause of aging is mitochondrial dysfunction that also involves oxidative damages (Bonawitz & Shadel 2007). While subcellular compartmentalization confines TAG synthesis and storage to ER and lipid droplets, respectively, a number of reports have demonstrated physical association of

mitochondria with ER and LD (Barbosa et al. 2015), lending support for functional crosstalk between neutral lipid metabolism and mitochondria biogenesis (Haemmerle et al. 2011). Moreover, mitochondria also possess a type II fatty acid synthesis pathway (Hiltunen et al. 2009). Deleting enzymes within this pathway causes mouse embryonic lethality and yeast respiratory defects (Yi & Maeda 2005; Kastaniotis et al. 2004). Fatty acids trafficking between mitochondria and LD may help achieve mitochondrial lipid homeostasis. Importantly, mitochondria are a major source for reactive oxygen species. Free radicals that would otherwise escape from mitochondria and cause pleiotropic cellular damages might enter LD and attack the fatty acyl chains of the storage TAG molecules (Niki 2009). It is possible that the high density of peroxidated fatty acids in LD facilitates crosslinking of neighboring radicalized molecules, hence terminating the vicious propagation of radicals. This “radicals sink” model appears to be consistent with the experimental findings presented above.

TAG metabolism and many aspects of cellular aging are conserved. It is thus possible that the cytoprotective role of TAG also exists in higher organisms. For example, Bailey *et al.* recently reported an anti-oxidant role of lipid droplets in the stem cell niche of *Drosophila* during neurodevelopment by limiting the levels of reactive oxygen species and inhibiting the oxidation of polyunsaturated fatty acids (Bailey et al. 2015). In transgenic mice, overexpression of DGAT1 in the skeletal muscle and heart increased intracellular TAG abundance as well as insulin sensitivity of the underlying animals (Liu et al. 2009; Liu et al. 2007). Similarly, deleting adipose triglyceride lipase (ATGL)

protected animals from high-fat diet-induced insulin resistance (Hoy et al. 2011). However, excessive TAG in heart muscle resulting from ATGL knockout also was associated with cardiac dysfunction (Haemmerle et al. 2011; Haemmerle et al. 2006). These transgenic animal studies underscore the complexity of mammalian metabolism and the interdigitating relationships between triglycerides (dietary, circulating, and in different tissues) and other nutrients. While the positive influence of intracellular TAG on chronological lifespan in yeast is reminiscent of the so-called obesity paradox in humans, that is, the overweight population has the lowest mortality under a number of medical conditions (Flegal et al. 2013; Lavie et al. 2015), we caution that the comparatively simple yeast may not be immediately applicable to the complex human system. An integrative strategy combining metabolomics, lipidomics, and transcriptomics of representative yeast strains will help elucidate the molecular basis of this novel function of TAG, which might provide a toolbox for a better understanding of the benefits of intracellular TAG in humans.

Materials and methods

Strains and media

Yeast strains used in this study are shown in Table 2.2. YPD medium contained 2% glucose (Sigma-Aldrich) (unless otherwise stated in the text), 2% peptone (BD Difco), and 1% yeast extract (BD Difco). SC medium (synthetic complete) contained 2% glucose, 5 g/l ammonium sulfate (Sigma-Aldrich), 1.7 g/l yeast nitrogen base without

amino acids or ammonium sulfate (BD Difco), and complete amino acids as described in (Murakami & Kaeberlein 2009). Auxotrophic nutrients were supplied at four-fold excess as recommended (Longo et al. 2012). Citrate phosphate buffering was done as described (Burtner et al. 2009). Rapamycin (Sigma-Aldrich) and paraquat dichloride (Fluka) were added from 10 μM and 250 mM stocks to SC medium to make final concentrations of 10 nM and 10 mM, respectively.

Yeast methods

Yeast transformation was performed using the lithium acetate method (Gietz et al. 1992). Deletion of *TGL3* and *TGL4* was described in (Li et al. 2012). To delete *DGA1*, PCR reactions using primers ATGTCAGGAACATTCAATGATATAAGAAGAAGGAAGAAGG AAGATCCCCGGGTTAATTAA and TTACCCAACTATCTTCAATTCTGCATCCGGTACCCC ATATTTATTCGAGCTCGTTTAAAC and template pFA6a-KanMX6 (W. Wei et al. 2007) were conducted. To delete *LRO1*, primers TATCCATATGACGTTCCAGATTACGCTGCTCAGT GCG*GCCGC*ATGTCAGGAACATTCAAT and GAATTTCGACGGTATCGGGGGGATCC ACTAGTTCTAGCTAGATTACCCAACTATCTTCAA were used with pBS1539 as the template to amplify *K. lactis URA3* gene as the selective marker (Markgraf et al. 2014). To delete *TOR1*, primers GAACCGCATGAGGAGCAGATTTGGAAGAGTAAACTTTTGAAATGAAGC TTGATATCGAAT and CCAGAATGGGCACCATCCAATATAATGTTGACATAACCTTTC TACGACTCACTATAGGGC were used with pBS1539 to amplify *K. lactis URA3*. For *RAS2* deletion, primers CCTTTGAACAAGTCGAACATAAGAGAGTACAAGCTAGTCGTCTGAAGC TTGATATCGAAT and ACTTATAATACAACAGCCACCCGATCCGCTCTTGGAGGCTTCTACG

ACTCACTATAGGGC were used to amplify *K. lactis URA3* on pBS1539. For *SOD2* deletion, primers TTCGCGAAAACAGCAGCTGCTAATTTAACCAAGAAGGGTGGTTGAAGCTTG ATATCGAAT and GATCTTGCCAGCATCGAATCTTCTGGATGCTTCTTTCCAGTTT ACGACTCACTATAGGGC were used to amplify *K. lactis URA3* on pBS1539. The PCR products were gel-purified for yeast transformation. Genomic PCR was used to verify the correct insertion. To overproduce Dga1p, a yeast genomic PCR product was co-transformed with *Not* I-linearlized pMK595 (Luo et al. 2010) for *ADH1*-controlled expression (pMK595-*DGA1*). A second multicopy *DGA1* overexpression plasmid with *DGA1* under its own promoter control (pMK595 P_{DGA1}-DGA1) was constructed similarly, except that the *DGA1* promoter (961 bp) was included in the transforming PCR DNA, using primers ATCCATATGACGTTCCAGATTACGCTGCTCAGTGCGGGTAAAGAATCTAAA TCGAGCTAC and ATCGGGGGGATCCACTAGTTCTAGCTAGAGCGGCCTAGATAGGTAC AATCGACTTAAAGC.

The *tgl3*Δ */tgl3*Δ diploid strain yWH74 was generated by first transforming yXL004 with YCp50-HO (Herskowitz & Jensen 1991) to induce mating type switch and subsequently spontaneous mating of cells in the same colony. Homozygous diploid cells were identified by their inability to mate as either a MATa and MATalpha strain. Diploid cells were then grown in YPD for two days to allow for the loss of YCp50-HO, resulting in 5-FOA resistant, *ura3*$^{-}$ cells.

For growth curve analyses, yeast cells were seeded at an initial concentration of 0.1 OD_{600} in 150 μl of YPD medium in 96-well plates with biological and technical duplicates. The plates were examined by measuring OD_{630} every 30 minutes via a BioTex PowerWave XS plate reader until cells reached saturation. The machine was programmed to shake at the high-speed setting and to control temperature at 30°C.

Lifespan analyses

Chronological lifespan was measured by the outgrowth method as described in (Murakami & Kaeberlein 2009). Briefly, yeast from stab cultures were inoculated to YPD broth and grown at 30°C overnight or until late log phase. Cultures were then diluted into 5 ml SC medium at 0.1 OD_{600}. The seeded cultures, in 15-ml glass tubes with a loose metal cap, were incubated in a rotator drum at 30°C. At selected time points, 5 μl of stationary phase cultures were sampled out and mixed with 145 μl of fresh liquid YPD in a 96-well plate. The plates were sealed with parafilm to prevent evaporation, and incubated in the BioTex PowerWave XS plate reader. Cell density (OD_{630}) was monitored every 30 minute for 48 hours. Growth curves, doubling times, and survival fractions were calculated according to (Murakami & Kaeberlein 2009). To compare the quantitative differences in lifespan of different strains, the time by which each culture reached 10%, 1%, and 0.1% survival fractions was obtained from three independent survival curves. The cultures which survived beyond 30 days before reaching the specified survival fractions were not included in the statistical calculation and represented as >30 days.

For spot assays, stationary phase cultures at selective time points were adjusted to 1 OD_{600} with sterile water in 96-well plates and ten-fold serially diluted. 5 μl of cells from each well were spotted to a YPD plate and grown at 30°C for two days. The culture viability was quantified by counting visible colonies at the most diluted spot. The number of colonies multiplied by the dilution factor of that spot was regarded as the viability. This method was adapted from the Tadpole assay as described in (Welch & Koshland 2013).

Replicative lifespan was performed according to previously described (Steffen et al. 2009) by counting number of progeny produced by 60 – 90 virgin cells from young mother of each strain. Daughter cells were removed every 90 minutes by a micromanipulator. The lifespan analyses were performed by using R software, version 3.0.3 with survival and KMsurv packages. Breslow test was used for statistic analysis.

Lipid analysis and Nile red staining

Total lipid extraction was conducted essentially as described before (Zhang et al. 2003) with modifications. Briefly, 3 OD_{600} cells from selected time points were harvested by centrifugation at 5,000 rpm for 5 minutes at room temperature, followed by washing once with 1 ml water, and were kept at -80°C if lipid extraction was not done immediately after cell collection. To extract total lipids, cells, if frozen, were removed from the freezer and mixed directly with 300 μl of glass beads (425-600 μm, Sigma-Aldrich) and 1 ml of chloroform : methanol (17:1, v/v) (JT Baker) by vortexing twice for

90 seconds at 4 °C. The mixtures were briefly spun and the supernatant was moved to a new glass tube. The remaining cell debris and glass beads were vortexed with an additional 1 ml of chloroform : methanol (2:1, v/v). The supernatant was collected as above and pooled with the previous fraction. 1 ml of 0.2 M phosphoric acid and 1 M KCl, was added to the pooled organic fraction and vortexed vigorously for 30 seconds, and spun at 3,000 rpm, 4°C for 5 minutes to separate the organic and aqueous phases. The chloroform phase at the bottom was collected and dried under nitrogen gas. This lipid extract served as the total lipid fraction. To purify TAG, total lipids were developed by thin-layer chromatography (TLC) on a G60 silica plate (EMD Chemicals). The mobile phase was composed of petroleum ether (35 – 60°C, Macron) : diethyl ether (JT Baker): acetic acid (JT Baker) = 80: 20: 1 (v/v/v). Following development, the TLC plates were briefly stained with iodine vapor to reveal the position of TAG. Spots co-migrating with a TAG control (olive oil, Dante) were isolated and converted to fatty acyl methyl esters (FAME) by reacting with 1 ml of 1 N Methanolic HCl (Sigma-Aldrich) at 80°C for 25 minutes (C Benning 1992). A universal internal control of 5 μg of pentadecanoic acid (Sigma-Aldrich) was included in all samples for FAME derivatization and gas chromatography (GC). 1 ml of 0.9% NaCl was added to stop the FAME reaction, followed by the addition of 1 ml of hexane, and vortexed for 30 sec to extract FAME. Centrifugation at 3,000 rpm for 5 min at 4°C was conducted before the hexane layer was aspirated to another glass tube, and the volume reduced to 30 μl under nitrogen blowing. 2 μl of the FAME in hexane was injected to a gas chromatography system (Agilent Technology, 7890A) for quantification.

To visualize lipid droplets in yeast cells, approximately 0.5 OD_{600} cells were collected by centrifugation (14,000 rpm for 1 min in a microfuge) and washed once by 1 ml TE buffer (pH 7.4). Cell pellets were suspended in 100 μl of TE buffer and stained with 1 mg/ml Nile red in the presence of 3.7% formaldehyde for concomitant fixation, and let sit in the dark for 20 min. Cells were collected again by microcentrifugation and re-suspended in 100 μl TE buffer and stored in the dark for no more than two days. For microscopy, an Olympus BX51 station with a Exfo X-cite 120 UV light fixture and a DP30-BW CCD camera were used. A GFP filter was used for lipid droplet fluorescence detection. For semi-quantitative comparison of lipid droplets, a fixed exposure (typically 2 seconds) for fluorescence was applied to all samples.

Sporulation and mating analysis

Sporulation efficiency was determined by microscopically examining the percent of diploid cells forming asci. Overnight YPD cultures of diploid strains were transferred to PSP2 medium (Potassium phthalate (Sigma-Aldrich) 8.3 g/l, yeast extract 1 g/l, 1.7 g/l yeast nitrogen base without amino acids or ammonium sulfate, ammonium sulfate 5 g/l, potassium acetate 10 g/l, pH 5.4 at 0.1 OD_{600} and grown at 30°C under vigorous shaking (200 – 250 rpm). After 24 hours, cells were harvested by centrifugation (14,000 rpm, 30 sec in a microfuge), washed once with sterile water, and re-suspended in 1 ml SPM medium (potassium acetate 3 g/l, raffinose 0.2 g/l). Cultures were shaken vigorously at 200 – 250 rpm at 30°C for 48 – 72 hours. A small amount of cells were removed from the culture, spun, and suspended in 1 mg/ml DAPI (4,6-diamidino-2-

phenylindole) in a mounting medium (1 mg/ml p-phenylenediamine, 0.9% glycerol, 2.25 μg/ml DAPI). Percent of cells forming asci with four DAPI foci (i.e., four spores) were counted.

Mating efficiency was quantified by mixing 0.1 OD_{600} of "tested" strains with 0.5 OD_{600} of tester strains of the opposite mating type (227a or 70α), all in early log phase, in 1 ml of YPD. Cell mixtures were let sit at 30°C for 5 hours. The tested and tester stains were also incubated separately as the negative control. Cells were washed once with sterile water and plated on SD medium (2% glucose, 1.7 g/l nitrogen base with amino acids or ammonium sulfate, 5 g/l ammonium sulfate, 20 g/l agar). Mating between the tested and tester strains generated prototroph diploid cells that were able to form colonies on the SD medium plate.

Wild strains segregation

The strains B454, B756, B779, B359, B370, B357 and B390 were segregants of isolates collected in the wild (see Table 1 for source and reference). In order to generate isogenic haploid strains, the heterozygous wild isolates were sporulated and self diploidized due to homothallism. We randomly selected one of the four homozygous segregants from each tetrad. Next, strains were made heterothallic via removal of the HO gene, using homologous gene replacement with either a Hgh cassette (pAG32) (Goldstein & McCusker 1999) (strain B454 due to a natural kanamycin resistance) or a KanMX6 cassette (pFA6a) (Wach et al. 1994) (strains B756, B779, B359, B370, B357 and

B390). Transformed strains were sporulated and dissected to verify 2:2 segregation of either hygromycin or kanamycin resistance. One MATa and MATalpha haploid transformant was retained from each strain. Proper integration at the *HO* locus was verified via PCR. Strain B653 was obtained from John McCusker.

Table 2.2 yeast strains used in this study

Strains	**Relevant genotypes**	**Sources or references**
yMK839	*MATa leu2-3 trp1 ura3-52*	Siliciano & Tatchell 1984
yXL004	From yMK839 *MATa leu2-3 trp1 ura3-52 tgl3Δ ::TRP1*	Li et al. 2012
yXL001	From yMK839 *MATa leu2-3 trp1 ura3-52 tgl4Δ ::TRP1*	Li et al. 2012
yXL005	From yMK839 *MATa leu2-3 trp1 ura3-52 tgl3Δ ::KanMX; tgl4Δ ::TRP1*	Li et al. 2012
yXL172	From yMK839 *MATa leu2-3 ura3-52 dga1Δ ::KanMX; lro1Δ ::URA3*	This study
yWH001	From yMK839 *MATa leu2-3 trp1 ura3-52 tgl3Δ ::TRP1; dga1Δ ::KanMX; lro1Δ ::URA3*	This study
yXL023	From yMK839 *MATa leu2-3 trp1 ura3-52 pMK595 [2μ URA3]*	Li et al. 2012
yXL041	From yMK839 *MATa leu2-3 trp1 ura3-52 tgl3Δ ::TRP1 pMK595 [2μ URA3]*	This study
yXL183	From yMK839 *MATa leu2-3 trp1 ura3-52 pMK595-DGA1 [2μ URA3]*	This study

Table 2.2 (cont'd)

yWH083	From yMK839 *MATa leu2-3 trp1 ura3-52 pMK595 P_{DGA1}-DGA1 [2μ URA3]*	This study
yXL180	From yMK839 *MATa leu2-3 trp1 ura3-52 tgl3Δ ::TRP1 pMK595-DGA1 [2μ URA3]*	This study
yWH087	From yMK839 *MATa leu2-3 trp1 ura3-52 tgl3Δ ::TRP1 pMK595 P_{DGA1}-DGA1 [2μ URA3]*	This study
W303a	*MAT*a *leu2-3,112 trp1-1 can1-100 ura3-1 ade2-1 his3-11,15*	
BY4742	*MAT*α *his3Δ 1 leu2Δ 0 lys2Δ 0 ura3Δ 0*	
yWH47	BY4742 with *tgl3Δ ::URA3*	This study
EJ72	*MATa/a gal⁻ trp1 leu2 ura3-52 his4*	Siliciano & Tatchell 1984
yWH036	EJ72 with *tgl3Δ ::URA3/TGL3*	This study
yWH74	EJ72 with *tgl3Δ ::TRP1/tgl3Δ ::TRP1*	This study
70α	*MATa thr3 met*	Clemons et al. 1994
227a	*MATa lys1*	Clemons et al. 1994
yXL189 (B454α ; clinical sample)	*MAT*α *ho::Hygromycin*	This study. Haploid isoform of YJM454 from J. McCusker
yXL190 (B653α ; clinical sample)	*MAT*α *ho::hisG lys2 gal2*	
yXL191 (B756α ; clinical sample)	*MAT*α *ho::KanMX6*	This study. Haploid isoform of YJM450 from J. McCusker
yXL192 (B779α ; clinical sample)	*MAT*α *ho::KanMX6*	This study. Haploid isoform of YJM326 from J. McCusker

Table 2.2 (cont'd)

yXL193 (B359α ; vineyard)	*MAT*α *ho::KanMX6*	This study. Haploid isoform of YCD51-4 from Burgundy region of France, 1948
yXL194 (B370α ; vineyard)	*MAT*α *ho::KanMX6*	This study. Haploid isoform of M5-2 from Italy in 1993 by R. Mortimer
yXL195 (B357α ; oak exudate)	*MAT*α *ho::KanMX6*	This study. Haploid isoform of YPS1009-2 from Mettler's Woods, New Jersey in 2000 by P. Sniegowski
yXL196 (B390α ; oak exudate)	*MAT*α *ho::KanMX6*	This study. Haploid isoform of YPS1000-1 from Mettler's Woods, New Jersey in 2000 by P. Sniegowski
yXD188	From yMK839 *MATa leu2-3 trp1 ura3-52 tor1Δ ::URA3*	This study
yXD189	From yMK839 *MATa leu2-3 trp1 ura3-52 ras2Δ ::URA3*	This study
yXD190	From yMK839 *MATa leu2-3 trp1 ura3-52 sod2Δ ::URA3*	This study
yXD191	From yMK839 *MATa leu2-3 trp1 ura3-52 tgl3Δ ::TRP1; tor1Δ ::URA3*	This study
yXD192	From yMK839 *MATa leu2-3 trp1 ura3-52 tgl3Δ ::TRP1; ras2Δ ::URA3*	This study
yXD193	From yMK839 *MATa leu2-3 trp1 ura3-52 tgl3Δ ::TRP1; sod2Δ ::URA3*	This study

Table 2.2 (cont'd)

yXD200	From yMK839 *MATa leu2-3 trp1 ura3-52 dga1Δ ::KanMX; lro1Δ ::TRP1*	This study
yXD201	From yMK839 *MATa leu2-3 trp1 ura3-52 dga1Δ ::KanMX; lro1Δ ::TRP1; tor1Δ ::URA3*	This study
yXD202	From yMK839 *MATa leu2-3 trp1 ura3-52 dga1Δ ::KanMX; lro1Δ ::TRP1; ras2Δ ::URA3*	This study
yXD203	From yMK839 *MATa leu2-3 trp1 ura3-52 dga1Δ ::KanMX; lro1Δ ::TRP1; sod2Δ ::URA3*	This study

Acknowledgements

We thank Zhiying You for assisting statistical analysis; Eve Gardner, Jaikishan Prasad, Rachel Green, Hao Nguyen, Jan Stoltin, and Rebecca Roston for technical assistance; and Kelly Tatchell and Paul Siliciano for tracing the history of yMK839 and EG123. Barbara Sears, Astrid Vieler, and Neil Bowlby are thanked for their advice on TAG analysis. We acknowledge Erik Martinez-Hackert, David Arnosti, Tom Sharkey, and John Wang for their critical reading and suggestions for this manuscript.

CHAPTER III:

Triacylglycerol accumulation affects endogenous reactive oxygen species

Abstract

Triacylglycerol (TAG) is one of the most common neutral lipids found in all eukaryotes. The previous Chapter shows evidence that TAG, despite its main function of storing and controlling energy, has an energy-independent role in lifespan control in the budding yeast *Saccharomyces cerevisiae*. High levels of intracellular TAG abundance prolongs lifespan independent of the nutrient awaits delineation pathway and dietary restriction; however, the detailed molecular mechanism by which TAG extends lifespan awaits delineation.

While it remains a hotly debated issue regarding the underpinning of cellular and organismal senescence, accepted pro- and anti-aging factors support the mitochondrial free radical theory of aging, that is, aging is a result of the accumulation of oxidative damage caused by free radicals originating primarily from mitochondria. If true, this theory predicts that enhancing the cellular ability to resist or to prevent oxidative damages leads to lifespan extension. In light of this mitochondria free radical theory of aging, and of our previous findings for the pro-longevity function of intracellular TAG, we set out to develop a fluorescence-based quantitative approach for the comparison of cellular ROS levels. Using this approach, we demonstrate for the first time an inverse correlation between the cellular levels of TAG and reactive oxygen species (ROS). Fluorescent microscopy further reveals unique distribution patterns of ROS in the stationary-phase cells that are reminiscent of lipid droplets, the primary storage organelles for TAG. Together, these data are consistent with the role of TAG to function

as a sink that dampens the toxicity of ROS. Further studies to test this Radicals Sink model will be discussed.

Introduction

Aging is a complex condition whereby the biological functions of organisms progressively decay over time (Harman 2003). Many studies have discovered lifespan determinants, such as genomic instability, telomere length, and deregulated nutrient sensing that function in most organisms (López-Otín et al. 2013). An organisms' lifespan is controlled by two main factors: genetic (the programmed factors) and environment (the damaged factors) (Jin 2010). Typically, two criteria are used to compare both inter- and intraspecies lifespans: the mean lifespan, which describes the average age of individuals in a certain population, and the maximum lifespan, which refers to the longest lifespan a species can reach (Sanz & Stefanatos 2008). Between these two criteria, most researchers agree that the maximum lifespan is in fact the true longevity factor; this is because while a longer mean lifespan without a higher maximum lifespan demonstrates that the individual organisms are healthier on average, they do not live any longer (Sanz & Stefanatos 2008). Therefore, it is preferable in aging research to focus on conditions that can extend the maximum lifespan of a species.

Genetic and molecular tools have helped uncover many factors for lifespan control, as well as different theories for the mechanisms underlying aging. Among these, the mitochondrial free radical theory of aging (MFRTA), introduced by Harman in 1972,

is still considered one of the most influential determinants in the history of aging (Harman 1972). This theory suggests that aging is the result of the long-term accumulation of toxic free radicals and/or their by-products (Harman 1972; Harman 1956). These free radicals are mostly produced during normal cellular respiration in mitochondria (Harman 2003; Kushnareva et al. 2002; Miwa & Brand 2005). Importantly, the oxygen molecules utilized in the respiratory process are not always completely reduced into water. Approximately 0.1%-4% of the consumed oxygen has a partial reduction; this results in reactive oxygen species (ROS or, if produced from mitochondria, mtROS), highly aggressive molecules such as hydrogen peroxide and singlet oxygen (Boveris & Chance 1973). The ROS are very unstable and tend to react with nearby macromolecules such as proteins, DNA, or lipids, leading to oxidative damages (Harman 2003). If cells fail either to repair or to rid this impairment, the defective molecules can accumulate and become a senescent factor. Cells also have another protective mechanism to intercept ROS through antioxidants or anti-free radical enzymes; these molecules have the specific ability to seize radicals and either turn the ROS (or the antioxidant-ROS complex) into less deleterious species or, in some cases, neutralize the ROS (Halliwell 2007).

Although MFRTA is well supported by many studies, the theory garners some skepticism. For instance, even though the quantification of mtROS is shown to correlate with maximum lifespan in many organisms (Barja et al. 1994; Sohal et al. 1989; Ku & Sohal 1993), the results are inconsistent. Some animals, such as pigeons, produce high

levels of ROS and a high amount of oxidative damage but display higher maximum lifespans compared to other animals of the same size (Ku & Sohal 1993). Additionally, many studies have shown that the overexpression of anti-oxidative enzymes or treatment with exogenous antioxidants does not always result in longer lifespans (Magwere et al. 2006; Muller et al. 2007). Nonetheless, these findings do not entirely contradict MFRTA. It is known today that a simple modification in one small factor is not always sufficient to alter the maximum lifespan of an organism, which is considered the result of millions of years of evolution (Sanz & Stefanatos 2008). However, it is an undeniable claim that free radicals play a crucial role in pushing cell metabolisms that affect lifespan. Taking these reports together and the MFRTA, it is likely that long-lived organisms may require two important properties: less ROS production and a high resistance to oxidative damages.

Several recent reports demonstrate that mitochondria and lipid droplet (LD) can associate physically under physiological conditions (Shaw et al. 2008; Novikoff et al. 1980; Blanchette-Mackie & Scow 1983; Kalashnikova & Fadeeva 2006). These studies theorize that the physical contact between these organelles provides a channel to translocate metabolites; i.e., LD supplies hydrolyzed fatty acid to mitochondria for ß-oxidation, and mitochondria produces phospholipids for LD to expand (Shaw et al. 2008; Barbosa et al. 2015). Mitochondrial membrane lipids are also known as major oxidative damage site because mtROS is produced in abundance at complexes I and III of the electron transport chain, which is located on the mitochondrial inner membrane

(Kushnareva et al. 2002; Miwa & Brand 2005). It is critical that mitochondria can re-localize membrane components, as it suggests that mitochondria may use this function to dispose of lipids with oxidative damage to LD, which then may turn them into an inert neutral fat. The latest findings by Bailey et al. (2015) suggest that LD is critical for counteracting ROS, safeguarding the development of neural stem cells (Bailey et al. 2015). The authors also indicate that ROS-targeted unsaturated lipids can redistribute into LD where they are safely stored in hydrophobic goblets (Bailey et al. 2015). Although the underlying mechanism is still unknown, the existence of mito-LD channels suggests that TAG accumulation also serves to protect mitochondria. Interestingly, unsaturated fatty acids are prone to oxidation by free radicals. Indeed, the degree of mitochondria membrane fatty acid unsaturation has been reported to be negatively correlated with longevity of the underlying animals (Pamplona et al. 2002). Given these reports, the MFRTA, and our findings of the pro-longevity function of TAG, this Chapter aims to test a Radicals Sink model (Figure 3.1) that explains the molecular mechanism by which TAG preserves lifespan during chronological aging.

Results

Measuring cellular ROS with a new fluorescence approach

There are several approaches to measuring intracellular ROS, with each method measuring a certain type of ROS, such as hydrogen peroxide (H_2O_2), oxide anion (O^-), hydrochlorous acid (HOCl), and hydroxyl radical ($HO^\bullet$) (Halliwell & Gutteridge 2007). The 2',7' -dichlorofluorescein diacetate (DCFDA) is an inexpensive fluorescent probe

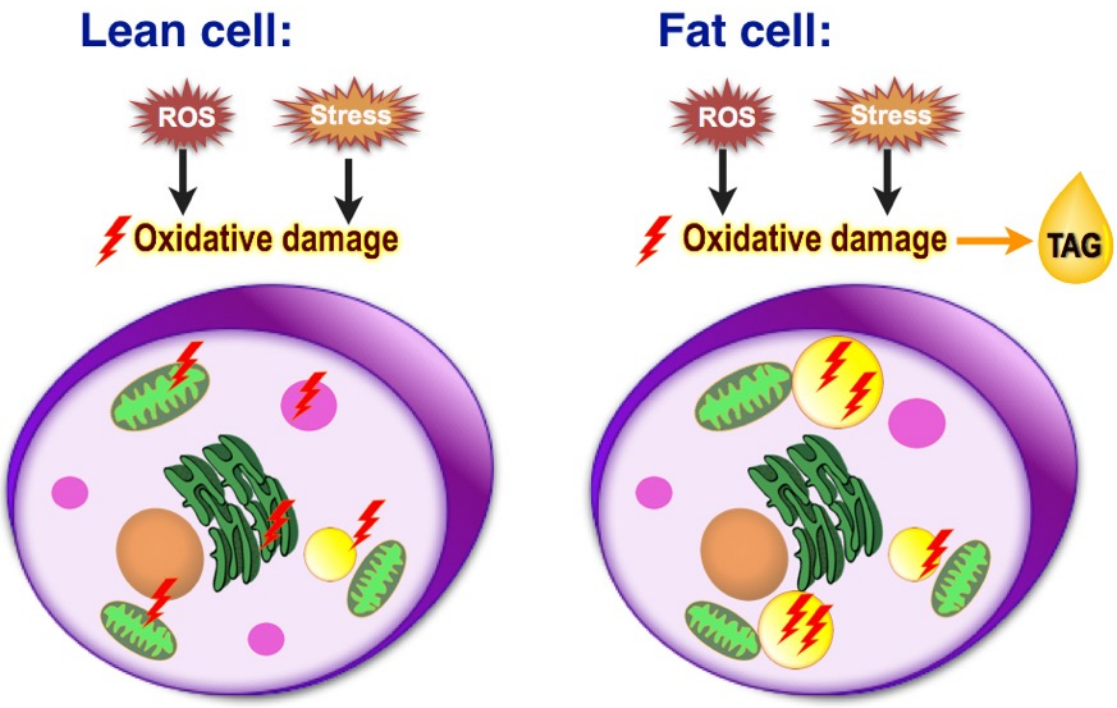

Figure 3.1 The proposed "radicals sink" model for the lifespan extension role of TAG. Stress and ROS (red lightening) can induce cellular damages of nearby biomolecules and organelles (e.g., mitochondria, endoplasmic reticulum, and peroxisome). Higher levels of TAG may attract ROS and other free radicals to lipid droplets and away from other biomolecules, leading to cellular protection and preservation of cell viability over time.

used in many studies and is compatible with various cell types (Hempel et al. 1999; Bass et al. 1983). The dye itself is non-fluorescent, but after its reaction with ROS it can produce strong green florescence (Figure 3.2A) (Burow & Valet 1987). DCFDA has been frequently applied for a quantification of intracellular H_2O_2 (Carter et al. 1994). However, recent evidence suggests that the DCFDA signal does not come from direct interaction with H_2O_2 (Kalyanaraman et al. 2012; Karlsson et al. 2010; Bonini et al.

2006). Instead, DCFDA can reduce various compounds such as HO•, HOCl, peroxynitrite (ONOO/ONOOH), and cytochrome c (Burkitt & Wardman 2001; Bonini et al. 2006; Hempel et al. 1999; Qian & Buettner 1999; Kalyanaraman et al. 2012). In the presence

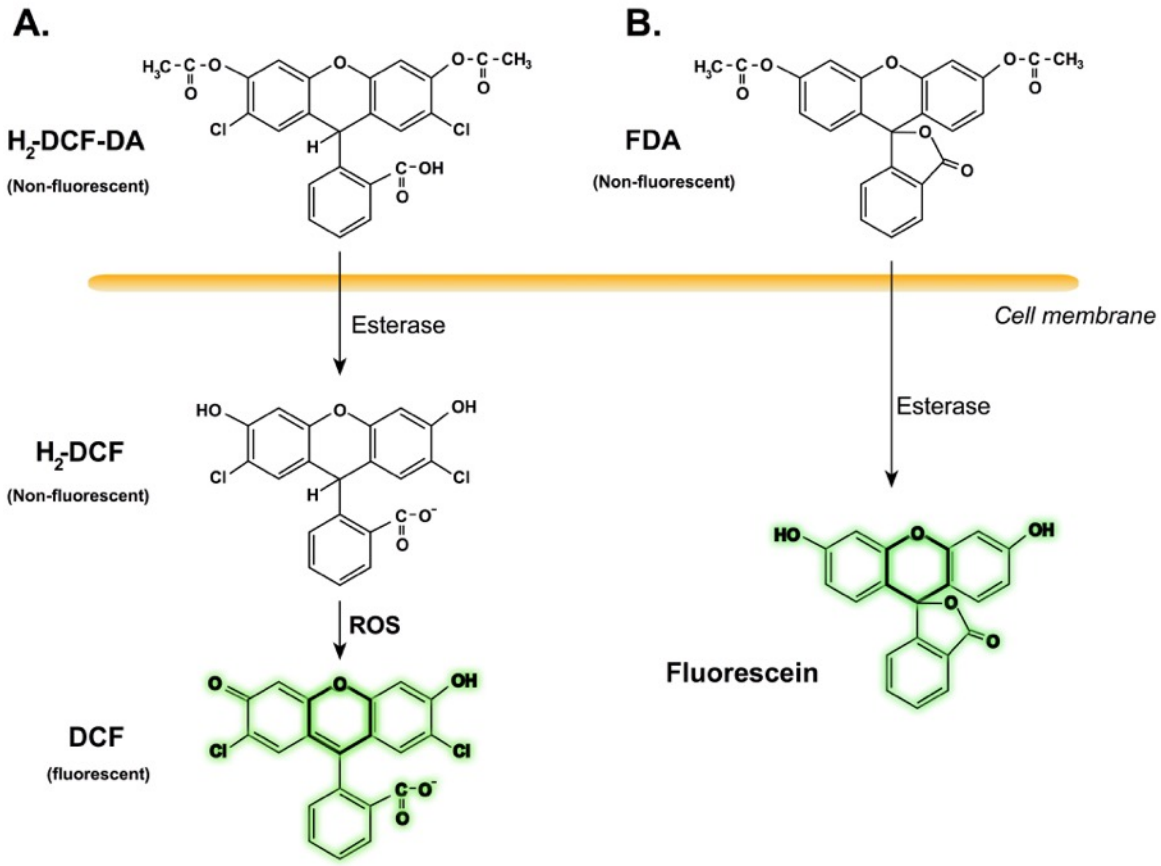

Figure 3.2 DCFDA requires two reactions to become fluorescent. (A) 2',7'-dichlorofluorescin diacetate (DCFDA) can freely cross the plasma membrane, which then can interact with an esterase to cleave two acetate groups. The product is impermeable but highly reactive with ROS such as hydroxyl and peroxyl. The oxidized form, 2',7'-dichlorofluorescein (DCF), is a fluorescene that can be detected by fluorescence spectroscopy with maximum excitation and emission spectra of 495 nm and 529 nm, respectively. (B) Fluorescein diacetate (FDA) has a similar mechanism to DCFDA, but after the reaction with an esterase it becomes fluorescent with maximum excitation and emission spectra of 490 nm and 514 nm, respectively.

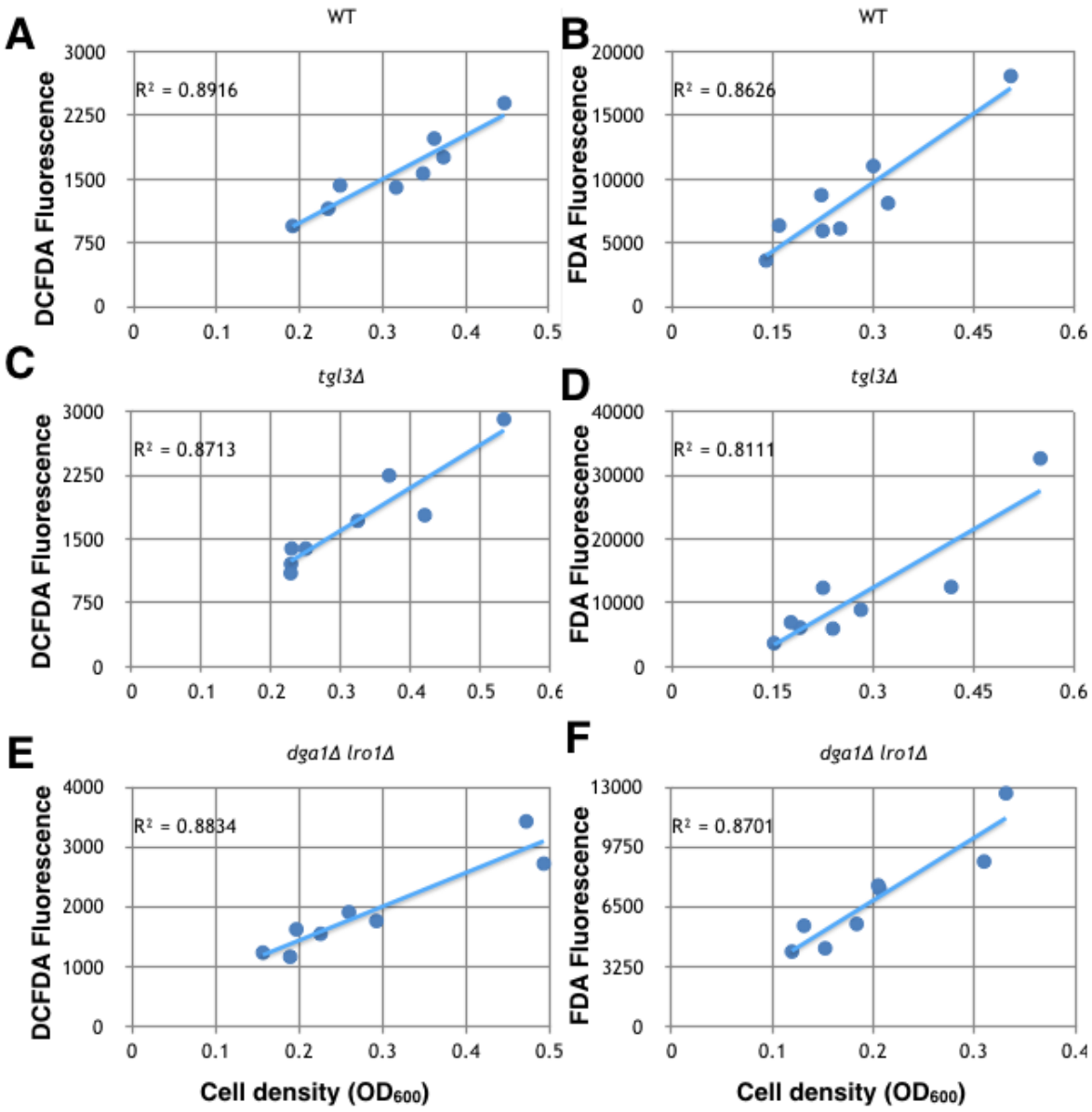

Figure 3.3 DCFDA and FDA emissions are linearly correlated with cell numbers. The three core budding yeast strains were diluted in water to the range of 0.1-0.5 OD_{600}, with DCFDA and FDA fluorescent signals then measured as stated in Materials and Methods. The data were obtained from 4 replications. (A.) yMK839 wild type (WT), DCFDA. (B.) WT, FDA. (C.) *tgl3*Δ, DCFDA. (D.) *tgl3*Δ, FDA. (E.) *dga1*Δ*lro1*Δ, DCFDA. (F.) *dga1*Δ*lro1*Δ, FDA.

of O_2 and light, the DCFDA intermediate (DCF) can undergo photoreduction to produce more superoxides (Marchesi et al. 1999). With appropriate controls and caution in data analysis, DCFDA can thus be used as an indicator for the amount of general ROS.

One concern for using DCFDA in an aging study is that the dye needs to be first modified by an esterase enzyme (Figure 3.2A) (Robinson et al. 1988). As a result, only live cells with active esterase can be measured. This requirement adds a challenge in the use of DCFDA to gauge ROS in aging cells, for the mortality increases over time and that different strains at a given time point of the experiment may exhibit different population viability. To ensure that differences in viability and metabolic capacity (i.e., the esterase activity) are calibrated, we incorporated fluorescein diacetate, FDA, into the DCFDA assay. FDA shares a similar structure and chemistry of activation with DCFDA, that is, FDA is converted to the fluorescein only after the very same esterase action that activates DCFDA (Figure 3.2B) (Braunstein et al. 1979). The difference is that FDA becomes fluorescent right after the reaction with esterase, which is ideal for differentiating live from dead cells, while dichlorofluorescein becomes fluorescent only after it is reduced by a radical (Sugita et al. 1986; Boyd et al. 2008). The ratio of the fluorescence derived from DCFDA to that from FDA thus affords a reliable means to compare the ROS levels of multiple samples, regardless of the percent of cellular viability.

To devise a quantitative DCFDA assay calibrated with FDA fluorescence, we first examined the dose responses of these two dyes. Figure 3.3 shows that with 0.1-0.5 OD_{600}

of cells, linear dose responses were obtained with 0.5-1.0 μg/ml of DCFDA, and 1.0-5.0 μg/ml of FDA. These number were in good agreement with literature (Rastogi et al. 2010; Crow 1997; Karlsson et al. 2010). We then tested the FDA and DCFDA fluorescence as a function of a increasing number of yeast cells (Figure 3.3). With 0.5

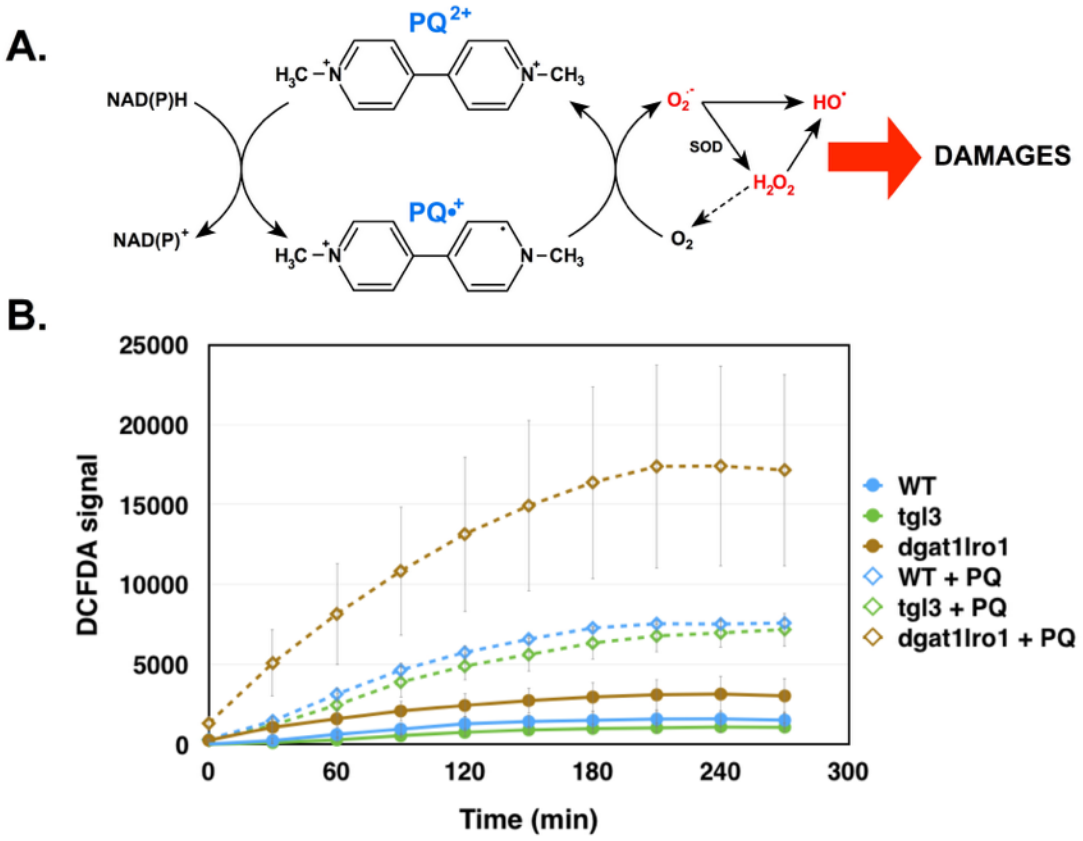

Figure 3.4 Thin cells are more sensitive to the paraquat treatment. (A.) The mechanism of paraquat dichloride (PQ). PQ can switch between two redox states, by which common cellular reducing agents such as NAD(P)H can create the reduced PQ, which can further oxidize oxygen molecules partially into oxygen radicals. The radicals can turn into $HO^{\bullet}$ or H_2O_2 by the enzyme superoxide dismutase (SOD). These ROS can damage nearby molecules. (B.) The yeast strains were grown in SC medium for 3 days, then either treated with 20 mM PQ or water (control). DCFDA was added to the final concentration of 0.1 μg/ml in the 100 μl samples. After the 30-min incubation, the microplates were read fluorescent signals every 30 min, 10 times with the kinetic mode.

μg/ml of DCFDA and 5.0 μg/ml of FDA, cell suspensions between approximately 0.2 and 0.45 OD_{600} reproducibly yielded fluorescence units proportional to the cell density. Based on these results, all the subsequent experiments were conducted with 0.25 OD_{600} cells and 0.5 μg/ml of DCFDA and 5.0 μg/ml of FDA.

In addition to the steady-state ROS, it is a common practice to trigger ROS production by the use of paraquat. Paraquat (PQ [1,1-dimethyl-4,4-bipyridinium dichloride]), is a herbicide widely used in over 120 countries (Wesseling et al. 2001). PQ cytotoxicity results from the production of ROS by a redox cycle by which NADPH is partially reduced by NADPH-cytochrome c reductase and O_2 is half-oxidized into a superoxide anion ($O^{\bullet -}$) (Figure 3.4A) (Fukushima et al. 2002; Day et al. 1999). Superoxide is a highly hazardous, unstable compound; it either quickly interacts with superoxide dismutase (SOD) to yield H_2O_2, or it degrades into $HO^{\bullet}$ (Fukushima et al. 2002). In addition to NADPH exhaustion, there are many targets that these radicals can injure, such as mitochondrial DNA, and cytoskeleton. However, most evidence strongly suggests that membrane lipids in mitochondria receive the majority of the attack by radicals produced under physical or induced conditions leading to prominent lipid peroxidation and membrane dysfunction (Bus et al. 1976; Shimada et al. 2009). Given the link between ROS and lipid peroxidation, we set out to use DCFDA to examine the relationship between ROS and TAG.

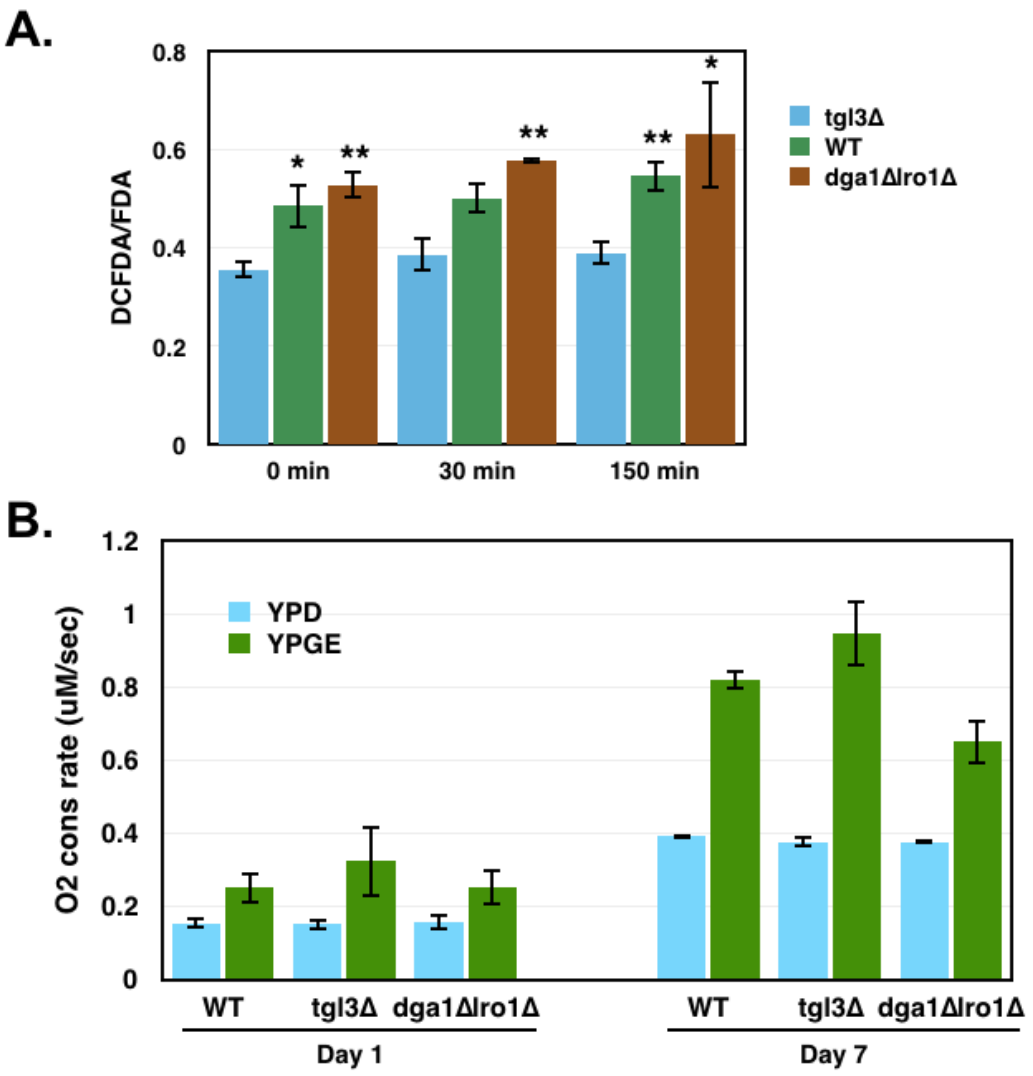

Figure 3.5 Intracellular TAG level has no significant effect to levels of oxygen consumption but is negatively correlated with ROS levels. (A.) The yeast strains, wild type (WT), high TAG (*tgl3*Δ), and low TAG (*dga1*Δ *lro1*Δ), were grown in the SC medium for 3 days; 20 mM paraquat were subsequently added to the cultures. Levels of ROS were quantified by the fluorescent technique at 0 (before paraquat addition), 30, and 150 min after the treatment. The measurement of DCFDA and FDA fluorescent signals were described in the Materials and Methods. Data were obtained from 4 independent experiments and analyzed with the ANOVA test. * $p < 0.05$; ** $p < 0.01$. (B.) The oxygen consumption of cells grew in logarithmic phase (24 hr after the inoculation) or in stationary phase (7-day-old culture) in either YPD or YPGE. Data were obtained from 2 biological and 3 technical replicates.

To first ensure that DCFDA can be used to quantify changes of ROS levels, 3-day old stationary-phase cells were exposed to PQ and DCFDA, and the fluorescence was measured every 30 min for five hours. Figure 3.4B shows that PQ-induced ROS elevation was readily detectable by changes of fluorescence derived form DCFDA and that, importantly, the *dga1*Δ *lro1*Δ lean cells showed significantly higher levels of ROS upon PQ treatment. Furthermore, the *dga1*Δ *lro1*Δ cells also exhibited slightly higher endogenous ROS even in the control, paraquat-free condition. We thus surmise that DCFDA is sensitive to ROS detection and quantitatively reliable under our experimental setting.

Intracellular TAG abundance inversely correlates with ROS levels.

Glucose, the most preferred energy source for yeast and many organisms, can be catabolized via two processes: anaerobic glycolysis (i.e., fermentation) in cytoplasm and aerobic respiration in mitochondria. Both ethanol and glycerol are non-fermentable carbon sources that require the full function of mitochondrial electron transport chains to be metabolized (Grauslund & Rønnow 2000; Ferguson & Borstel 1992). Therefore, the YPGE medium, in which glucose is replaced with ethanol and glycerol, affords a better tool for the assessment of mitochondrial function. Figure 3.5A shows that the oxygen consumption rates of all three strains were higher when grown in YPGE, consistent with the expectation that glycerol and ethanol forced cells to obtain energy from respiration. The rate of oxygen consumption was further increased in 7-day old stationary-phase cells. Intriguingly, the *dga1*Δ *lro1*Δ double knockout cells consumed oxygen at a lower

rate when compared with the wildtype or the *tgl3*Δ cells, even though these cells showed the highest level of PQ-triggered ROS production (Figure 3.4B). At least in YPGE cultures, the oxygen consumption rate appears to be inversely correlated to the TAG level, in particular in the stationary phase. It is tempting to speculate that cells with more TAG preserve the mitochondrial function better, hence a more robust rate of oxygen consumption.

Our radical sink hypothesis (Figure 3.1) posits that TAG intercepts mtROS that may otherwise attack other biomolecules key to cells to maintain viability in the stationary phase. Accordingly, cells with high TAG abundance (i.e., *tgl3*Δ) should have lower ROS than WT. On the other hand, the *dga1*Δ *lro1*Δ strain, which has almost no TAG, should display higher intracellular ROS. To test this hypothesis, the paraquat-induced ROS production from three selected yeast strains (WT, *tgl3*Δ, and *dga1*Δ *lro1*Δ) were examined. To this end, yeast cultures were grown in an SC medium until they reached the stationary phase (72 hr after the inoculation). Then, cells were treated with 20 mM PQ for 30 and 150 minutes. Results in Figure 3-4B demonstrate that before the paraquat treatment (time point 0), *tgl3*Δ cells had the lowest, while *dga1*Δ *lro1*Δ cells exhibited the greatest DCFDA/FDA level, consistent with the notion that TAG prevents the buildup of ROS produced under physiological conditions. In the presence of the ROS inducer paraquat, all three strains showed increased ROS over time (Figure 3.5A), with the *dga1*Δ *lro1*Δ cells having the highest concentration. We thus conclude that the

intracellular ROS level, steady state or induced by paraquat, correlates inversely with the TAG concentration.

It is known that the endogenous ROS amount is highly sensitive to the level of respiration (Lin et al. 2002; Barja et al. 1994; Halliwell 2009). To test whether the higher ROS detected in *dga1*Δ *lro1*Δ resulted from higher oxygen uptake, the three yeast strains were measured for their oxygen consumption rates during logarithmic phase (1-day-old) and in stationary phase (7-day-old). Figure 3.5B demonstrates that all three yeast strains consumed oxygen at a similar rate (light blue bars), suggesting that under the normal laboratory conditions, these three strains had similar overall metabolic rates.

Intracellular distribution of ROS is not random.

DCFDA is membrane permeable and can thus move freely across lipid membranes. However, after the actions of esterase and ROS, the fluorochrome DCF loses the ability to pass the phospholipid layer (Rota et al. 1999; Marchesi et al. 1999; Afri et al. 2004). If TAG can intercept ROS, as stated in the radical sink hypothesis, ROS may get buried inside LD, where TAG is located. Alternatively, lipid peroxidation from the mitochondrial membrane may get transferred to LD, as suggested by Bailey et al. (2015). Therefore, it is possible that the DCF signal may co-localize with or appear juxtaposed to the LD.

In the present study, we examined the DCF signal distribution in WT, *tgl3*Δ, and *dga1*Δ *lro1*Δ cells. Surprisingly, we found that ROS distribution in yeast cells is not

random; rather, the fluorescent signals showed different patterns including diffused cytoplasmic staining, aggregation into varying numbers of puncta, and co-localization with a disrupted plasma membrane (Figure 3.6B-G). These results suggest that radicals that can oxidize DCFH were concentrated at selective locations. We further quantified the proportion of each class of DCF distribution. Firstly, approximately 50% of wt and *tgl3*Δ cells and 70% *dga1*Δ *lro1*Δ cells showed diffused cytoplasmic staining. Secondly, the majority of the remaining wt and *tgl3*Δ cells exhibited DCF punctate signals. Conversely, the *dga1*Δ *lro1*Δ cells barely had any cells in this category. A closer look at the number of puncta further showed that the weight of such staining shifted up in *tgl3*Δ cells, that is, there were more three-and-more dots per cells than one- and two-dotted cells. These differential punctate staining patterns were reminiscent of the TAG level as well as the number of LD in each of these three strains. We suspected that these DCF dots overlapped with lipid droplets. Unfortunately, the use of Nile red to label TAG and LD failed to definitively reveal the identity of the DCF puncta due to leakage of fluorescence of Nile red and DCF. The optimal conditions for radicals and LD staining remain to be delineated. The last class of DCF fluorescence distribution was bright fluorescence associated with abnormal membranes. This class appeared to be highly enriched in the *dga1*Δ *lro1*Δ cells. It has been shown that yeast cells deprived of neutral lipid biosynthetic capability suffered from early death (Handee et al. 2016) and excessive membrane proliferation (Petschnigg et al. 2009). Again, the DCF staining was in excellent agreement of a phenotype of lean cells. Together, these results support the

major premise of the radicals sink model, that is, increased TAG level reduces the production of and damage from ROS.

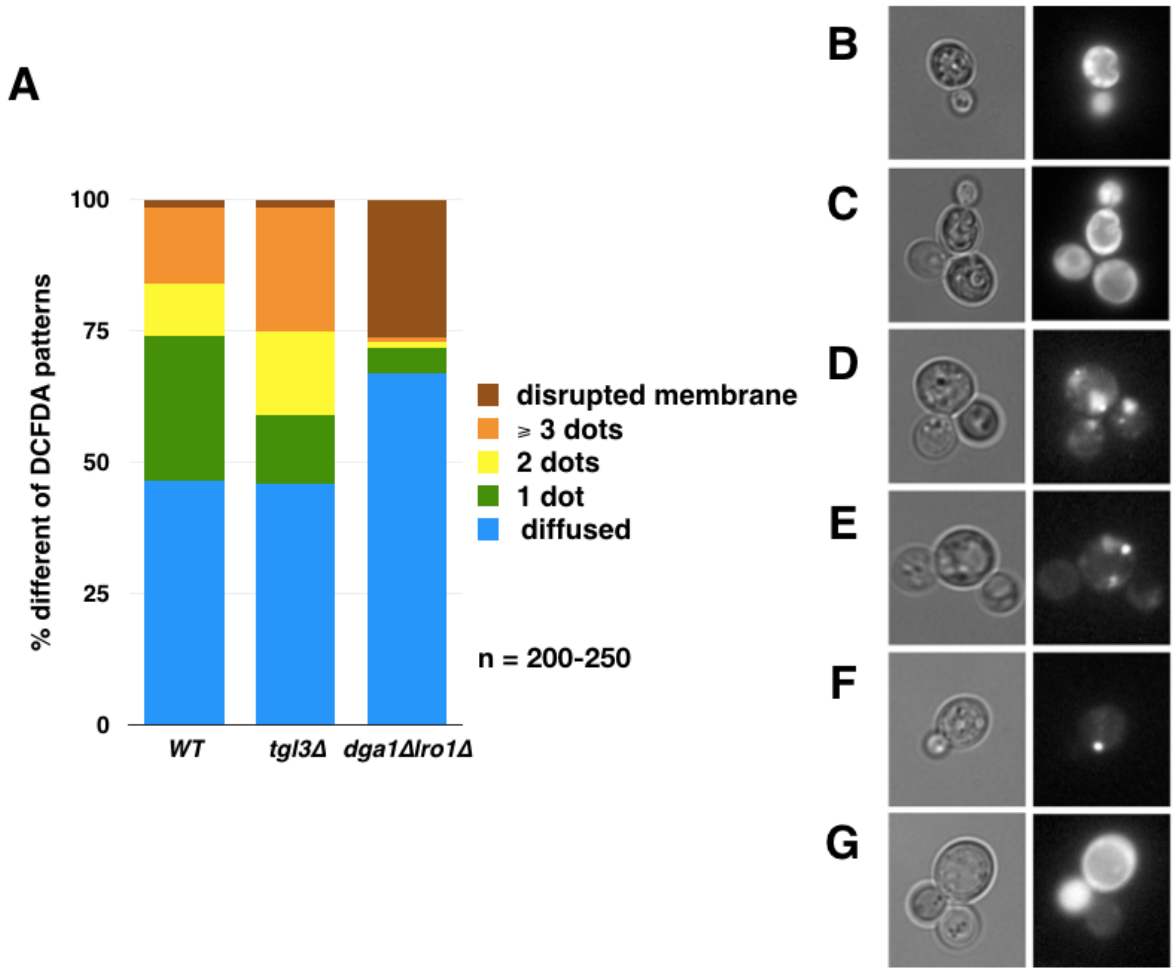

Figure 3.6 ROS distribution in cells is not random and likely linked to TAG abundance. The 3-day-old cultures in SC media were treated with 20 mM paraquat for 24 hr. Cells were then treated with DCFDA for 30 min before the microscopic characterization. (A) Percent distributions of fluorescent signals are classified into 6 groups: (B-C) disrupted membrane, (D-E) more than 3 dots of signals, (F) 1-dot signal, (G) dispersive signal in cytoplasm, and no signal. Data were obtained from two independent experiments; n = 200-250.

Discussion

The MFRTA states that one way to make an organism live longer is to minimize oxidative damages caused by ROS (Pérez-Campo et al. 1998). While this notion is widely tested with means that enhance the activities of antioxidants and anti-radical enzymes, evidence suggests that such approaches are usually insufficient to extend the maximum lifespan because organisms generally balance the antioxidant level just enough to guarantee their normal lifespan (Sanz & Stefanatos 2008). This argument is logical in terms of evolutionary processes, since cells do not waste extra energy to maintain high levels of antioxidants under either normal or stressed conditions (Sanz & Stefanatos 2008). The second strategy involves the reduction of oxidative damages. This process includes autophagy (Martinez-Lopez et al. 2015; Shaik et al. 2016) and protein degradation (Russell et al. 2007; Shringarpure & Davies 2002), both of which have been shown to play a role in lifespan regulation via the nutrient sensing pathways (Jiang 2016; Hansen et al. 2013; van Zutphen et al. 2014). Recent discoveries of the physical contact between mitochondria and LD have shed light on the function of lipid homeostasis, which is crucial for cellular stress response and lifespan control (Jägerström et al. 2009; Barbosa et al. 2015). Our lab has demonstrated that high TAG accumulation, either by knocking out TAG lipases or by overexpressing DGAT (i.e., the TAG biosynthesis enzymes), can significantly extend the maximum chronological lifespan of the budding yeast. The pro-longevity function of TAG is unlikely to rely on canonical nutrient sensing pathways or dietary restriction (Handee et al. 2016).

In this study, we present evidence that TAG may prolong yeast lifespan by decreasing oxidative damages (Figure 3.5 and Figure 3.6). Based on our ROS quantification results, the high TAG content in *tgl3*Δ cells is accompanied by lower ROS signals, whereas *dga1*Δ *lro1*Δ cells, which have essentially no TAG, contain significantly higher ROS amounts (Figure 3.5A). Together, these findings suggest a ROS-reduction ability of TAG. Moreover, there is a significant number of *dga1*Δ *lro1*Δ cells with apparently abnormal membrane that lit up with DCF (Figure 3.6A). Together these observations support our Radicals Sink model that TAG enhances survival of aging cells by reducing ROS the oxidative damages from ROS (Figure 3.1).

It is known that TAG does not accumulate in actively dividing yeast cells; instead, TAG level increases steeply after cells are shifted into unwelcome environments, including those with low carbon or nitrogen sources and high stress (Taylor & Parks 1979; Gray et al. 2004). These stress inducers commonly cause one notable feature, the alteration of membrane composition that is occasionally coupled with losing membrane potential (Knorre et al. 2013). The damages if occur at inner membrane of mitochondria at which the electron transport chain complexes are located may cause high ROS production. Some reports show that medium acidification or nitrogen starvation (the common stress found at stationary phase) causes mitochondria membrane damages and subsequently induce mitochondrial stress responses such as mitochondrial fusion-fission, mitochondrial adaptive ROS singing (MARS), mitochondrial DNA response, or program cell death (Knorre et al. 2013; Ždralević et al. 2012; Shadel 2014; Schroeder and Shadel

2014). Many genes and proteins related to these pathways are identified, but very little is known about roles of lipids or lipid homeostasis dealing with such stress. Intriguingly, one study reported that yeast cells treated with oligomycin (a mitochondrial ATP synthase inhibitor) or antimycin A (a respiratory chain complex III inhibitor) in stationary phase display lower ROS and better chronological lifespan (CLS) compared to adding these compounds in logarithmic-phase (Ocampo et al. 2012). This suggests that cells in logarithmic phase contain limited ability to detoxify ROS and oxidative damages. The remaining damages if exceed the capacity of initial ROS defense mechanisms, are carried over to stationary phase which sequentially can lead to shorten CLS (Ocampo et al. 2012). Conversely, cells in stationary phase may develop a mechanism for higher ROS tolerance (Ocampo et al. 2012). Even though there is no current evidence showing a function of TAG in ROS defense mechanisms, it is intriguing that higher TAG abundance is positively correlated with increased ROS resistance (Daum et al. 2007; Ocampo et al. 2012). Possibly, TAG is produced in stationary phase in order to serve as a ROS defense mechanism in addition to those of in logarithmic phase.

One outstanding question is how TAG counteracts oxidative stress. A possible mechanism of how TAG decreases oxidative stress is through the reduction of lipid peroxidation at the mitochondria or the nearby organelles, such as endoplasmic reticulum (ER) and the cell membrane (Pamplona 2008; Pamplona et al. 2002). It has been demonstrated that cells possess mechanisms to reshuffle these damaged lipids into the LD (Bailey et al. 2015). Although the details of the mechanism are currently

unknown, the research to date shows that mitochondria can redistribute their phospholipids into LD. This process is also similar to how ER cleans toxic fatty acids by converting them into TAG and moving into LD (Hapala et al. 2011; Kohlwein & Petschnigg 2007). It has been shown that after LD is generated from the ER, it has multiple contacts with all membrane organelles, including the ER, mitochondria, peroxisome, vacuole, lysosome, and plasma membrane (Wolinski et al. 2011; Shaw et al. 2008; Knoblach & Rachubinski 2015; Kohlwein et al. 2013). Therefore, it is possible that TAG accumulation after the stationary phase is a cytoprotective function that translocates damaged and toxic lipids into LD.

Blocking TAG lipases not only means that cells must use alternative ways to extract energy from neutral lipids (e.g., the engulfment to central vacuole); it also means that the communication with mitochondria flows in a single direction, that is, only PL (intact or damaged) can move toward LD, but no FFA are produced in LD (at least by the major TAG lipases) for further metabolism in mitochondria (Rambold et al. 2015; Barbosa et al. 2015). This leads to two possible consequences. Firstly, β-oxidation in the mitochondria matrix may be reduced. Therefore, mitochondrial ROS production is likely to decrease along with lipid peroxidation. This is consistent with other findings that show that cells tend to avoid glycolysis and Krebs's cycle when they are under stress (Österlund et al. 2013; Jewett et al. 2013). Instead, the metabolic flux is likely to shift to the pentose phosphate pathway, which favors more lipid production (Perl et al. 2011; Matsufuji et al. 2008). It is possible that this metabolic shift occurs in order to avoid

utilizing electron transport chains and to pump impaired lipids into LD (Lee et al. 2013; Girotti 1998). However, if this hypothesis is true, it cannot explain how cells extract energy from TAG in order to maintain normal cellular functions. Interestingly, a recent study shows that TAG can become hydrolyzed via a novel pathway that is independent to regular TAG lipases on the LD surface. This process involves the engulfing of LD into the vacuole and LD digesting inside the vacuole lumen (van Zutphen et al. 2014). Therefore, it is possible that cells may use this alternative mechanism to harvest energy from TAG without direct contact with the mitochondria. However, this hypothesis requires further investigations.

Dietary restriction (DR), or calorie restriction (CR), is a well-established means of prolonging lifespan in most organisms, and it also supports the MFRTA (Trifunovic et al. 2004; Lin et al. 2002; Schriner et al. 2005). Research has shown that animals that consume fewer calories produce lower ROS compared to the same species fed with a normal diet (Gredilla & Barja 2005). However, until now, it was unclear how DR regulates ROS production. One interesting fact about DR is that DR has no effect on naked mole-rats (*Heterocephalus glaber*), an exceptional organism that has extremely long lifespans but low anti-oxidation activity (Andziak et al. 2005; Buffenstein 2005; Andziak et al. 2006). Therefore, it seems that the MFRTA and DR cannot explain how naked mole-rats have developed a long-life phenotype. The naked mole-rat is a poikilotherm, meaning that it cannot control its body temperature like other mammals (Kramer & Buffenstein 2004). It has been shown that they have developed special

adipose tissues inserted among internal organs, and they have a high volume of LD closely attached to the mitochondria (Daly & Williams 1997). This assumes that LD can quickly supply fatty acids to mitochondria for more energy during winter. At the same time, if the radicals sink hypothesis is correct, the physical association between mitochondria and LD could serve as a channel for damaged lipids to transfer to LD. This could be the longevity secret of *H. glaber*.

In summary, aging is a complicated phenomenon that cannot be ascribed to only a single factor. Most studies on aging theories, including MFRTA, can predict certain aging mechanisms, but there are exceptions left to explore. The evidence that TAG can potentially counteract ROS-initiated damages opens a new perspective on how lipid homeostasis can play a critical role in lifespan regulation. However, many questions still remain. In addition, it is unknown if the same mechanism is present in higher eukaryotes. Nevertheless, our findings may provide a deeper understanding of how mammals age and may lead to more effective human health care.

Materials and methods

Yeast methods, media, and reagents

The yeast strains, yMK839 wild type, *tgl3*Δ, and *dga1*Δ *lro1*Δ, were derived from Handee et al. 2016 (also listed in Table 2.2). The preparation of YPD and SC media is described in the Materials and Methods section of chapter 2. YPGE medium is composed of 2% (w/v) peptone (BD Difco), 1% (w/v) yeast extract (BD Difco), 1% (v/v) glycerol

(J.T.Baker), and 1% (v/v) ethyl alcohol (Koptec-VWR). Paraquat dichloride (Fluke) was diluted from 100 mM stock (in water) to the described media. The fluorescent dye stocks were made from dissolving DCFDA (Sigma-Aldrich) powders in ethyl alcohol to 10 mg/ml, and FDA (Sigma-Aldrich) in DMSO (J.T.Baker) to 0.5 mg/ml. The dyes were allocated into small tubes, kept in -80ºC, and sealed with aluminum foil to protect from light. Yeast cultures were prepared by the standard yeast protocol (Sherman 2003). The newly formed yeast colonies are obtained from stab cultures preserved in -80˚C by streaking them on a YPD agar plate. Colonies are generally developed after 48-hr incubation at 30ºC. A single colony from each strain is randomly selected and cultivated overnight in 3 ml YPD medium in 15 ml glass tubes. Finally, the cultures are diluted 100 times to the experimental media (SC, YPD, or YPGE). After 72-hour incubation (otherwise stated in the text), the cultures are ready for further analysis.

Fluorescent spectroscopy

For fluorescent measurement, the DCFDA and FDA stocks were diluted into working solutions in sterile water briefly before loading into a 96-well plate. Final concentrations of DCFDA and FDA were 0.5 μg/ml and 5 μg/ml, respectively. Cell samples were diluted into 0.2 OD_{600}. The combined volume of cells and the dye is 100 μl in each well. Sample plates were prepared at room temperature with dim surroundings, then tightly sealed with aluminum foil to minimize light and oxygen exposure. After 30-min incubation, the fluorescent signals were read by Tecan Infinite M1000 Pro

Microplate Reader, with the gain setting at 150 UV, the excitation at 495 nm, and emission at 535 nm.

To visualize DCFDA signals in yeast cells, approximately 0.5 OD_{600} cells were harvested and washed with TE buffer (pH 7.4). Cells were incubated with 0.5 μg/ml DCFDA in the dark at room temperature for 30 min, then quickly viewed under a fluorescent microscope with a GFP filter (500- 550 nm). An Olympus BX51 station with a Exfo X-cite 120 UV light fixture and a DP30-BW CCD camera were used. Approximately 200-250 cells from each condition were recorded and classified twice by one researcher.

Oxygen consumption measurement

The oxygen consumption was measured by a Clark oxygen electrode (model YSI 5331), with a probe from Yellow Springs Instrument. The rate of oxygen uptakes in the function of time were recorded by the oxygen monitor (model 53000). Sample conditions were described in figure legends. During the measurements, the ice-cold buffer (100 mM HEPES-KOH, 24 mM KCl, pH 7.4) was added periodically to the samples to increase O_2 in the solutions. All experiments were conducted at room temperature. Data were obtained from 3 biological and 3 technical replications.

Data and statistical analyses

The correlation between fluorescent dyes and cell numbers was computed by Numbers, version 3.6.2 (Apple Inc.). The oxygen consumption rate and ROS levels were analyzed by a factorial ANOVA test by SAS, University Edition (SAS Institute Inc.).

CHAPTER IV:

Summary and discussion:
The slim, the fat and the obese: guess who lives the longest?[1]

[1] This research was published in: Li, X., Handee, W., & Kuo, M.-H. (2016). The slim, the fat, and the obese: guess who lives the longest? *Current Genetics*. I contributed to all of the figures.

Abstract

In a modern society that is increasingly older and “heavier”, it is understandable that the majority favors a slimmer body that helps to sail smoothly into the dusk of life. Given the association between obesity and many metabolic and cardiovascular disorders, there are stern criticisms over such a thought of “good fat”. Ironically, a phenomenon called “obesity paradox”, that is, the overweight population purportedly enjoys the lowest all-cause mortality, baffles open-minded clinicians and scientists. Lipids are essential to all life forms. Fat, in particular triacylglycerol, also exists in different forms and in different locations in the human body, making any simple statement that vilifies all fat invalid. Whether the phenomenon of obesity paradox indeed has its root in a hitherto unrealized pro-survival function of fat deserves a serious look. Indeed, a recent publication using yeast as the model showed that elevation in the cellular storage of triacylglycerol extends lifespan in an energy expenditure independent fashion. In stark contrast, lean cells devoid of triacylglycerol biosynthetic capability die upon entering the senescence phase. Together, a new cytoprotective function of fat emerges. This mini-review aims to discuss potential mechanisms for the observed lifespan preservation function of triacylglycerol.

Is fat always bad?

The question of body shape and health has puzzled humans for centuries. People are often described as slim, chubby, fat or obese, with a modern quantitative indicator of the body mass index (BMI), which is calculated by dividing the body weight (kg) to the

square of height (m) (Keys et al. 1972). Obesity (BMI>30) has been observed to be associated with cardiovascular diseases, type 2 diabetes and hypertension (Eckel et al. 2011; Poirier et al. 2006; Rahmouni et al. 2005). This is why the seemingly opposite observations – overweight and obese people have longer life expectancy among some disease populations – are referred to as the "obesity paradox" (Hainer & Aldhoon-Hainerova 2013; Oreopoulos et al. 2008). The phenomenon of "obesity paradox", if indeed exists, may suggest an unrecognized, protective benefit of fat. Based on recent findings that the intracellular triacylglycerol (or fat) exerts a pro-longevity function in yeast (Handee et al. 2016), and that lipid droplets, in which triacylglycerol is stored, play an antioxidant role in protecting Drosophila stem cells during development (Bailey et al. 2015), this minireview attempts to discuss possible mechanisms for the energy-independent cytoprotective role of fat that may underlie the obesity paradox in humans. We suggest a "radicals sink" hypothesis for a pro-survival function of intracellular triacylglycerol.

Fat (triacylglycerol) is accumulated in various organisms in storage tissues or under stresses

Is there really a paradox? To answer this question, we need to understand what fat is and why it is made. Biochemically, the fat we talk about in our daily lives is primarily composed of hydrophobic compounds called triacylglycerols (TAGs), or triglycerides (TGs). A TAG molecule consists of a three-carbon glycerol backbone with three esterified acyl chains from fatty acids (Figure 4.1A). TAG is used as a universal

storage lipid in eukaryotes and in some bacterial species (Figure 4.1B). It is also known as “oil” when it is accumulated in plant tissues, mainly seeds of food crops (Li-Beisson et al. 2013). Rather than nutrient excess, many unicellular eukaryotes such as algae and fungi, accumulate TAG upon stresses, such as nutrient deprivation, high light and higher salinity (Fan et al. 2011; Hu et al. 2008; Kohlwein 2010).

The biochemical pathways and the major players of TAG metabolism have been elucidated (Figure 4.1A and 4.1C). Two acyltransferases sequentially transfer acyl-CoAs (or Acyl-ACPs in plastids; ACP: acyl carrier protein) to glycerol-3-phosphate to form phosphatidic acid (PA), which is then dephosphorylated into diacylglycerol (DAG) (Carman & Han 2009). The final step of TAG assembly is catalyzed by acyl-CoA:diacylglycerol acyltransferases (DGATs) (Yen et al. 2008). In recent years, one alternative mechanism, the phospholipid:diacylglycerol acyltransferase (PDAT) reaction, has been found in plants, algae and fungi (Dahlqvist et al. 2000; Yoon et al. 2012; Zhang et al. 2009). While PA and DAG are also precursors for glycerolipids that make up biological membranes (Fagone & Jackowski 2009; Ohlrogge & Browse 1995), DGATs and PDATs function exclusively in the biosynthesis of TAG. The turnover of TAG has also received increased attention in recent years. TAG is mobilized upon improved environmental conditions for microbes, germination for plants, and hunger for animals by lipases that sequentially hydrolyze TAG, DAG and monoacylglycerol (MAG) (Watt & Steinberg 2008). A series of beta-oxidation reactions in mitochondria and peroxisomes convert fatty acids extracted from TAG to multiple molecules of acetyl-CoA, which are a

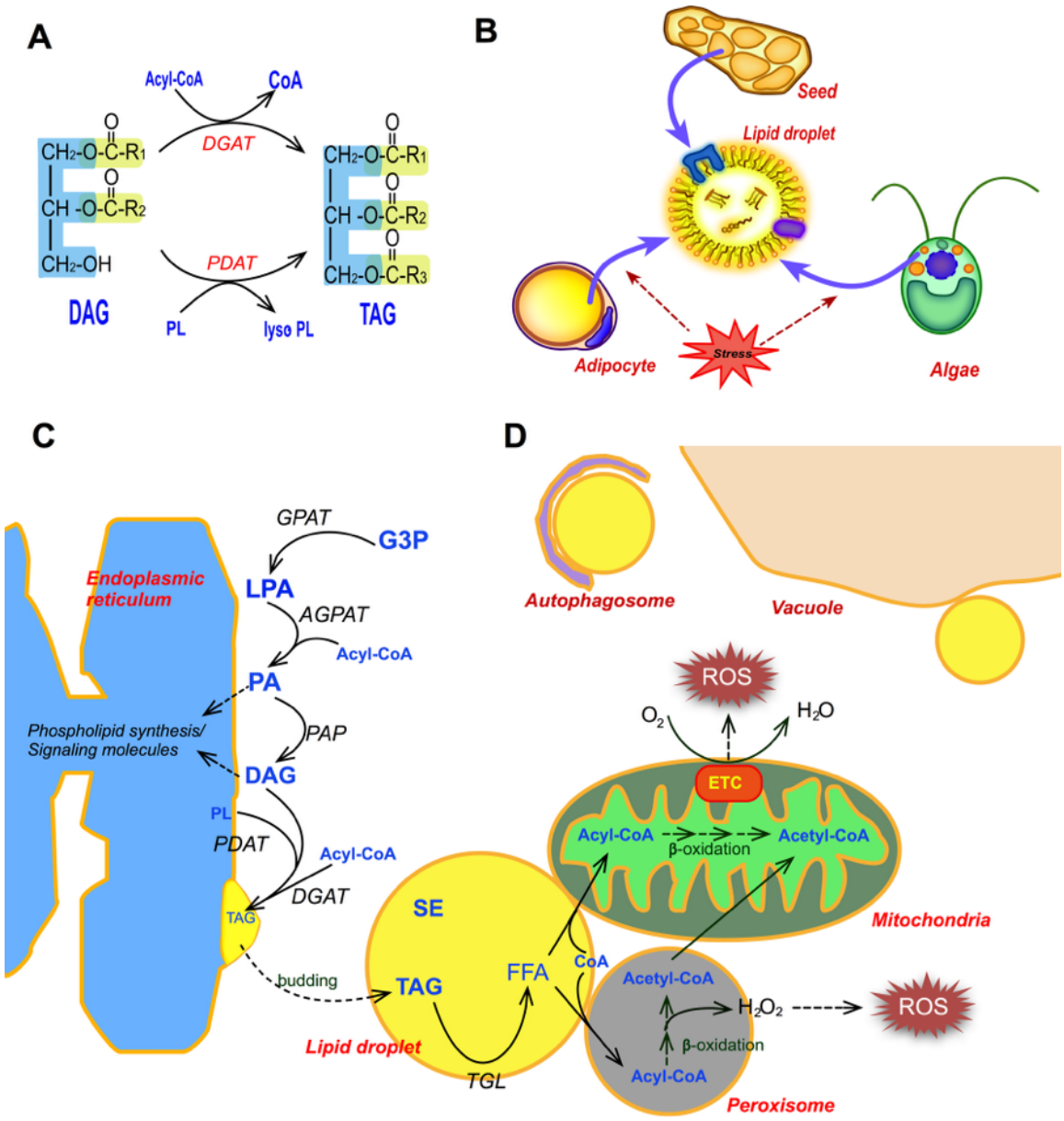

Figure 4.1 TAG is a ubiquitous molecule that is part of crosstalks involving different organelles for homeostasis. (A) Each TAG molecule consists of a glycerol backbone with three fatty acyl chains esterified. (B) TAG and lipid droplets are accumulated in storage tissues for multicellular organisms or under stress conditions for unicellular organisms. Shown here are an adipocyte of animals, a seed of plants, and a photosynthetic microalga. (C) Metabolism of TAG. Biosynthesis of TAG in endoplastic reticulum is accomplished through multiple acylation steps that esterify fatty acids to the glycerol backbone. Increasing TAG content locally causes the formation of lipid droplets that also store steryl esters,

Figure 4.1 (cont'd)

another category of neutral, storage lipids. TAG hydrolysis takes place in lipid droplets via the action of TAG lipases (TGL). Free fatty acids (FFA) resulting from lipolysis are subjected to sequential β-oxidation reactions for the generation of multiple molecules of acetyl-CoA that are fed into TCA cycle and other anabolic pathways. Mitochondria and peroxisomes are the major locations for β-oxidation. (D) Lipid droplets interact physically with many other organelles, including the endoplasmic reticulum, mitochondria, peroxisomes, autophagosomes and vacuoles. Abbreviations: DAG, diacylglycerol; G3P, glycerol-3-phosphate; LPA, lysophosphatidic acid; PA, phosphatidic acid; PL, phospholipids; ROS, reactive oxygen species; R_1, R_2 and R_3, alkyl group; SE, steryl ester; TAG, triacylglycerol. Abbreviations for enzymes: AGPAT, 1-acylglycerol-3-phosphate acyltransferase; DGAT, acyl CoA:diacylglycerol acyltransferase; GPAT, glycerol-3-phosphate acyltransferase; PDAT, phospholipid:diacylglycerol acyltransferase; PAP, phosphatidic acid phosphatase; TGL, triacylglycerol lipase; ETC, electron transport chain.

common substrate for anabolism (Eaton et al. 1996; Reddy & Hashimoto 2001).

In cells, TAG biosynthesis takes place in the endoplasmic reticulum (ER). Accumulation of TAG in ER causes ER membrane to bulge, eventually leading to the budding of lipid droplets off ER (Figure 4.1C) (Choudhary et al. 2015; Farese & Walther 2009). Instead of being an inert storage organelle, lipid droplets are actually highly dynamic in their composition (e.g., proteomes), number, size, and intracellular distribution (Guo et al. 2008; Yang et al. 2012). They also interact dynamically with many other organelles (Figure 4.1D) (Murphy et al. 2009), consistent with their roles in establishing lipid homeostasis (Kohlwein et al. 2013; Yu & Ginsberg 2005). Physical interactions between lipid droplets and peroxisomes and mitochondria effectively couple

lipolysis to fatty acid beta-oxidation (Binns et al. 2006; Jagerstrom et al. 2009). During autophagy, lipid droplets are enclosed by autophagosomes and targeted to lysosomes for nutrient recycling (Singh et al. 2009).

Yeast is a good model for fat metabolism and aging

Given the association between higher body mass and lower mortality (i.e., longer life expectancy), it is tempting to speculate a novel function of fat that protects the underlying cells and organism. On the other hand, in mammals, the effect of TAG on lifespan is confounded by the fact that TAG is present both intracellularly and in the circulation. Fortunately, the ubiquitous presence and the conserved metabolism of TAG justify the use of model organisms to understand the roles of TAG in different cellular functions, including perhaps the human obesity paradox and lifespan regulation. The unicellular organism *Saccharomyces cerevisiae*, commonly known as the budding yeast or the Baker's yeast, affords a variety of advantages for the molecular and functional dissection of TAG. The unparalleled genetic toolset, fast growth rate, well-defined and conserved metabolic pathways, and, importantly, the finite lifespan of yeast cells render this species a particularly attractive model.

Budding yeast can undergo two independent aging paradigms: replicative aging and chronological aging (Figure 4.2) (Kaeberlein 2010). The main principle behind replicative lifespan (RLS) is that a mother cell can only produce a finite number of progeny before it enters the post-replicative state when cell division stops (Mortimer &

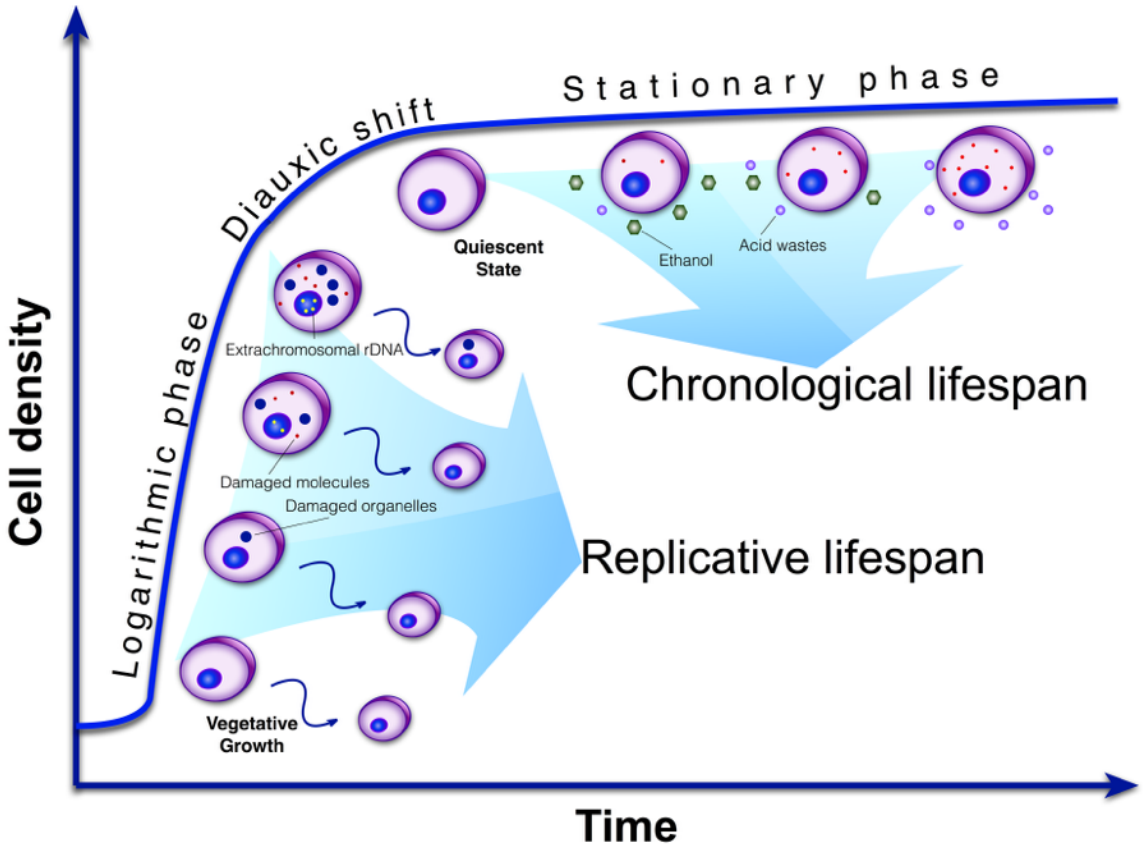

Figure 4.2 The yeast lifespan assessment samples cells with a different physiological and mitotic status. The yeast replicative lifespan measures the proliferative potential, while chronological lifespan describes how long a cell survives in a non-dividing condition. For RLS, cells are kept on a rich agar plate and are continually dividing until they reach a state of irreversible growth arrest. The number of division that each cell can accomplish is described as the RLS. On the other hand, CLS is obtained from sampling cells in the stationary phase over a period of time (ranging from days to weeks) in which individual cells are metabolically active but mitotically inactive. The portion of cells capable of forming colonies upon seeding on fresh medium decreases over time. The time of each strain to change from 100% survival to a pre-determined survival rate (e.g., 10% or 1%) is the CLS of that strain. Both RLS and CLS can be influenced by environmental (e.g., glucose concentration, increased osmolarity, in the presence of certain compounds) and genetic factors (e.g., up- or down-regulation of the Target of Rapamycin, TOR, pathway). Some of the known senescence factors of RLS and CLS are shown.

Johnson 1959; Kaeberlein 2010). When a yeast cell divides, senescence factors such as damaged proteins, toxic materials, and extrachromosomal ribosomal DNA circles (ERCs) stay preferentially with the mother cell (Figure 4.2). The daughter cell thus receives primarily fresh, undamaged biomolecules and hence nearly full potential of replication. On the other hand, the replicative potential of the mother cell becomes increasingly restricted over time, eventually leading to cessation of division (Sinclair & Guarente 1997). The yeast RLS is conceptually similar to the maintenance of stem cell viability in animals.

Chronological lifespan (CLS) on the other hand concerns the time-dependent loss of viability of the post-mitotic, stationary phase cells (Fabrizio & Longo 2007). The CLS is quantified by the colony forming capability of a population kept in the stationary phase for an increasing period of time, a situation similar to post-mitotic cells in humans, such as the neurons. When nutrients including sugar and alcohols are consumed, cells enter the mitotically inactive, yet metabolically active stationary phase. Meanwhile, certain cells adapt a quiescent state (Allen et al. 2006) that is thought to be key to maintaining cellular viability. Like normal human cells, the stationary phase yeast cells rely on mitochondria-driven respiration for energy flux and metabolism. Consequently, the accumulated oxidative damages and toxic wastes impair the cells' ability to return to a proliferative cell cycle when conditions improve (Fabrizio &Longo 2008).

Genetics and omics studies have uncovered mechanisms that control yeast RLS and/or CLS. Critically, many yeast aging and longevity factors and pathways are conserved in worms, flies and mammals (Kaeberlein 2010; Kaeberlein et al. 2015; Fabrizio et al. 2010). Most notable among these lifespan regulators include dietary restriction (DR), oxidative stresses (Weindruch & Walford 1988; Kaeberlein et al. 2005; Spindler 2010), and the Sch9/S6 kinase-TOR (target of rapamycin) pathway (Laplante & Sabatini 2009; Raught et al. 2001).

TAG is a longevity factor in yeast

Recently, our group sought to investigate the effects of TAG on lifespan in budding yeast (Handee et al. 2016). We initially observed a positive correlation between TAG content and chronological lifespan among strains used in the lab (lower TAG and shorter lifespan) and strains collected from wild (higher TAG and longer lifespan). We then manipulated a lab strain toward higher TAG content through two independent means: removal of one or both TAG lipases (*TGL3* and *TGL4*) or overexpression of the major DGAT (*DGA1*). Both manipulations successfully increased the TAG content and extended chronological lifespan. The pro-longevity role of TAG was further demonstrated by creating a "lean" strain that lacked *DGA1* and *LRO1*, the yeast PDAT. The *dga1lor1* double mutant exhibited significantly shortened CLS (Figure 4.3) without a clear growth defect in the logarithmically growing phase.

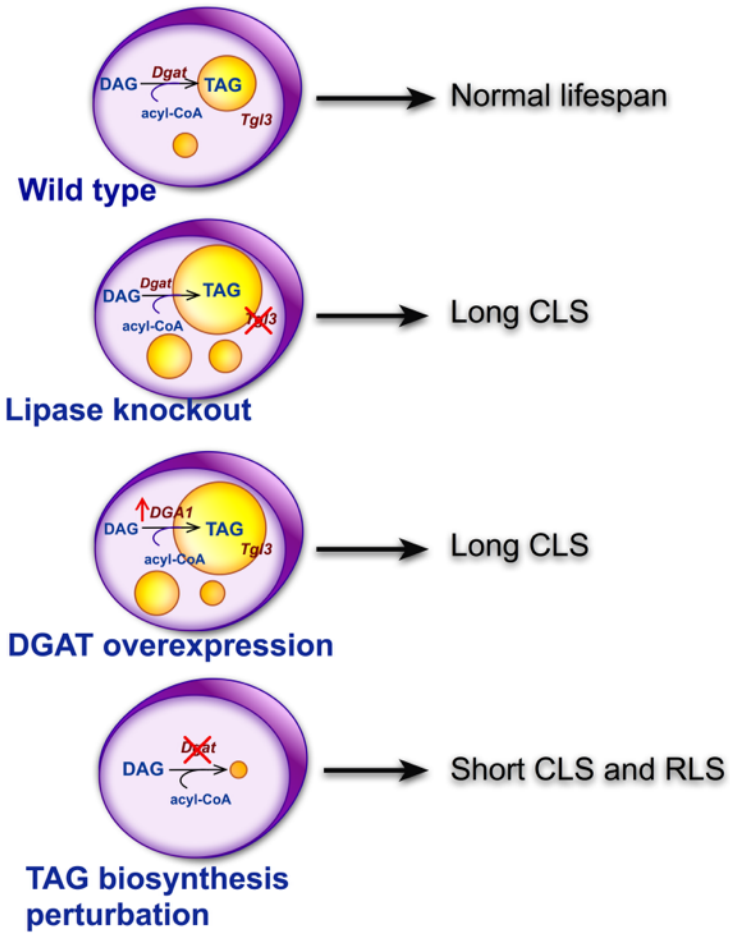

Figure 4.3 Controlling lifespan by modulating TAG metabolism in yeast. Yeast chronological lifespan is critically regulated by the level of intracellular triacylglycerol. Genetic measures that deplete or enrich TAG molecules create lean and fat cells with shortened or extended lifespan, respectively.

Yeast aging is regulated by pathways that are conserved through evolution (Longo et al. 2012). Considering that TAG is a critical biomolecule for the homeostasis of lipids and even other biological processes such as signaling (Coleman & Lee 2004), it is important to delineate the mechanistic distinction and overlap between TAG and other senescence and longevity factors. Genetic and growth tests using the above fat and lean

strains with additional treatments that alter yeast lifespan further demonstrate that TAG extends lifespan independently from such factors as dietary restriction, medium acidification, and the pathways involving Tor1, Sch9, Ras2, and Sod2 (Handee et al. 2016). Intracellular TAG thus exerts a pro-longevity function that operates in a manner that is distinct from other known lifespan regulators.

Why is TAG "healthful"?

So how does TAG protect yeast cells from aging? An intuitive answer would be that the elevated TAG stockpile provides additional energy for cells to sustain the crisis longer than those without. This notion may explain why fatter yeast cells live longer when there are extra copies of the *DGA1* gene that produce more TAG. However, over-accumulation of TAG can also be achieved by deleting TAG lipases, which effectively deprives cells of the ability to extract energy from TAG. We therefore do not think the hypothesis of saving-for-later-use is likely. Another hypothesis is that TAG accumulation defers aging by sequestering the otherwise cytotoxic free fatty acids (Listenberger et al. 2003). Indeed, in the short-living *dga1 lor1* mutant cells, the level of free fatty acids is greater and are hypersensitive to exogenous fatty acids (Handee & Kuo, unpublished observation), consistent with the report that yeast cells depleted of their neutral lipid biosynthetic capability lose viability while entering the stationary phase (Petschnigg et al. 2009). On the other hand, the long-living, fatter cells do not have significantly lower free fatty acids than their normal counterparts (Li, Handee, & Kuo, published data). Sequestering the toxic molecules of free fatty acids thus is important but unlikely to be a

major reason underlying the lifespan extension by TAG. Additional potential roles of TAG are worth considering.

Given that lipid droplets, in which TAG is stored, physically and dynamically interact with organelles including mitochondria, peroxisomes, and autophagosomes that all are involved in the production and/or elimination of reactive oxygen species and their radicalized derivatives (Beach & Titorenko 2013; Scherz-Shouval & Elazar 2007), and that the fate of cellular senescence or proliferation is critically dependent on pathways in stress responses (Ho & Gasch, 2015; Jiang 2016; Saarikangas & Barral 2016; Kourtis & Tavernarakis 2011), we suggest that TAG is part of a conserved pro-survival factor for cells to cope with many stresses in an energy-independent fashion. Indeed, TAG accumulation can be induced by a variety of stresses (Li et al. 2012; Li et al. 2009; Pal et al. 2011; Younce & Kolattukudy 2012; Lee et al. 2013). Also critical to this anti-stress function of TAG is the report of an antioxidant role of lipid droplets in Drosophila stem cells (Bailey et al. 2015). Taking these considerations together, we hypothesize that intracellular TAG may act as a “radicals sink” that protects the underlying cells from oxidative damages (Ziegler et al. 2015). This model (Figure 4.4) is based on the fact that unsaturated fatty acids, free or esterified into TAG or phospholipids, are highly susceptible to radicals attack. In fact, the membrane phospholipids are believed to be a physiologically relevant target of radicals attack in aging (Pamplona 2008; Pamplona et al. 2002). Assuming that the normal, lean (short-living), and fat (long-living) yeast cells have comparable rates of metabolism, the amounts of reactive oxygen species produced

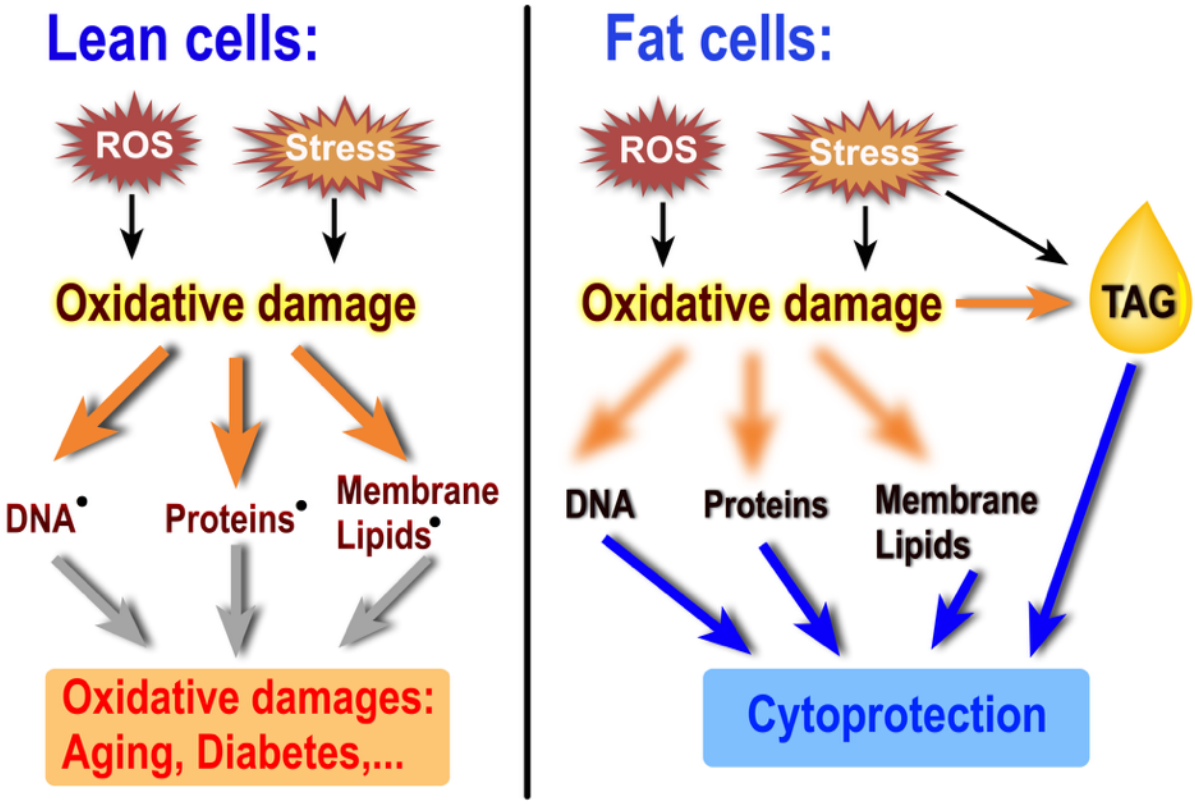

Figure 4.4 A "radicals sink" model for the lifespan extension role of TAG. Reactive oxygen species, ROS, can cause pleiotropic damages of a variety of biomolecules and organelles. Higher levels of TAG may draw ROS and other radicals to lipid droplets and away from other biomolecules, leading to cytoprotection and preservation of cell viability over time.

during metabolism therefore should be similar among these strains as well. In the fatter yeast cells in which the TAG content is effectively raised, oxidative radicals may be drawn to TAG, thus sparing other biomolecules or organelles key to the maintenance of cellular viability during aging. Another potential bonus of using TAG as the radicals sink is that these highly hydrophobic molecules are confined in lipid droplets, so they are less likely to cause diffused damages. Together, the accumulation of pro-senescence damages

in cytoplasm, membranes, and/or nucleus will be deferred. In contrast, the lean cells that can not incorporate fatty acids into TAG not only are devoid of the protective TAG molecules but also are enriched for fatty acids that may become radicalized and further cause diffusible damages, thus shortening lifespan.

Besides yeast, many other unicellular organisms also raise their TAG synthesis and storage when encountering environmental hardships (Fan et al. 2011; Hu et al. 2008; Kohlwein 2010). For laboratory mice and *C. elegans*, restricting food supply (i.e., caloric restriction) may cause an increase of fat-to-protein ratio (Li et al. 2009; Zasedatelev 1988), suggesting that TAG being part of a stress response may be widely conserved. On the other hand, the intricate balance involving multiple tissues and organs, as well as the existence of circulating and stored TAG in the human body render the delineation of TAG's role in lifespan regulation and in the phenomenon of obesity paradox a very complicated task. The statement that higher TAG equates longer lifespan clearly is oversimplification and can potentially lead to ill consequences in individual and public health. Unbiased scrutiny of the role of TAG, in particular that synthesized and stored in cells, is needed. We suggest that whether TAG exerts an energy-independent pro-survival function in animals can be first examined at the cellular level by the use of a variety of transformed and primary cells for, e.g., DGAT overexpression (Yen et al. 2008) and TAG lipase knockdown or deletion (Nielsen et al. 2014). If indeed intracellular TAG has a cytoprotective function besides its canonical role in storing surplus energy, a new array of studies linking intracellular TAG to other lifespan and stress pathways are expected,

ultimately leading to a balanced guideline seeking effective bodyweight control and, at the same time, assuming the benefit of TAG.

APPENDIX

APPENDIX

Raw data from “radicals sink” model’s experiments

Table A1. DCFDA and FDA fluorescence signals and cell density data in Figure 3.3

Strain	Sample No.	OD_{600}	DCFDA	OD_{600}	FDA
WT	1	0.2488	1428	0.3002	11044
WT	2	0.3734	1760	0.2228	8759
WT	3	0.3164	1404	0.2507	6140
WT	4	0.3488	1569	0.2247	5970
WT	5	0.4468	2395	0.5048	18084
WT	6	0.2345	1155	0.16	6380
WT	7	0.3623	1979	0.3221	8133
WT	8	0.1917	952	0.1406	3644
*tgl3*Δ	1	0.3238	1714	0.1911	6140
*tgl3*Δ	2	0.4198	1780	0.2401	5970
*tgl3*Δ	3	0.2493	1388	0.2819	8929
*tgl3*Δ	4	0.2291	1389	0.2253	12365
*tgl3*Δ	5	0.5333	2907	0.5499	32626
*tgl3*Δ	6	0.2283	1207	0.1775	6961
*tgl3*Δ	7	0.3689	2246	0.4167	12496
*tgl3*Δ	8	0.2279	1099	0.1522	3701
*dga1*Δ *lro1*Δ	1	0.2255	1548	0.1524	4247
*dga1*Δ *lro1*Δ	2	0.2923	1763	0.1836	5568
*dga1*Δ *lro1*Δ	3	0.2594	1909	0.2064	7466
*dga1*Δ *lro1*Δ	4	0.1965	1623	0.205	7659
*dga1*Δ *lro1*Δ	5	0.4924	2721	0.3098	8959
*dga1*Δ *lro1*Δ	6	0.1891	1164	0.1195	4068
*dga1*Δ *lro1*Δ	7	0.4715	3427	0.3315	12663
*dga1*Δ *lro1*Δ	8	0.1565	1235	0.1314	5474

Table A1. The data represent DCFDA and FDA readings from the 3 core strains in Figure 3.3. The data show 2 biological and 4 technical replicates (8 samples in total).

Table A2. DCFDA readings from the time-point treatments with PQ in Figure 3.4

Time (min)	Strains					
	WT	***tgl3*Δ**	***dga1*Δ *lro1*Δ**	**WT + PQ**	***tgl3*Δ + PQ**	***dga1*Δ *lro1*Δ+ PQ**
0	-4.00 ± 14.84	-31.50 ± 39.60	236.50 ± 76.37	291.50 ± 38.18	256.50 ± 9.90	1298.00 ± 482.50
30	218.00 ± 200.81	90.00 ± 74.95	1052.50 ± 499.92	1449.00 ± 295.57	1182.50 ± 430.63	5068.50 ± 2101.50
60	600.21 ± 216.37	261.21 ± 132.94	1,581.71 ± 574.88	3,123.71 ± 392.44	2,444.71 ± 719.13	8,143.21 ± 3215.00
90	936.57 ± 377.60	523.57 ± 145.66	2,071.07 ± 655.49	4,633.07 ± 464.57	3,877.07 ± 993.49	10,831.07 ± 4051.50
120	1,269.64 ± 466.69	735.64 ± 257.39	2,416.64 ± 743.88	5,737.14 ± 434.87	4,878.14 ± 863.38	13,143.14 ± 4849.50
150	1,411.00 ± 415.78	887.00 ± 280.01	2,723.00 ± 832.97	6,567.50 ± 245.36	5,604.50 ± 1041.57	14,926.00 ± 5392.00
180	1,488.43 ± 556.49	972.93 ± 298.40	2,947.93 ± 946.11	7,266.43 ± 135.05	6,324.93 ± 1004.09	16,379.43 ± 6036.50
210	1,565.86 ± 505.58	1,018.86 ± 338.70	3,086.86 ± 970.86	7,536.36 ± 79.20	6,768.86 ± 976.51	17,382.36 ± 6392.00
240	1,577.07 ± 519.72	1,073.07 ± 396.69	3,130.57 ± 1129.96	7,516.07 ± 185.97	6,954.07 ± 934.09	17,406.07 ± 6290.50
270	1,500.28 ± 542.35	1,054.79 ± 329.51	3,017.79 ± 1137.03	7,579.79 ± 281.43	7,168.79 ± 1038.03	17,156.29 ± 6005.50

Table A2. The data represent DCFDA readings demonstrated in Figure 3.4. Three yeast strains (WT, *tgl3*Δ, and *dga1*Δ *lro1*Δ) grown in YPD cultures for 3 days were either throated with or without 0.1 μg/ml paraquat (PQ). DCFDA was added 30 min before the fluorescence measurement. The signals were read every 30 min for 5 hr. Each cell represents the mean and standard deviation from the 3 replicates.

Table A3. Least square means of DCFDA/FDA signals after the PQ treatment at 30 and 150 min in Figure 3.5A

Strain	Time (min)	Estimate	Standard Error	DF	t Value	Pr > |t|
WT	0	0.4848	0.01826	3	26.55	0.0001
WT	30	0.5010	0.04482	3	11.18	0.0015
WT	150	0.5457	0.02857	3	19.10	0.0003
*tgl3*Δ	0	0.3555	0.03520	3	10.10	0.0021
*tgl3*Δ	30	0.3861	0.03107	3	12.42	0.0011
*tgl3*Δ	150	0.3900	0.006906	3	56.47	<.0001
*dga1*Δ *lro1*Δ	0	0.5273	0.02624	3	20.10	0.0003
*dga1*Δ *lro1*Δ	30	0.5773	0.03233	3	17.86	0.0004
*dga1*Δ *lro1*Δ	150	0.6301	0.1091	3	5.77	0.0103

Table A3. The DCFDA/FDA data form the three core strains treated with 20 mM PQ for 0, 30, and 150 min shown in Figure 3.5A. The DCFDA signals were normalized to the FDA readings conducted at the same time. The mean values of 4 independent experiments are reported in the Estimate columns which were derived from maximum likelihood of a two-way ANOVA test. The variance-covariance analysis was performed using a compound symmetry structure with Kenward-Roger correction for the unequal variance. DF, degree of freedom; Pr > |t|, p-value of two-tail probability computed using t distribution.

Table A4. Pair-wise differences of Least Squares Means of DCFDA/FDA signals from Table A3.

Strain	Time (min)	Strain	Time (min)	Estimate	Standard Error	DF	t Value	Pr > |t|
WT	0	WT	30	-0.01619	0.04840	3.97	-0.33	0.7549
WT	0	WT	150	-0.06094	0.03391	5.1	-1.80	0.1311
WT	0	*dga1*Δ *lro1*Δ	0	-0.04252	0.03196	5.35	-1.33	0.2373
WT	0	*dga1*Δ *lro1*Δ	30	-0.09251	0.03713	4.74	-2.49	0.0578
WT	0	*dga1*Δ *lro1*Δ	150	-0.1454	0.1106	3.17	-1.31	0.2759
WT	0	*tgl3*Δ	0	0.1293	0.03965	4.51	3.26	0.0261

Table A4. (cont'd)

Strain	Time (min)	Strain	Time (min)	Estimate	Standard Error	DF	t Value	Pr > |t|
WT	0	*tgl3*Δ	30	0.09871	0.03604	4.85	2.74	0.0422
WT	0	*tgl3*Δ	150	0.09479	0.01952	3.84	4.86	0.0092
WT	30	WT	150	-0.04475	0.05315	5.09	-0.84	0.4376
WT	30	*dga1*Δ *lro1*Δ	0	-0.02633	0.05193	4.84	-0.51	0.6345
WT	30	*dga1*Δ *lro1*Δ	30	-0.07632	0.05526	5.46	-1.38	0.2211
WT	30	*dga1*Δ *lro1*Δ	150	-0.1292	0.1180	3.98	-1.09	0.3353
WT	30	*tgl3*Δ	0	0.1455	0.05699	5.68	2.55	0.0455
WT	30	*tgl3*Δ	30	0.1149	0.05454	5.34	2.11	0.0854
WT	30	*tgl3*Δ	150	0.1110	0.04535	3.14	2.45	0.0880
WT	150	*dga1*Δ *lro1*Δ	0	0.01842	0.03879	5.96	0.47	0.6518
WT	150	*dga1*Δ *lro1*Δ	30	-0.03158	0.04315	5.91	-0.73	0.4923
WT	150	*dga1*Δ *lro1*Δ	150	-0.08443	0.1128	3.41	-0.75	0.5025
WT	150	*tgl3*Δ	0	0.1902	0.04534	5.76	4.20	0.0063
WT	150	*tgl3*Δ	30	0.1597	0.04221	5.96	3.78	0.0093
WT	150	*tgl3*Δ	150	0.1557	0.02940	3.35	5.30	0.0099
*dga1*Δ *lro1*Δ	0	*dga1*Δ *lro1*Δ	30	-0.05000	0.04164	5.76	-1.20	0.2769
*dga1*Δ *lro1*Δ	0	*dga1*Δ *lro1*Δ	150	-0.1029	0.1122	3.35	-0.92	0.4206
*dga1*Δ *lro1*Δ	0	*tgl3*Δ	0	0.1718	0.04390	5.55	3.91	0.0092
*dga1*Δ *lro1*Δ	0	*tgl3*Δ	30	0.1412	0.04067	5.84	3.47	0.0139
*dga1*Δ *lro1*Δ	0	*tgl3*Δ	150	0.1373	0.02713	3.41	5.06	0.0108
*dga1*Δ *lro1*Δ	30	*dga1*Δ *lro1*Δ	150	-0.05285	0.1138	3.52	-0.46	0.6696
*dga1*Δ *lro1*Δ	30	*tgl3*Δ	0	0.2218	0.04779	5.96	4.64	0.0036
*dga1*Δ *lro1*Δ	30	*tgl3*Δ	30	0.1912	0.04484	5.99	4.26	0.0053
*dga1*Δ *lro1*Δ	30	*tgl3*Δ	150	0.1873	0.03306	3.27	5.67	0.0086
*dga1*Δ *lro1*Δ	150	*tgl3*Δ	0	0.2747	0.1147	3.62	2.40	0.0815
*dga1*Δ *lro1*Δ	150	*tgl3*Δ	30	0.2441	0.1135	3.48	2.15	0.1080

Table A4. (cont'd)

Strain	Time (min)	Strain	Time (min)	Estimate	Standard Error	DF	t Value	Pr > |t|
*dga1*Δ *lro1*Δ	150	*tgl3*Δ	150	0.2402	0.1093	3.02	2.20	0.1148
*tgl3*Δ	0	*tgl3*Δ	30	-0.03058	0.04695	5.91	-0.65	0.5393
*tgl3*Δ	0	*tgl3*Δ	150	-0.03450	0.03587	3.23	-0.96	0.4025
*tgl3*Δ	30	*tgl3*Δ	150	-0.00392	0.03183	3.3	-0.12	0.9091

Table A4. The pair-wise comparison of DCFDA/FDA data for the 3 core strains shown in Table A3 are treated with 20 mM PQ for 0, 30, and 150 min. A pair of means of each strain at different time points were compared using a two-way ANOVA analysis, as described in Table A3. The Estimate values describe least squares means of a pair of different means. DF: degrees of freedom; Pr > $|t|$, *p*-value of two-tail probability computed using the *t* distribution.

Table A5. The rate of oxygen consumption data from Figure 3.5B

Strain	Media	Age	Estimate	Standard Error	DF	t Value	Pr > |t|
WT-1	YPD	log	0.1013	0.03560	8	2.84	0.0217
WT-2	YPD	log	0.1635	0.03560	8	4.59	0.0018
WT-3	YPD	log	0.1558	0.03560	8	4.38	0.0024
*tgl3*Δ-1	YPD	log	0.1414	0.03560	8	3.97	0.0041
*tgl3*Δ-2	YPD	log	0.1632	0.03560	8	4.58	0.0018
*tgl3*Δ-3	YPD	log	0.1685	0.03560	8	4.73	0.0015
*dga1*Δ *lro1*Δ-1	YPD	log	0.1619	0.03560	8	4.55	0.0019
*dga1*Δ *lro1*Δ-2	YPD	log	0.1821	0.03560	8	5.12	0.0009
WT-1	YPD	7-day	0.03810	0.1803	24	0.21	0.8345
WT-2	YPD	7-day	0.3635	0.1803	24	2.02	0.0552

Table A5. (cont'd)

Strain	Media	Age	Estimate	Standard Error	DF	t Value	Pr > |t|
WT-3	YPD	7-day	0.3324	0.1803	24	1.84	0.0777
*tgl3*Δ-1	YPD	7-day	0.4810	0.1803	24	2.67	0.0135
*tgl3*Δ-2	YPD	7-day	0.2563	0.1803	24	1.42	0.1681
*tgl3*Δ-3	YPD	7-day	0.4910	0.1803	24	2.72	0.0119
*dga1*Δ *lro1*Δ-1	YPD	7-day	0.6337	0.1803	24	3.51	0.0018
*dga1*Δ *lro1*Δ-2	YPD	7-day	0.4554	0.1803	24	2.53	0.0186
WT-1	YPGE	log	0.1587	0.1460	8	1.09	0.3088
WT-2	YPGE	log	0.2808	0.1460	8	1.92	0.0907
WT-3	YPGE	log	0.2358	0.1460	8	1.61	0.1451
*tgl3*Δ-1	YPGE	log	0.3348	0.1460	8	2.29	0.0511
*tgl3*Δ-2	YPGE	log	0.2282	0.1460	8	1.56	0.1568
*tgl3*Δ-3	YPGE	log	0.3978	0.1460	8	2.72	0.0261
*dga1*Δ *lro1*Δ-2	YPGE	log	0.2403	0.1460	8	1.65	0.1385
*dga1*Δ *lro1*Δ-2	YPGE	log	0.2403	0.1460	8	1.65	0.1385
WT-1	YPGE	7-day	0.6654	0.1803	24	3.69	0.0011
WT-2	YPGE	7-day	1.0171	0.1803	24	5.64	<.0001
WT-3	YPGE	7-day	0.7540	0.1803	24	4.18	0.0003
*tgl3*Δ-1	YPGE	7-day	1.1138	0.1803	24	6.18	<.0001
*tgl3*Δ-2	YPGE	7-day	0.7310	0.1803	24	4.05	0.0005
*tgl3*Δ-3	YPGE	7-day	1.0705	0.1803	24	5.94	<.0001
*dga1*Δ *lro1*Δ-1	YPGE	7-day	0.6139	0.1803	24	3.40	0.0023
*dga1*Δ *lro1*Δ-2	YPGE	7-day	0.6352	0.1803	24	3.52	0.0017

Table A5 (cont'd). The oxygen consumption rate data from the 3 core strains grown in either YPD or YPGE for 24 hr (log) or 7 days, as shown in Figure 3.5B. The Estimate values represent the oxygen consumption rate (μM/sec) calculated from the maximum likelihood of a two-way ANOVA test. DF: degrees of freedom; Pr $> |t|$, p-value of two-tail probability computed using the t distribution.

Table A6. DCFDA signal distribution data in Figure 3.6

Strain	Diffused	1 dot	2 dots	⩾ 3 dots	Disrupted membrane
WT	46.49 ± 15.09	27.68 ± 7.63	9.71 ± 2.02	14.60 ± 7.84	1.52 ± 0.52
*tgl3*Δ	45.82 ± 2.05	13.07 ± 3.98	16.13 ± 6.03	23.51 ± 10.75	1.47 ± 0.45
*dga1*Δ *lro1*Δ	67.04 ± 13.98	4.76 ± 1.92	1.19 ± 0.48	0.89 ± 0.36	26.11 ± 18.59

Table A6. The quantified DCFDA distribution demonstrated in Figure 3.6. Data in the table show the means and standard deviations of 2 biological replicates (n = 200 to 250 cells).

REFERENCES

REFERENCES

Abell, B.M., Hahn, M., Holbrook, L.A. & Moloney, M.M. (2004) Membrane topology and sequence requirements for oil body targeting of oleosin. *The Plant Journal: for Cell and Molecular Biology*. 37 (4), pp. 461–470.

Adeyo, O., Horn, P.J., Lee, S., Binns, D.D., Chandrahas, A., Chapman, K.D. & Goodman, J.M. (2011) The yeast lipin orthologue Pah1p is important for biogenesis of lipid droplets. *The Journal of Cell Biology*. 192 (6), pp. 1043–1055.

Afri, M., Frimer, A.A. & Cohen, Y. (2004) Active oxygen chemistry within the liposomal bilayer. Part IV: Locating 2',7'-dichlorofluorescein (DCF), 2',7'-dichlorodihydrofluorescein (DCFH) and 2‘,7’-dichlorodihydrofluorescein diacetate (DCFH-DA) in the lipid bilayer. *Chemistry and Physics of Lipids*. 131 (1), pp. 123–133.

Aguilaniu, H., Gustafsson, L., Rigoulet, M. & Nystrom, T. (2003) Asymmetric inheritance of oxidatively damaged proteins during cytokinesis. *Science*. 299 (5613), pp. 1751–1753.

Allen, C., Büttner, S., Aragon, A.D., Thomas, J.A., Meirelles, O., Jaetao, J.E., Benn, D., Ruby, S.W., Veenhuis, M., Madeo, F. & Werner-Washburne, M. (2006) Isolation of quiescent and nonquiescent cells from yeast stationary-phase cultures. *The Journal of Cell Biology*. 174 (1), pp. 89–100.

Andziak, B., O'Connor, T.P. & Buffenstein, R. (2005) Antioxidants do not explain the disparate longevity between mice and the longest-living rodent, the naked mole-rat. *Mechanisms of Ageing and Development*. 126 (11), pp. 1206–1212.

Andziak, B., O'Connor, T.P., Qi, W., DeWaal, E.M., Pierce, A., Chaudhuri, A.R., Van Remmen, H. & Buffenstein, R. (2006) High oxidative damage levels in the longest-living rodent, the naked mole-rat. *Aging Cell*. 5 (6), pp. 463–471.

Athenstaedt, K. & Daum, G. (2003) YMR313c/TGL3 encodes a novel triacylglycerol lipase located in lipid particles of Saccharomyces cerevisiae. *The Journal of Biological Chemistry.* 278 (26), pp. 23317–23323.

Athenstaedt, K. & Daum, G. (2005) Tgl4p and Tgl5p, two triacylglycerol lipases of the yeast Saccharomyces cerevisiae are localized to lipid particles. *The Journal of Biological Chemistry*. 280 (45), pp. 37301–37309.

Athenstaedt, K., Zweytick, D., Jandrositz, A., Kohlwein, S.D. & Daum, G. (1999) Identification and characterization of major lipid particle proteins of the yeast Saccharomyces cerevisiae. *Journal of Bacteriology*. 181 (20), pp. 6441–6448.

Bailey, A.P., Koster, G., Guillermier, C., Hirst, E.M.A., MacRae, J.I., Lechene, C.P., Postle, A.D. & Gould, A.P. (2015) Antioxidant Role for Lipid Droplets in a Stem Cell Niche of Drosophila. *Cell*. 163 (2), pp. 340–353.

Barbosa, A.D., Savage, D.B. & Siniossoglou, S. (2015) Lipid droplet–organelle interactions: emerging roles in lipid metabolism. *Current Opinion in Cell Biology*. 35pp. 91–97.

Barja, G., Cadenas, S., Rojas, C., Pérez-Campo, R. & López-Torres, M. (1994) Low mitochondrial free radical production per unit O_2 consumption can explain the simultaneous presence of high longevity and high aerobic metabolic rate in birds. *Free Radical Research*. 21 (5), pp. 317–327.

Barker, M.G. & Walmsley, R.M. (1999) Replicative ageing in the fission yeast Schizosaccharomyces pombe. *Yeast*. 15 (14), pp. 1511–1518.

Bartz, R., Li, W.-H., Venables, B., Zehmer, J.K., Roth, M.R., Welti, R., Anderson, R.G.W., Liu, P. & Chapman, K.D. (2007) Lipidomics reveals that adiposomes store ether lipids and mediate phospholipid traffic. *The Journal of Lipid Research*. 48 (4), pp. 837–847.

Bass, D.A., Parce, J.W., Dechatelet, L.R., Szejda, P., Seeds, M.C. & Thomas, M. (1983) Flow cytometric studies of oxidative product formation by neutrophils: a graded response to membrane stimulation. *Journal of Immunology*. 130 (4), pp. 1910–1917.

Beach, A. & Titorenko, V.I. (2013) Essential roles of peroxisomally produced and metabolized biomolecules in regulating yeast longevity. *Sub-Cellular Biochemistry*. 69 (Chapter 9), pp. 153–167.

Benning, C.R.S. (1992) Isolation and genetic complementation of a sulfolipid-deficient mutant of Rhodobacter sphaeroides. *Journal of Bacteriology*. 174 (7), pp. 2352.

Binns, D., Januszewski, T., Chen, Y., Hill, J., Markin, V.S., Zhao, Y., Gilpin, C., Chapman, K.D., Anderson, R.G.W. & Goodman, J.M. (2006) An intimate collaboration between peroxisomes and lipid bodies. *The Journal of Cell Biology*. 173 (5), pp. 719–731.

Blanchette-Mackie, E.J. & Scow, R.O. (1983) Movement of lipolytic products to mitochondria in brown adipose tissue of young rats: an electron microscope study. *The Journal of Lipid Research*. 24 (3), pp. 229–244.

Bonawitz, N.D. & Shadel, G.S. (2007) Rethinking the mitochondrial theory of aging: the role of mitochondrial gene expression in lifespan determination. *Cell Cycle*. 6 (13), pp. 1574–1578.

Bonawitz, N.D., Rodeheffer, M.S. & Shadel, G.S. (2006) Defective mitochondrial gene expression results in reactive oxygen species-mediated inhibition of respiration and reduction of yeast life span. *Molecular and Cellular Biology*. 26 (13), pp. 4818–4829.

Bonini, M.G., Rota, C., Tomasi, A. & Mason, R.P. (2006) The oxidation of 2‘,7’-dichlorofluorescin to reactive oxygen species: a self-fulfilling prophesy? *Free Radical Biology and Medicine*. 40 (6), pp. 968–975.

Boveris, A. & Chance, B. (1973) The mitochondrial generation of hydrogen peroxide. General properties and effect of hyperbaric oxygen. *Biochemical Journal*. 134 (3), pp. 707–716.

Boyd, V., Cholewa, O.M. & Papas, K.K. (2008) Limitations in the Use of Fluorescein Diacetate/Propidium Iodide (FDA/PI) and Cell Permeable Nucleic Acid Stains for Viability Measurements of Isolated Islets of Langerhans. *Current Trends in Biotechnology and Pharmacy*. 2 (2), pp. 66–84.

Braunstein, J.D., Schwartz, G., Good, R.A., Sharpless, T.K. & Melamed, M.R. (1979) Quantitation of lymphocyte response to PHA by flow cytofluorometry. III. Heterogeneity of induction period. *The Journal of Histochemistry and Cytochemistry: official Journal of the Histochemistry Society*. 27 (1), pp. 474–477.

Buffenstein, R. (2005) The naked mole-rat: a new long-living model for human aging research. *The Journals of Gerontology. Series A, Biological Sciences and Medical Sciences*. 60 (11), pp. 1369–1377.

Burhans, W.C. & Weinberger, M. (2009) Acetic acid effects on aging in budding yeast: are they relevant to aging in higher eukaryotes? *Cell Cycle*. 8 (14), pp. 2300–2302.

Burkitt, M.J. & Wardman, P. (2001) Cytochrome C is a potent catalyst of dichlorofluorescin oxidation: implications for the role of reactive oxygen species in apoptosis. *Biochemical and Biophysical Research Communications*. 282 (1), pp. 329–333.

Burow, S. & Valet, G. (1987) Flow-cytometric characterization of stimulation, free radical formation, peroxidase activity and phagocytosis of human granulocytes with 2,7-dichlorofluorescein (DCF). *European Journal of Cell Biology*. 43 (1), pp. 128–133.

Burtner, C.R., Murakami, C.J., Kennedy, B.K. & Kaeberlein, M. (2009) A molecular mechanism of chronological aging in yeast. *Cell Cycle*. 8 (8), pp. 1256–1270.

Burtner, C.R., Murakami, C.J., Olsen, B., Kennedy, B.K. & Kaeberlein, M. (2011) A genomic analysis of chronological longevity factors in budding yeast. *Cell Cycle*. 10 (9), pp. 1385–1396.

Bus, J.S., Aust, S.D. & Gibson, J.E. (1976) Paraquat toxicity: proposed mechanism of action involving lipid peroxidation. *Environmental Health Perspectives*. 16pp. 139–146.

Çakmak, Z.E., Ölmez, T.T., Çakmak, T., Menemen, Y. & Tekinay, T. (2014) Induction of triacylglycerol production in Chlamydomonas reinhardtii: comparative analysis of different element regimes. *Bioresource Technology*. 155pp. 379–387.

Carman, G.M. & Han, G.-S. (2009a) Phosphatidic acid phosphatase, a key enzyme in the regulation of lipid synthesis. *Journal of Biological Chemistry*. 284 (5), pp. 2593–2597.

Carman, G.M. & Han, G.-S. (2009b) Regulation of phospholipid synthesis in yeast. *The Journal of Lipid Research*. 50 Suppl. S69–S73.

Carman, G.M. & Henry, S.A. (2007) Phosphatidic acid plays a central role in the transcriptional regulation of glycerophospholipid synthesis in Saccharomyces cerevisiae. *Journal of Biological Chemistry*. 282 (52), pp. 37293–37297.

Carmona-Gutierrez, D., Eisenberg, T., Büttner, S., Meisinger, C., Kroemer, G. & Madeo, F. (2010) Apoptosis in yeast: triggers, pathways, subroutines. *Cell Death and Differentiation*. 17 (5), pp. 763–773.

Carter, W.O., Narayanan, P.K. & Robinson, J.P. (1994) Intracellular hydrogen peroxide and superoxide anion detection in endothelial cells. *Journal of Leukocyte Biology*. 55 (2), pp. 253–258.

Choi, H.-S., Su, W.-M., Morgan, J.M., Han, G.-S., Xu, Z., Karanasios, E., Siniossoglou, S. & Carman, G.M. (2011) Phosphorylation of phosphatidate phosphatase regulates its membrane association and physiological functions in Saccharomyces cerevisiae: identification of SER(602), THR(723), AND SER(744) as the sites phosphorylated by CDC28 (CDK1)-encoded cyclin-dependent kinase. *The Journal of Biological Chemistry*. 286 (2), pp. 1486–1498.

Choudhary, V., Ojha, N., Golden, A. & Prinz, W.A. (2015) A conserved family of proteins facilitates nascent lipid droplet budding from the ER. *The Journal of Cell Biology*. 211 (2), pp. 261–271.

Clemons, K.V., McCusker, J.H., Davis, R.W. & Stevens, D.A. (1994) Comparative pathogenesis of clinical and nonclinical isolates of Saccharomyces cerevisiae. *The Journal of Infectious Diseases*. 169 (4), pp. 859–867.

Coleman, R.A. & Lee, D.P. (2004) Enzymes of triacylglycerol synthesis and their regulation. *Progress in Lipid Research*. 43 (2), pp. 134–176.

Crow, J.P. (1997) Dichlorodihydrofluorescein and Dihydrorhodamine 123 are sensitive indicators of peroxynitrite in vitro: implications for intracellular measurement of reactive nitrogen and oxygen species. *Nitric oxide: Biology and Chemistry*. 1 (2), pp. 145–157.

D'mello, N.P., Childress, A.M., Franklin, D.S., Kale, S.P., Pinswasdi, C. & Jazwinski, S.M. (1994) Cloning and characterization of LAG1, a longevity-assurance gene in yeast. *The Journal of Biological Chemistry*. 269 (22), pp. 15451–15459.

Dahlqvist, A., Stahl, U., Lenman, M., Banas, A., Lee, M., Sandager, L., Ronne, H. & Stymne, S. (2000). Phospholipid:diacylglycerol acyltransferase: an enzyme that catalyzes the acyl-CoA-independent formation of triacylglycerol in yeast and plants. *Proceedings of the National Academy of Sciences*. 97, pp. 6487–6492.

Daly, T. & Williams, L.A. (1997) Catecholaminergic innervation of interscapular brown adipose tissue in the naked mole−rat (Heterocephalus glaber). *Journal of Anatomy*. 190, pp. 321–326.

Daum, G., Lees, N.D., Bard, M. & Dickson, R. (1998) Biochemistry, cell biology and molecular biology of lipids of Saccharomyces cerevisiae. *Yeast*. 14 (16), pp. 1471–1510.

Daum, G., Wagner, A., Czabany, T. & Athenstaedt, K. (2007) Dynamics of neutral lipid storage and mobilization in yeast. *Biochimie*. 89 (2), pp. 243–248.

Day, B.J., Patel, M., Calavetta, L., Chang, L.Y. & Stamler, J.S. (1999) A mechanism of paraquat toxicity involving nitric oxide synthase. *Proceedings of the National Academy of Sciences*. 96 (22), pp. 12760–12765.

Dejean, L., Beauvoit, B., Guérin, B. & Rigoulet, M. (2000) Growth of the yeast Saccharomyces cerevisiae on a non-fermentable substrate: control of energetic yield by the amount of mitochondria. *Biochimica et Biophysica Acta - Bioenergetics*. 1457 (1-2), pp. 45–56.

Department of Economic and Social Affairs: Population Devision (2012) *Population Facts*. United Nations. 1, pp. 1–2.

Dickinson, J.R. & Schweizer, M. (2004) *The Metabolism and Molecular Physiology of Saccharomyces cerevisiae*, 2nd edn. London: CRC Press.

Ding, Y., Yang, L., Zhang, S., Wang, Y., Du, Y., Pu, J., Peng, G., Chen, Y., Zhang, H., Yu, J., Hang, H., Wu, P., Yang, F., Yang, H., et al. (2012) Identification of the major functional proteins of prokaryotic lipid droplets. *Journal of Lipid Research*. 53 (3), pp. 399–411.

Eaton, S., Bartlett, K. & Pourfarzam, M. (1996) Mammalian mitochondrial beta-oxidation. *Biochemical Journal*. 320 (2), pp. 345–357.

Eckel, R.H., Kahn, S.E., Ferrannini, E., Goldfine, A.B., Nathan, D.M., Schwartz, M.W., Smith, R.J. & Smith, S.R. (2011) Obesity and type 2 diabetes: what can be unified and what needs to be individualized? *The Journal of Clinical Endocrinology and Metabolism*. 96 (6), pp. 1654–1663.

Eisenberg, T. & Büttner, S. (2013) Lipids and cell death in yeast. *FEMS Yeast Research*. 14 (1), pp. 179–197.

Eldakak, A., Rancati, G., Rubinstein, B., Paul, P., Conaway, V. & Li, R. (2010) Asymmetrically inherited multidrug resistance transporters are recessive determinants in cellular replicative ageing. *Nature Cell Biology*. 12 (8), pp. 799–805.

Fabrizio, P. & Longo, V.D. (2008) Chronological aging-induced apoptosis in yeast. *Biochimica et Biophysica Acta - Molecular Cell Research*. 1783 (7), pp. 1280–1285.

Fabrizio, P. & Longo, V.D. (2003) The chronological life span of Saccharomyces cerevisiae. *Aging Cell*. 2 (2), pp. 73–81.

Fabrizio, P. & Longo, V.D. (2007) The chronological life span of Saccharomyces cerevisiae. *Methods in Molecular Biology*. 371pp. 89–95.

Fabrizio, P., Battistella, L., Vardavas, R., Gattazzo, C., Liou, L.-L., Diaspro, A., Dossen, J.W., Gralla, E.B. & Longo, V.D. (2004) Superoxide is a mediator of an altruistic aging program in Saccharomyces cerevisiae. *Journal of Cell Biology*. 166 (7), pp. 1055–1067.

Fabrizio, P., Hoon, S., Shamalnasab, M., Galbani, A., Wei, M., Giaever, G., Nislow, C. & Longo, V.D. (2010) Genome-wide screen in Saccharomyces cerevisiae identifies vacuolar protein sorting, autophagy, biosynthetic, and tRNA methylation genes involved in life span regulation. *PLoS Genetics*. 6 (7), pp. e1001024.

Fabrizio, P., Liou, L.-L., Moy, V.N., Diaspro, A., Valentine, J.S., Gralla, E.B. & Longo, V.D. (2003) SOD2 functions downstream of Sch9 to extend longevity in yeast. *Genetics*. 163 (1), pp. 35–46.

Fabrizio, P., Pozza, F., Pletcher, S.D., Gendron, C.M. & Longo, V.D. (2001) Regulation of longevity and stress resistance by Sch9 in yeast. *Science*. 292 (5515), pp. 288–290.

Fagone, P. & Jackowski, S. (2009) Membrane phospholipid synthesis and endoplasmic reticulum function. *The Journal of Lipid Research*. 50 Suppl. S311–S316.

Fan, J., Andre, C. & Xu, C. (2011) A chloroplast pathway for the de novo biosynthesis of triacylglycerol in Chlamydomonas reinhardtii. *FEBS Letters*. 585 (12), pp. 1985–1991.

Farese, R.V. & Walther, T.C. (2009) Lipid droplets finally get a little R-E-S-P-E-C-T. *Cell*. 139 (5), pp. 855–860.

Fenner, G.P. & Parks, L.W. (1989) Gas chromatographic analysis of intact steryl esters in wild type Saccharomyces cerevisiae and in an ester accumulating mutant. *Lipids*. 24 (7), pp. 625–629.

Ferguson, L.R. & Borstel, von, R.C. (1992) Induction of the cytoplasmic 'petite' mutation by chemical and physical agents in Saccharomyces cerevisiae. *Mutation Research/ Fundamental and Molecular Mechanisms of Mutagenesis*. 265 (1), pp. 103–148.

Flegal, K.M., Kit, B.K., Orpana, H. & Graubard, B.I. (2013) Association of All-Cause Mortality With Overweight and Obesity Using Standard Body Mass Index Categories A Systematic Review and Meta-analysis. *The Journal of the American Medical Association*. 309 (1), pp. 71–82.

Fukushima, T., Tanaka, K., Lim, H. & Moriyama, M. (2002) Mechanism of cytotoxicity of paraquat. *Environmental Health and Preventive Medicine*. 7 (3), pp. 89–94.

Gaber, R.F., Copple, D.M., Kennedy, B.K., Vidal, M. & Bard, M. (1989) The yeast gene ERG6 is required for normal membrane function but is not essential for biosynthesis of the cell-cycle-sparking sterol. *Molecular and Cellular Biology*. 9 (8), pp. 3447–3456.

Gao, Q. & Goodman, J.M. (2015) The lipid droplet—a well-connected organelle. *Frontiers in Cell and Developmental Biology*. 3pp. 367.

Garay, E., Campos, S.E., Gonzalez de la Cruz, J., Gaspar, A.P., Jinich, A. & Deluna, A. (2014) High-resolution profiling of stationary-phase survival reveals yeast longevity factors and their genetic interactions. *PLoS Genetics*. 10 (2), pp. e1004168.

Garbarino, J., Padamsee, M., Wilcox, L., Oelkers, P.M., D'Ambrosio, D., Ruggles, K.V., Ramsey, N., Jabado, O., Turkish, A. & Sturley, S.L. (2009) Sterol and

diacylglycerol acyltransferase deficiency triggers fatty acid-mediated cell death. *The Journal of Biological Chemistry*. 284 (45), pp. 30994–31005.

Gasch, A.P., Spellman, P.T., Kao, C.M., Carmel-Harel, O., Eisen, M.B., Storz, G., Botstein, D. & Brown, P.O. (2000) Genomic expression programs in the response of yeast cells to environmental changes. *Molecular Biology of the Cell*. 11 (12), pp. 4241–4257.

Gietz, D., St Jean, A., Woods, R.A. & Schiestl, R.H. (1992) Improved method for high efficiency transformation of intact yeast cells. *Nucleic Acids Research*. 20 (6), pp. 1425.

Girotti, A.W. (1998) Lipid hydroperoxide generation, turnover, and effector action in biological systems. *The Journal of Lipid Research*. 39 (8), pp. 1529–1542.

Goffeau, A., Barrell, B.G., Bussey, H., Davis, R.W., Dujon, B., Feldmann, H., Galibert, F., Hoheisel, J.D., Jacq, C., Johnston, M., Louis, E.J., Mewes, H.W., Murakami, Y., Philippsen, P., et al. (1996) Life with 6000 Genes. *Science*. 274 (5287), pp. 546–567.

Goldberg, A.A., Bourque, S.D., Kyryakov, P., Gregg, C., Boukh-Viner, T., Beach, A., Burstein, M.T., Machkalyan, G., Richard, V., Rampersad, S., Cyr, D., Milijevic, S. & Titorenko, V.I. (2009) Effect of calorie restriction on the metabolic history of chronologically aging yeast. *Experimental Gerontology*. 44 (9), pp. 555–571.

Goldstein, A.L. & McCusker, J.H. (1999) Three new dominant drug resistance cassettes for gene disruption in Saccharomyces cerevisiae. *Yeast*. 15 (14), pp. 1541–1553.

Grauslund, M. & Rønnow, B. (2000) Carbon source-dependent transcriptional regulation of the mitochondrial glycerol-3-phosphate dehydrogenase gene, GUT2, from Saccharomyces cerevisiae. *Canadian Journal of Microbiology*. 46 (12), pp. 1096–1100.

Gray, J.V., Petsko, G.A., Johnston, G.C., Ringe, D., Singer, R.A. & Werner-Washburne, M. (2004) 'Sleeping beauty': quiescence in Saccharomyces cerevisiae. *Microbiology and Molecular Biology Reviews*. 68 (2), pp. 187–206.

Gredilla, R. & Barja, G. (2005) Minireview: the role of oxidative stress in relation to caloric restriction and longevity. *Endocrinology*. 146 (9), pp. 3713–3717.

Grillitsch, K., Connerth, M., Köfeler, H., Arrey, T.N., Rietschel, B., Wagner, B., Karas, M. & Daum, G. (2011) Lipid particles/droplets of the yeast Saccharomyces cerevisiae revisited: lipidome meets proteome. *Biochimica et Biophysica Acta*. 1811 (12), pp. 1165–1176.

Guo, Y., Walther, T.C., Rao, M., Stuurman, N., Goshima, G., Terayama, K., Wong, J.S., Vale, R.D., Walter, P. & Farese, R.V. (2008) Functional genomic screen reveals genes involved in lipid-droplet formation and utilization. *Nature*. 453 (7195), pp. 657–661.

Haemmerle, G., Lass, A., Zimmermann, R., Gorkiewicz, G., Meyer, C., Rozman, J., Heldmaier, G., Maier, R., Theussl, C., Eder, S., Kratky, D., Wagner, E.F., Klingenspor, M., Hoefler, G., et al. (2006) Defective lipolysis and altered energy metabolism in mice lacking adipose triglyceride lipase. *Science*. 312 (5774), pp. 734–737.

Haemmerle, G., Moustafa, T., Woelkart, G., Büttner, S., Schmidt, A., van de Weijer, T., Hesselink, M., Jaeger, D., Kienesberger, P.C., Zierler, K., Schreiber, R., Eichmann, T., Kolb, D., Kotzbeck, P., et al. (2011) ATGL-mediated fat catabolism regulates cardiac mitochondrial function via PPAR-α and PGC-1. *Nature Medicine*. 17 (9), pp. 1076–1085.

Hainer, V. & Aldhoon-Hainerova, I. (2013) Obesity Paradox Does Exist. *Diabetes Care*. 36 Suppl 2, pp. S276–S281.

Halliwell, B. (2007) Biochemistry of oxidative stress. *Biochemical Society Transactions*. 35pp. 1147–1150.

Halliwell, B. (2009) The wanderings of a free radical. *Free Radical Biology and Medicine*. 46 (5), pp. 531–542.

Halliwell, B. and Gutteridge J. M. C. (2007) Free radicals in biology and medicine 4th ed. Oxford University Press Inc. New York. pp.268-337

Han, G.-S., O'Hara, L., Siniossoglou, S. & Carman, G.M. (2008) Characterization of the yeast DGK1-encoded CTP-dependent diacylglycerol kinase. *The Journal of Biological Chemistry*. 283 (29), pp. 20443–20453.

Han, G.-S., Wu, W.-I. & Carman, G.M. (2006) The Saccharomyces cerevisiae Lipin homolog is a $Mg2^{+}$-dependent phosphatidate phosphatase enzyme. *The Journal of Biological Chemistry*. 281 (14), pp. 9210–9218.

Handee, W., Li, X., Hall, K.W., Deng, X., Li, P., Benning, C., Williams, B.L. & Kuo, M.-H. (2016) An Energy-Independent Pro-longevity Function of Triacylglycerol in Yeast. *PLoS Genetics*. 12 (2), pp. e1005878.

Hansen, M., Flatt, T. & Aguilaniu, H. (2013) Reproduction, fat metabolism, and life span: what is the connection? *Cell Metabolism*. 17 (1), pp. 10–19.

Hapala, I., Marza, E. & Ferreira, T. (2011) Is fat so bad? Modulation of endoplasmic reticulum stress by lipid droplet formation. *Biology of the Cell / under the auspices of the European Cell Biology Organization*. 103 (6), pp. 271–285.

Harman, D. (1956) Aging: a theory based on free radical and radiation chemistry. *Journal of Gerontology*. 11 (3), pp. 298–300.

Harman, D. (1972) Free radical theory of aging: dietary implications. *The American Journal of Clinical Nutrition*. 25 (8), pp. 839–843.

Harman, D. (2003) The free radical theory of aging. *Antioxidants & Redox Signaling*. 5 (5), pp. 557–561.

Harrison, D.E., Strong, R., Sharp, Z.D., Nelson, J.F., Astle, C.M., Flurkey, K., Nadon, N.L., Wilkinson, J.E., Frenkel, K., Carter, C.S., Pahor, M., Javors, M.A., Fernandez, E. & Miller, R.A. (2009) Rapamycin fed late in life extends lifespan in genetically heterogeneous mice. *Nature*. 460 (7253), pp. 392–395.

Hayflick, L. & Moorhead, P.S. (1961) The serial cultivation of human diploid cell strains. *Experimental Cell Research*. 25 (3), pp. 585–621.

Hempel, S.L., Buettner, G.R., O'Malley, Y.Q., Wessels, D.A. & Flaherty, D.M. (1999) Dihydrofluorescein diacetate is superior for detecting intracellular oxidants: comparison with 2',7'-dichlorodihydrofluorescein diacetate, 5(and 6)-carboxy-2‘, 7’-dichlorodihydrofluorescein diacetate, and dihydrorhodamine 123. *Free Radical Biology and Medicine*. 27 (1-2), pp. 146–159.

Herman, P.K. (2002) Stationary phase in yeast. *Current Opinion in Microbiology*. 5 (6), pp. 602–607.

Herskowitz, I. & Jensen, R.E. (1991) Putting the HO gene to work: practical uses for mating-type switching. *Methods in Enzymology*. 194pp. 132–146.

Hiltunen, J.K., Schonauer, M.S., Autio, K.J., Mittelmeier, T.M., Kastaniotis, A.J. & Dieckmann, C.L. (2009) Mitochondrial fatty acid synthesis type II: more than just fatty acids. *Journal of Biological Chemistry*. 284 (14), pp. 9011–9015.

Ho, Y.-H. & Gasch, A.P. (2015) Exploiting the yeast stress-activated signaling network to inform on stress biology and disease signaling. *Current Genetics*. 61 (4), pp. 503–511.

Hodges, B.D.M. & Wu, C.C. (2010) Proteomic insights into an expanded cellular role for cytoplasmic lipid droplets. *Journal of Lipid Research*. 51 (2), pp. 262–273.

Hoy, A.J., Bruce, C.R., Turpin, S.M., Morris, A.J., Febbraio, M.A. & Watt, M.J. (2011) Adipose triglyceride lipase-null mice are resistant to high-fat diet-induced insulin resistance despite reduced energy expenditure and ectopic lipid accumulation. *Endocrinology*. 152 (1), pp. 48–58.

Hörl, G., Wagner, A., Cole, L.K., Malli, R., Reicher, H., Kotzbeck, P., Köfeler, H., Höfler, G., Frank, S., Bogner-Strauss, J.G., Sattler, W., Vance, D.E. & Steyrer, E. (2011) Sequential synthesis and methylation of phosphatidylethanolamine promote lipid droplet biosynthesis and stability in tissue culture and in vivo. *The Journal of Biological Chemistry*. 286 (19), pp. 17338–17350.

Hu, Q., Sommerfeld, M., Jarvis, E., Ghirardi, M., Posewitz, M., Seibert, M. & Darzins, A. (2008) Microalgal triacylglycerols as feedstocks for biofuel production: perspectives and advances. *The Plant Journal: for Cell and Molecular Biology*. 54 (4), pp. 621–639.

Huh, W.-K., Falvo, J.V., Gerke, L.C., Carroll, A.S., Howson, R.W., Weissman, J.S. & O'Shea, E.K. (2003) Global analysis of protein localization in budding yeast. *Nature*. 425 (6959), pp. 686–691.

Ingelmo-Torres, M., González-Moreno, E., Kassan, A., Hanzal-Bayer, M., Tebar, F., Herms, A., Grewal, T., Hancock, J.F., Enrich, C., Bosch, M., Gross, S.P., Parton, R.G. & Pol, A. (2009) Hydrophobic and basic domains target proteins to lipid droplets. *Traffic*. 10 (12), pp. 1785–1801.

Jacquier, N., Choudhary, V., Mari, M., Toulmay, A., Reggiori, F. & Schneiter, R. (2011) Lipid droplets are functionally connected to the endoplasmic reticulum in Saccharomyces cerevisiae. *Journal of Cell Science*. 124 (14), pp. 2424–2437.

Jägerström, S., Polesie, S., Wickström, Y., Johansson, B.R., Schröder, H.D., Højlund, K. & Boström, P. (2009) Lipid droplets interact with mitochondria using SNAP23. *Cell Biology International*. 33 (9), pp. 934–940.

Jewett, M.C., Workman, C.T., Nookaew, I., Pizarro, F.A., Agosin, E., Hellgren, L.I. & Nielsen, J. (2013) Mapping condition-dependent regulation of lipid metabolism in Saccharomyces cerevisiae. *G3; Genes|Genomes|Genetics*. 3 (11), pp. 1979–1995.

Jiang, Y. (2016) Regulation of TORC1 by ubiquitin through non-covalent binding. *Current Genetics*. 62 (3), pp. 553–555.

Jin, K. (2010) Modern Biological Theories of Aging. *Aging and Disease*. 1 (2), pp. 72–74.

Kaeberlein, M. (2010) Lessons on longevity from budding yeast. *Nature*. 464 (7288), pp. 513–519.

Kaeberlein, M. (2007a) Longevity genomics across species. *Current Genomics*. 8 (2), pp. 73–78.

Kaeberlein, M. (2007b) Molecular basis of ageing. *European Molecular Biology Organization*. In: October 2007 EMBO Press. 8p. 907–911.

Kaeberlein, M., Hu, D., Kerr, E.O., Tsuchiya, M., Westman, E.A., Dang, N., Fields, S. & Kennedy, B.K. (2005) Increased life span due to calorie restriction in respiratory-deficient yeast. *PLoS Genetics*. 1 (5), pp. e69.

Kaeberlein, M., McVey, M. & Guarente, L. (1999) The SIR2/3/4 complex and SIR2 alone promote longevity in Saccharomyces cerevisiae by two different mechanisms. *Genes & development*. 13 (19), pp. 2570–2580.

Kaeberlein, M., Rabinovitch, P.S. & Martin, G.M. (2015) Healthy aging: The ultimate preventative medicine. *Science*. 350 (6265), pp. 1191–1193.

Kalashnikova, M.M. & Fadeeva, E.O. (2006) Ultrastructural study of liver cells from rooks living in ecologically unfavorable areas. *Biology Bulletin*. 33 (2), pp. 133–141.

Kalyanaraman, B., Darley-Usmar, V., Davies, K.J.A., Dennery, P.A., Forman, H.J., Grisham, M.B., Mann, G.E., Moore, K., Roberts, L.J. & Ischiropoulos, H. (2012) Measuring reactive oxygen and nitrogen species with fluorescent probes: challenges and limitations. *Free Radical Biology and Medicine*. 52 (1), pp. 1–6.

Karlsson, M., Kurz, T., Brunk, U.T., Nilsson, S.E. & Frennesson, C.I. (2010) What does the commonly used DCF test for oxidative stress really show? *Biochemical Journal*. 428 (2), pp. 183–190.

Kastaniotis, A.J., Autio, K.J., Sormunen, R.T. & Hiltunen, J.K. (2004) Htd2p/Yhr067p is a yeast 3-hydroxyacyl-ACP dehydratase essential for mitochondrial function and morphology. *Molecular Microbiology*. 53 (5), pp. 1407–1421.

Keys, A., Fidanza, F., Karvonen, M.J., Kimura, N. & Taylor, H.L. (2014) Indices of relative weight and obesity. *International Journal of Epidemiology*. 43 (3), pp. 655–665.

Khatchadourian, A., Bourque, S.D., Richard, V.R., Titorenko, V.I. & Maysinger, D. (2012) Dynamics and regulation of lipid droplet formation in lipopolysaccharide (LPS)-stimulated microglia. *Biochimica et Biophysica Acta*. 1821 (4), pp. 607–617.

Klinger, H., Rinnerthaler, M., Lam, Y.T., Laun, P., Heeren, G., Klocker, A., Simon-Nobbe, B., Dickinson, J.R., Dawes, I.W. & Breitenbach, M. (2010) Quantitation of (a)symmetric inheritance of functional and of oxidatively damaged mitochondrial aconitase in the cell division of old yeast mother cells. *Experimental Gerontology*. 45 (7-8), pp. 533–542.

Klug, L. & Daum, G. (2014) Yeast lipid metabolism at a glance. *FEMS Yeast Research*. 14 (3), pp. 369–388.

Knoblach, B. & Rachubinski, R.A. (2015) Transport and retention mechanisms govern lipid droplet inheritance in Saccharomyces cerevisiae. *Traffic*. 16 (3), pp. 298–309.

Koch, B., Schmidt, C., Ploier, B. & Daum, G. (2014) Modifications of the C terminus affect functionality and stability of yeast triacylglycerol lipase Tgl3p. *The Journal of Biological Chemistry*. 289 (28), pp. 19306–19316.

Kohlwein, S.D. (2010) Triacylglycerol Homeostasis: Insights from Yeast. *Journal of Biological Chemistry*. 285 (21), pp. 15663–15667.

Kohlwein, S.D. & Petschnigg, J. (2007) Lipid-induced cell dysfunction and cell death: lessons from yeast. *Current Hypertension Reports*. 9 (6), pp. 455–461.

Kohlwein, S.D., Veenhuis, M. & van der Klei, I.J. (2013) Lipid droplets and peroxisomes: key players in cellular lipid homeostasis or a matter of fat--store 'em up or burn 'em down. *Genetics*. 193 (1), pp. 1–50.

Kourtis, N. & Tavernarakis, N. (2011) Cellular stress response pathways and ageing: intricate molecular relationships. *The EMBO Journal*. 30 (13), pp. 2520–2531.

Köffel, R. & Schneiter, R. (2006) Yeh1 constitutes the major steryl ester hydrolase under heme-deficient conditions in Saccharomyces cerevisiae. *Eukaryotic Cell*. 5 (7), pp. 1018–1025.

Köffel, R., Tiwari, R., Falquet, L. & Schneiter, R. (2005) The Saccharomyces cerevisiae YLL012/YEH1, YLR020/YEH2, and TGL1 genes encode a novel family of membrane-anchored lipases that are required for steryl ester hydrolysis. *Molecular and Cellular Biology*. 25 (5), pp. 1655–1668.

Kramer, B. & Buffenstein, R. (2004) The pancreas of the naked mole-rat (Heterocephalus glaber): an ultrastructural and immunocytochemical study of the endocrine component of thermoneutral and cold acclimated animals. *General and Comparative Endocrinology*. 139 (3), pp. 206–214.

Ku, H.H. & Sohal, R.S. (1993) Comparison of mitochondrial pro-oxidant generation and anti-oxidant defenses between rat and pigeon: possible basis of variation in longevity and metabolic potential. *Mechanisms of Ageing and Development*. 72 (1), pp. 67–76.

Kumar, S., Kawałek, A. & van der Klei, I.J. (2014) Peroxisomal quality control mechanisms. *Current Opinion in Microbiology*. 22pp. 30–37.

Kurat, C.F., Natter, K., Petschnigg, J., Wolinski, H., Scheuringer, K., Scholz, H., Zimmermann, R., Leber, R., Zechner, R. & Kohlwein, S.D. (2006) Obese yeast: triglyceride lipolysis is functionally conserved from mammals to yeast. *The Journal of Biological Chemistry*. 281 (1), pp. 491–500.

Kurat, C.F., Wolinski, H., Petschnigg, J., Kaluarachchi, S., Andrews, B., Natter, K. & Kohlwein, S.D. (2009) Cdk1/Cdc28-dependent activation of the major triacylglycerol lipase Tgl4 in yeast links lipolysis to cell-cycle progression. *Molecular Cell*. 33 (1), pp. 53–63.

Kushnareva, Y., Murphy, A.N. & Andreyev, A. (2002) Complex I-mediated reactive oxygen species generation: modulation by cytochrome c and NAD(P)+ oxidation-reduction state. *Biochemical Journal*. 368 (Pt 2), pp. 545–553.

Kvitek, D.J., Will, J.L. & Gasch, A.P. (2008) Variations in stress sensitivity and genomic expression in diverse S. cerevisiae isolates. *PLoS Genetics*. 4 (10), pp. e1000223.

Laplante, M. & Sabatini, D.M. (2009) mTOR signaling at a glance. *Journal of Cell Science*. 122 (20), pp. 3589–3594.

Lavie, C.J., De Schutter, A. & Milani, R.V. (2015) Healthy obese versus unhealthy lean: the obesity paradox. *Nature Reviews. Endocrinology*. 11 (1), pp. 55–62.

Lee, S.-J., Zhang, J., Choi, A.M.K., Kim, H.P., Lee, S.-J., Zhang, J., Choi, A.M.K. & Kim, H.P. (2013) Mitochondrial Dysfunction Induces Formation of Lipid Droplets as a Generalized Response to Stress. *Oxidative Medicine and Cellular Longevity*. 2013 (1–3), pp. 1–10.

Li, X., Benning, C. & Kuo, M.-H. (2012) Rapid triacylglycerol turnover in Chlamydomonas reinhardtii requires a lipase with broad substrate specificity. *Eukaryotic Cell*. 11 (12), pp. 1451–1462.

Li, X., Cope, M.B., Johnson, M.S., Smith, D.L. & Nagy, T.R. (2010) Mild calorie restriction induces fat accumulation in female C57BL/6J mice. *Obesity*. 18 (3), pp. 456–462.

Li-Beisson, Y., Shorrosh, B., Beisson, F., Andersson, M.X., Arondel, V., Bates, P.D., Baud, S., Bird, D., Debono, A., Durrett, T.P., Franke, R.B., Graham, I.A., Katayama, K., Kelly, A.A., et al. (2013) Acyl-lipid metabolism. *The Arabidopsis book / American Society of Plant Biologists*. 11pp. e0161.

Lin, S.-J., Kaeberlein, M., Andalis, A.A., Sturtz, L.A., Defossez, P.-A., Culotta, V.C., Fink, G.R. & Guarente, L. (2002) Calorie restriction extends Saccharomyces cerevisiae lifespan by increasing respiration. *Nature*. 418 (6895), pp. 344–348.

Listenberger, L.L., Han, X., Lewis, S.E., Cases, S., Farese, R.V., Ory, D.S. & Schaffer, J.E. (2003) Triglyceride accumulation protects against fatty acid-induced lipotoxicity. *Proceedings of the National Academy of Sciences*. 100 (6), pp. 3077–3082.

Liti, G. & Louis, E.J. (2012) Advances in quantitative trait analysis in yeast. *PLoS Genetics*. 8 (8), pp. e1002912.

Liu, L., Shi, X., Bharadwaj, K.G., Ikeda, S., Yamashita, H., Yagyu, H., Schaffer, J.E., Yu, Y.H. & Goldberg, I.J. (2009) DGAT1 expression increases heart triglyceride content but ameliorates lipotoxicity. *The Journal of Biological Chemistry*. 284 (52), pp. 36312–36323.

Liu, L., Zhang, Y., Chen, N., Shi, X., Tsang, B. & Yu, Y.H. (2007) Upregulation of myocellular DGAT1 augments triglyceride synthesis in skeletal muscle and protects against fat-induced insulin resistance. *The Journal of Clinical Investigation*. 117 (6), pp. 1679–1689.

Loewith, R. & Hall, M.N. (2011) Target of rapamycin (TOR) in nutrient signaling and growth control. *Genetics*. 189 (4), pp. 1177–1201.

Longo, V.D. (1999) Mutations in signal transduction proteins increase stress resistance and longevity in yeast, nematodes, fruit flies, and mammalian neuronal cells. *Neurobiology of Aging*. 20 (5), pp. 479–486.

Longo, V.D. (2004) Ras: the other pro-aging pathway. *Science of Aging Knowledge Environment*. 2004 (39), pp. pe36–pe36.

Longo, V.D. & Fabrizio, P. (2012) Chronological Aging in Sacharomyces cerevisiae. In: Michael Breitenbach, S Michal Jazwinski, & Peter Laun (eds.). *Aging Research in Yeast*. pp. 1–21.

Longo, V.D., Gralla, E.B. & Valentine, J.S. (1996) Superoxide dismutase activity is essential for stationary phase survival in Saccharomyces cerevisiae. Mitochondrial production of toxic oxygen species in vivo. *Journal of Biological Chemistry*. 271 (21), pp. 12275–12280.

Longo, V.D., Shadel, G.S., Kaeberlein, M. & Kennedy, B. (2012) Replicative and Chronological Aging in Saccharomyces cerevisiae. *Cell Metabolism*. 16 (1), pp. 18–31.

Low, K.L., Shui, G., Natter, K., Yeo, W.K., Kohlwein, S.D., Dick, T., Rao, S.P.S. & Wenk, M.R. (2010) Lipid droplet-associated proteins are involved in the biosynthesis and hydrolysis of triacylglycerol in Mycobacterium bovis bacillus Calmette-Guerin. *The Journal of Biological Chemistry*. 285 (28), pp. 21662–21670.

López-Otín, C., Blasco, M.A., Partridge, L., Serrano, M. & Kroemer, G. (2013) The Hallmarks of Aging. *Cell*. 153 (6), pp. 1194–1217.

Luo, J., Xu, X., Hall, H., Hyland, E.M., Boeke, J.D., Hazbun, T. & Kuo, M.-H. (2010) Histone h3 exerts a key function in mitotic checkpoint control. *Molecular and Cellular Biology*. 30 (2), pp. 537–549.

Magwere, T., West, M., Riyahi, K., Murphy, M.P., Smith, R.A.J. & Partridge, L. (2006) The effects of exogenous antioxidants on lifespan and oxidative stress resistance in Drosophila melanogaster. *Mechanisms of Ageing and Development*. 127 (4), pp. 356–370.

Marchesi, E., Rota, C., Fann, Y.C., Chignell, C.F. & Mason, R.P. (1999) Photoreduction of the fluorescent dye 2'-7'-dichlorofluorescein: a spin trapping and direct electron spin resonance study with implications for oxidative stress measurements. *Free Radical Biology and Medicine*. 26 (1-2), pp. 148–161.

Markgraf, D.F., Klemm, R.W., Junker, M., Hannibal-Bach, H.K., Ejsing, C.S. & Rapoport, T.A. (2014) An ER protein functionally couples neutral lipid metabolism on lipid droplets to membrane lipid synthesis in the ER. *Cell Reports*. 6 (1), pp. 44–55.

Martinez-Lopez, N., Athonvarangkul, D. & Singh, R. (2015) Autophagy and aging. *Advances in Experimental Medicine and Biology*. 847 (Chap 3), pp. 73–87.

Matecic, M., Smith, D.L., Pan, X., Maqani, N., Bekiranov, S., Boeke, J.D. & Smith, J.S. (2010) A microarray-based genetic screen for yeast chronological aging factors. *PLoS Genetics*. 6 (4), pp. e1000921–e1000921.

Matsufuji, Y., Fujimura, S., Ito, T., Nishizawa, M., Miyaji, T., Nakagawa, J., Ohyama, T., Tomizuka, N. & Nakagawa, T. (2008) Acetaldehyde tolerance in Saccharomyces cerevisiae involves the pentose phosphate pathway and oleic acid biosynthesis. *Yeast*. 25 (11), pp. 825–833.

McCormick, M.A., Delaney, J.R., Tsuchiya, M., Tsuchiyama, S., Shemorry, A., Sim, S., Chou, A.C.-Z., Ahmed, U., Carr, D., Murakami, C.J., Schleit, J., Sutphin, G.L., Wasko, B.M., Bennett, C.F., et al. (2015) A Comprehensive Analysis of Replicative Lifespan in 4,698 Single-Gene Deletion Strains Uncovers Conserved Mechanisms of Aging. *Cell Metabolism*. 22 (5), pp. 895–906.

McDermott, M., Wakelam, M.J.O. & Morris, A.J. (2004) Phospholipase D. *Biochemistry and Cell Biology*. 82 (1), pp. 225–253.

Mirisola, M.G. & Longo, V.D. (2012) Acetic acid and acidification accelerate chronological and replicative aging in yeast. *Cell Cycle*. 11 (19), pp. 3532–3533.

Mirisola, M.G., Taormina, G., Fabrizio, P., Wei, M., Hu, J. & Longo, V.D. (2014) Serine- and Threonine/Valine-Dependent Activation of PDK and Tor Orthologs Converge on Sch9 to Promote Aging. *PLoS Genetics*. 10 (2), pp. e1004113.

Miwa, S. & Brand, M.D. (2005) The topology of superoxide production by complex III and glycerol 3-phosphate dehydrogenase in Drosophila mitochondria. *Biochimica et Biophysica Acta*. 1709 (3), pp. 214–219.

Mortimer, R.K. & Johnson, J.R. (1959) Life span of individual yeast cells. *Nature*. 183 (4677), pp. 1751–1752.

Muller, F.L., Lustgarten, M.S., Jang, Y., Richardson, A. & Van Remmen, H. (2007) Trends in oxidative aging theories. *Free Radical Biology and Medicine*. 43 (4), pp. 477–503.

Mullner, H. & Daum, G. (2004) Dynamics of neutral lipid storage in yeast. *Acta Biochimica Polonica*. 51 (2), pp. 323–347.

Murakami, C. & Kaeberlein, M. (2009) Quantifying Yeast Chronological Life Span by Outgrowth of Aged Cells. *Journal of Visualized Experiments*. (27).

Murakami, C.J., Burtner, C.R., Kennedy, B.K. & Kaeberlein, M. (2008) A method for high-throughput quantitative analysis of yeast chronological life span. *The Journals of Gerontology. Series A, Biological Sciences and Medical Sciences*. 63 (2), pp. 113–121.

Murphy, D.J. (2012) The dynamic roles of intracellular lipid droplets: from archaea to mammals. *Protoplasma*. 249 (3), pp. 541–585.

Murphy, S., Martin, S. & Parton, R.G. (2009) Lipid droplet-organelle interactions; sharing the fats. *Biochimica et Biophysica Acta*. 1791 (6), pp. 441–447.

Natter, K., Leitner, P., Faschinger, A., Wolinski, H., McCraith, S., Fields, S. & Kohlwein, S.D. (2005) The spatial organization of lipid synthesis in the yeast Saccharomyces cerevisiae derived from large scale green fluorescent protein tagging and high resolution microscopy. *Molecular & Cellular Proteomics*. 4 (5), pp. 662–672.

Neklesa, T.K. & Davis, R.W. (2008) Superoxide anions regulate TORC1 and its ability to bind Fpr1:rapamycin complex. *Proceedings of the National Academy of Sciences*. 105 (39), pp. 15166–15171.

Nielsen, T.S., Jessen, N., Jørgensen, J.O.L., Møller, N. & Lund, S. (2014) Dissecting adipose tissue lipolysis: molecular regulation and implications for metabolic disease. *Journal of Molecular Endocrinology*. 52 (3), pp. R199–R222.

Niki, E. (2009) Lipid peroxidation: physiological levels and dual biological effects. *Free Radical Biology and Medicine*. 47 (5), pp. 469–484.

Nomura, S., Horiuchi, T., Omura, S. & Hata, T. (1972) The action mechanism of cerulenin. I. Effect of cerulenin on sterol and fatty acid biosynthesis in yeast. *Journal of Biochemistry*. 71 (5), pp. 783–796.

Novikoff, A.B., Novikoff, P.M., Rosen, O.M. & Rubin, C.S. (1980) Organelle relationships in cultured 3T3-L1 preadipocytes. *Journal of Cell Biology*. 87 (1), pp. 180–196.

Nystrom, T. (2007) A bacterial kind of aging. *PLoS Genetics*. 3 (12), pp. e224.

Oelkers, P. (2001) The DGA1 Gene Determines a Second Triglyceride Synthetic Pathway in Yeast. *Journal of Biological Chemistry*. 277 (11), pp. 8877–8881.

Oelkers, P., Tinkelenberg, A., Erdeniz, N., Cromley, D., Billheimer, J.T. & Sturley, S.L. (2000) A lecithin cholesterol acyltransferase-like gene mediates diacylglycerol esterification in yeast. *The Journal of Biological Chemistry*. 275 (21), pp. 15609–15612.

Ohlrogge, J. & Browse, J. (1995) Lipid biosynthesis. *The Plant Cell*. 7 (7), pp. 957–970.

Oreopoulos, A., Padwal, R., Norris, C.M., Mullen, J.C., Pretorius, V. & Kalantar-Zadeh, K. (2008) Effect of obesity on short- and long-term mortality postcoronary revascularization: a meta-analysis. *Obesity*. 16 (2), pp. 442–450.

Oshiro, J., Han, G.-S. & Carman, G.M. (2003) Diacylglycerol pyrophosphate phosphatase in Saccharomyces cerevisiae. *Biochimica et Biophysica Acta*. 1635 (1), pp. 1–9.

Österlund, T., Nookaew, I., Bordel, S. & Nielsen, J. (2013) Mapping condition-dependent regulation of metabolism in yeast through genome-scale modeling. *BMC Systems Biology*. 7 (1), pp. 1–10.

Pal, D., Khozin-Goldberg, I., Cohen, Z. & Boussiba, S. (2011) The effect of light, salinity, and nitrogen availability on lipid production by Nannochloropsis sp. *Applied Microbiology and Biotechnology*. 90 (4), pp. 1429–1441.

Palgunow, D., Palgunow, D., Klapper, M., Klapper, M., Döring, F. & Döring, F. (2012) Dietary restriction during development enlarges intestinal and hypodermal lipid droplets in Caenorhabditis elegans. *PLoS ONE*. 7 (11), pp. e46198.

Pamplona, R. (2008) Membrane phospholipids, lipoxidative damage and molecular integrity: a causal role in aging and longevity. *Biochimica et Biophysica Acta*. 1777 (10), pp. 1249–1262.

Pamplona, R., Barja, G. & Portero-Otín, M. (2002) Membrane fatty acid unsaturation, protection against oxidative stress, and maximum life span: a homeoviscous-longevity adaptation? *Annals of the New York Academy of Sciences*. 959pp. 475–490.

Park, Y., Han, G.-S., Mileykovskaya, E., Garrett, T.A. & Carman, G.M. (2015) Altered Lipid Synthesis by Lack of Yeast Pah1 Phosphatidate Phosphatase Reduces Chronological Life Span. *Journal of Biological Chemistry*. 290 (42), pp. 25382–25394.

Perl, A., Hanczko, R., Telarico, T., Oaks, Z. & Landas, S. (2011) Oxidative stress, inflammation and carcinogenesis are controlled through the pentose phosphate pathway by transaldolase. *Trends in Molecular Medicine*. 17 (7), pp. 395–403.

Petschnigg, J., Wolinski, H., Kolb, D., Zellnig, G., Kurat, C.F., Natter, K. & Kohlwein, S.D. (2009) Good fat, essential cellular requirements for triacylglycerol synthesis to maintain membrane homeostasis in yeast. *The Journal of Biological Chemistry*. 284 (45), pp. 30981–30993.

Pérez-Campo, R., López-Torres, M., Cadenas, S., Rojas, C. & Barja, G. (1998) The rate of free radical production as a determinant of the rate of aging: evidence from the comparative approach. *Journal of Comparative Physiology. B, Biochemical, Systemic, and Environmental Physiology*. 168 (3), pp. 149–158.

Ploier, B., Scharwey, M., Koch, B., Schmidt, C., Schatte, J., Rechberger, G., Kollroser, M., Hermetter, A. & Daum, G. (2013) Screening for hydrolytic enzymes reveals Ayr1p as a novel triacylglycerol lipase in Saccharomyces cerevisiae. *The Journal of Biological Chemistry*. 288 (50), pp. 36061–36072.

Poirier, P., Giles, T.D., Bray, G.A., Hong, Y., Stern, J.S., Pi-Sunyer, F.X., Eckel, R.H., American Heart AssociationObesity Committee of the Council on Nutrition, Physical Activity, and Metabolism (2006) Obesity and cardiovascular disease: pathophysiology, evaluation, and effect of weight loss: an update of the 1997 American Heart Association Scientific Statement on Obesity and Heart Disease from the Obesity Committee of the Council on Nutrition, Physical Activity, and Metabolism. *Circulation*. 113pp. 898–918.

Postnikoff, S.D.L. & Harkness, T.A.A. (2014) Replicative and chronological life-span assays. *Methods in Molecular Biology*. 1163pp. 223–227.

Powers, R.W., Kaeberlein, M., Caldwell, S.D., Kennedy, B.K. & Fields, S. (2006) Extension of chronological life span in yeast by decreased TOR pathway signaling. *Genes & Development*. 20 (2), pp. 174–184.

Pu, J., Ha, C.W., Zhang, S., Jung, J.P., Huh, W.-K. & Liu, P. (2011) Interactomic study on interaction between lipid droplets and mitochondria. *Protein & Cell*. 2 (6), pp. 487–496.

Qian, S.Y. & Buettner, G.R. (1999) Iron and dioxygen chemistry is an important route to initiation of biological free radical oxidations: an electron paramagnetic resonance spin trapping study. *Free Radical Biology and Medicine*. 26 (11-12), pp. 1447–1456.

Radulovic, M., Knittelfelder, O., Cristobal-Sarramian, A., Kolb, D., Wolinski, H. & Kohlwein, S.D. (2013) The emergence of lipid droplets in yeast: current status and experimental approaches. *Current Genetics*. 59 (4), pp. 231–242.

Rahmouni, K., Correia, M.L.G., Haynes, W.G. & Mark, A.L. (2005) Obesity-associated hypertension: new insights into mechanisms. *Hypertension*. 45 (1), pp. 9–14.

Rajakumari, S. & Daum, G. (2010a) Janus-faced enzymes yeast Tgl3p and Tgl5p catalyze lipase and acyltransferase reactions. *Molecular Biology of the Cell*. 21 (4), pp. 501–510.

Rajakumari, S. & Daum, G. (2010b) Multiple functions as lipase, steryl ester hydrolase, phospholipase, and acyltransferase of Tgl4p from the yeast Saccharomyces cerevisiae. *Journal of Biological Chemistry*. 285 (21), pp. 15769–15776.

Rajakumari, S., Grillitsch, K. & Daum, G. (2008) Synthesis and turnover of non-polar lipids in yeast. *Progress in Lipid Research*. 47 (3), pp. 157–171.

Rambold, A.S., Cohen, S. & Lippincott-Schwartz, J. (2015) Fatty acid trafficking in starved cells: regulation by lipid droplet lipolysis, autophagy, and mitochondrial fusion dynamics. *Developmental Cell*. 32 (6), pp. 678–692.

Rando, T.A. (2006) Stem cells, ageing and the quest for immortality. *Nature*. 441 (7097), pp. 1080–1086.

Rastogi, R.P., Singh, S.P., Häder, D.-P. & Sinha, R.P. (2010) Detection of reactive oxygen species (ROS) by the oxidant-sensing probe 2‘,7’-dichlorodihydrofluorescein diacetate in the cyanobacterium Anabaena variabilis PCC 7937. *Biochemical and Biophysical Research Communications*. 397 (3), pp. 603–607.

Raught, B., Gingras, A.C. & Sonenberg, N. (2001) The target of rapamycin (TOR) proteins. *Proceedings of the National Academy of Sciences*. 98 (13), pp. 7037–7044.

Reddy, J.K. & Hashimoto, T. (2001) Peroxisomal beta-oxidation and peroxisome proliferator-activated receptor alpha: an adaptive metabolic system. *Annual Review of Nutrition*. 21 (1), pp. 193–230.

Robenek, H., Robenek, M.J. & Troyer, D. (2005) PAT family proteins pervade lipid droplet cores. *The Journal of Lipid Research*. 46 (6), pp. 1331–1338.

Robinson, J.P., Bruner, L.H., Bassoe, C.F., Hudson, J.L., Ward, P.A. & Phan, S.H. (1988) Measurement of intracellular fluorescence of human monocytes relative to oxidative metabolism. *Journal of Leukocyte Biology*. 43 (4), pp. 304–310.

Rockenfeller, P. & Madeo, F. (2008) Apoptotic death of ageing yeast. *Experimental Gerontology*. 43 (10), pp. 876–881.

Rota, C., Chignell, C.F. & Mason, R.P. (1999) Evidence for free radical formation during the oxidation of 2′-7′-dichlorofluorescin to the fluorescent dye 2′-7′-dichlorofluorescein by horseradish peroxidase: possible implications for oxidative stress measurements. *Free Radical Biology and Medicine*. 27 (7-8), pp. 873–881.

Russell, S.T., Eley, H. & Tisdale, M.J. (2007) Role of reactive oxygen species in protein degradation in murine myotubes induced by proteolysis-inducing factor and angiotensin II. *Cellular Signalling*. 19 (8), pp. 1797–1806.

Saarikangas, J. & Barral, Y. (2016) Protein aggregation as a mechanism of adaptive cellular responses. *Current Genetics*. pp. 1–14.

Sandager, L., Gustavsson, M.H., Stahl, U., Dahlqvist, A., Wiberg, E., Banas, A., Lenman, M., Ronne, H. & Stymne, S. (2002) Storage Lipid Synthesis Is Non-essential in Yeast. *Journal of Biological Chemistry*. 277 (8), pp. 6478–6482.

Sanz, A. & Stefanatos, R.K.A. (2008) The mitochondrial free radical theory of aging: a critical view. *Current Aging Science*. 1 (1), pp. 10–21.

Scherz-Shouval, R. & Elazar, Z. (2007) ROS, mitochondria and the regulation of autophagy. *Trends in Cell Biology*. 17 (9), pp. 422–427.

Schmidt, C., Athenstaedt, K., Koch, B., Ploier, B. & Daum, G. (2013) Regulation of the yeast triacylglycerol lipase TGl3p by formation of nonpolar lipids. *Journal of Biological Chemistry*. 288 (27), pp. 19939–19948.

Schrauwen, P., Schrauwen-Hinderling, V., Hoeks, J. & Hesselink, M.K.C. (2010) Mitochondrial dysfunction and lipotoxicity. *Biochimica et Biophysica Acta*. 1801 (3), pp. 266–271.

Schriner, S.E., Linford, N.J., Martin, G.M., Treuting, P., Ogburn, C.E., Emond, M., Coskun, P.E., Ladiges, W., Wolf, N., Van Remmen, H., Wallace, D.C. & Rabinovitch, P.S. (2005) Extension of murine life span by overexpression of catalase targeted to mitochondria. *Science*. 308 (5730), pp. 1909–1911.

Schroeder, E.A. & Shadel, G.S. (2014) Crosstalk between mitochondrial stress signals regulates yeast chronological lifespan. *Mechanisms of Ageing and Development*. 135pp. 41–49.

Shadel, G.S. (2014) Live longer on MARS: a yeast paradigm of mitochondrial adaptive ROS signaling in aging. *Microbial Cell*. 1pp. 140–144.

Shaik, A., Schiavi, A. & Ventura, N. (2016) Mitochondrial autophagy promotes healthy aging. *Cell Cycle*. pp. 1–2.

Shaw, C.S., Jones, D.A. & Wagenmakers, A.J.M. (2008) Network distribution of mitochondria and lipid droplets in human muscle fibres. *Histochemistry and Cell Biology*. 129 (1), pp. 65–72.

Sherman, F. (2003) Getting Started with Yeast. *Methods in Enzymology*. 350pp. 3–41.

Shimada, H., Hirai, K.-I., Simamura, E., Hatta, T., Iwakiri, H., Mizuki, K., Hatta, T., Sawasaki, T., Matsunaga, S., Endo, Y. & Shimizu, S. (2009) Paraquat toxicity induced by voltage-dependent anion channel 1 acts as an NADH-dependent oxidoreductase. *The Journal of Biological Chemistry*. 284 (42), pp. 28642–28649.

Shringarpure, R. & Davies, K.J.A. (2002) Protein turnover by the proteasome in aging and disease. *Free Radical Biology and Medicine*. 32 (11), pp. 1084–1089.

Siliciano, P.G. & Tatchell, K. (1984) Transcription and regulatory signals at the mating type locus in yeast. *Cell*. 37 (3), pp. 969–978.

Sinclair, D.A. (2005) Toward a unified theory of caloric restriction and longevity regulation. *Mechanisms of Ageing and Development*. 126 (9), pp. 987–1002.

Sinclair, D.A. & Guarente, L. (1997) Extrachromosomal rDNA circles—a cause of aging in yeast. *Cell*. 91 (7), pp. 1033–1042.

Singh, R., Kaushik, S., Wang, Y., Xiang, Y., Novak, I., Komatsu, M., Tanaka, K., Cuervo, A.M. & Czaja, M.J. (2009) Autophagy regulates lipid metabolism. *Nature*. 458 (7242), pp. 1131–1135.

Smith, E.D., Tsuchiya, M., Fox, L.A., Dang, N., Hu, D., Kerr, E.O., Johnston, E.D., Tchao, B.N., Pak, D.N., Welton, K.L., Promislow, D.E.L., Thomas, J.H., Kaeberlein, M. & Kennedy, B.K. (2008) Quantitative evidence for conserved longevity pathways between divergent eukaryotic species. *Genome Research*. 18 (4), pp. 564–570.

Smith, J., Wright, J. & Schneider, B.L. (2015) A budding yeast's perspective on aging: The shape I'm in. *Experimental Biology and Medicine*. 240 (6), pp. 701–710.

Sohal, R.S., Svensson, I., Sohal, B.H. & Brunk, U.T. (1989) Superoxide anion radical production in different animal species. *Mechanisms of Ageing and Development*. 49 (2), pp. 129–135.

Sorger, D. & Daum, G. (2002) Synthesis of triacylglycerols by the acyl-coenzyme A: diacyl-glycerol acyltransferase Dga1p in lipid particles of the yeast Saccharomyces cerevisiae. *Journal of Bacteriology*. 184 (2), pp. 519–524.

Sorger, D. & Daum, G. (2003) Triacylglycerol biosynthesis in yeast. *Applied Microbiology and Biotechnology*. 61 (4), pp. 289–299.

Spindler, S.R. (2010) Biological Effects of Calorie Restriction: Implications for Modification of Human Aging. In: *The Future of Aging*. Springer Science & Business Media.. pp. 367–438.

Steffen, K.K., Kennedy, B.K. & Kaeberlein, M. (2009) Measuring replicative life span in the budding yeast. *Journal of Visualized Experiments*. 2007 (28), pp. 1–5.

Stone, S.J., Levin, M.C. & Farese, R.V. (2006) Membrane topology and identification of key functional amino acid residues of murine acyl-CoA:diacylglycerol acyltransferase-2. *Journal of Biological Chemistry*. 281 (52), pp. 40273–40282.

Strauss, J.A., Shaw, C.S., Bradley, H., Wilson, O.J., Dorval, T., Pilling, J. & Wagenmakers, A.J.M. (2016) Immunofluorescence microscopy of SNAP23 in human skeletal muscle reveals colocalization with plasma membrane, lipid droplets, and mitochondria. *Physiological Reports*. 4 (1), pp. e12662.

Sugita, M., Muroya, T., Sugishita, T., Tenjin, Y. & Satoh, H. (1986) Sorting of living and dead cells by flow cytometry--staining principle and basic experiment. *Gan no Rinsho, Japan Journal of Cancer Clinics*. 32 (3), pp. 268–273.

Szymanski, K.M., Binns, D., Bartz, R., Grishin, N.V., Li, W.-P., Agarwal, A.K., Garg, A., Anderson, R.G.W. & Goodman, J.M. (2007) The lipodystrophy protein seipin is found at endoplasmic reticulum lipid droplet junctions and is important for droplet morphology. *Proceedings of the National Academy of Sciences*. 104 (52), pp. 20890–20895.

Taylor, F.R. & Parks, L.W. (1979) Triaglycerol metabolism in Saccharomyces cerevisiae. Relation to phospholipid synthesis. *Biochimica et Biophysica Acta*. 575 (2), pp. 204–214.

Thiam, A.R., Farese, R.V. & Walther, T.C. (2013) The biophysics and cell biology of lipid droplets. *Nature Reviews Molecular Cell Biology*. 14 (12), pp. 775–786.

Toda, T., Cameron, S., Sass, P. & Wigler, M. (1988) SCH9, a gene of Saccharomyces cerevisiae that encodes a protein distinct from, but functionally and structurally related to, cAMP-dependent protein kinase catalytic subunits. *Genes & Development*. 2 (5), pp. 517–527.

Trifunovic, A., Wredenberg, A., Falkenberg, M., Spelbrink, J.N., Rovio, A.T., Bruder, C.E., Bohlooly-Y, M., Gidlöf, S., Oldfors, A., Wibom, R., Törnell, J., Jacobs, H.T. & Larsson, N.-G. (2004) Premature ageing in mice expressing defective mitochondrial DNA polymerase. *Nature*. 429 (6990), pp. 417–423.

Unlu, E.S. & Koc, A. (2007) Effects of deleting mitochondrial antioxidant genes on life span. *Annuals of the New York Academy of Sciences*. 1100 (1), pp. 505–509.

van Zutphen, T., Todde, V., de Boer, R., Kreim, M., Hofbauer, H.F., Wolinski, H., Veenhuis, M., van der Klei, I.J. & Kohlwein, S.D. (2014) Lipid droplet autophagy in the yeast Saccharomyces cerevisiae. [online]. *Molecular Biology of the Cell*. 25 (2), pp. 290–301.

Vieler, A., Wu, G., Tsai, C.-H., Bullard, B., Cornish, A.J., Harvey, C., Reca, I.-B., Thornburg, C., Achawanantakun, R., Buehl, C.J., Campbell, M.S., Cavalier, D., Childs, K.L., Clark, T.J., et al. (2012) Genome, functional gene annotation, and nuclear transformation of the heterokont oleaginous alga Nannochloropsis oceanica CCMP1779. *PLoS Genetics*. 8 (11), pp. e1003064.

Wach, A., Brachat, A., Pöhlmann, R. & Philippsen, P. (1994) New heterologous modules for classical or PCR-based gene disruptions in Saccharomyces cerevisiae. *Yeast*. 10 (13), pp. 1793–1808.

Wagner, S. & Paltauf, F. (1994) Generation of glycerophospholipid molecular species in the yeast Saccharomyces cerevisiae. Fatty acid pattern of phospholipid classes and selective acyl turnover at sn-1 and sn-2 positions. *Yeast*. 10 (11), pp. 1429–1437.

Walther, T.C. & Farese, R.V. (2012) Lipid droplets and cellular lipid metabolism. *Annual Review of Biochemistry*. 81pp. 687–714.

Watt, M.J. & Steinberg, G.R. (2008) Regulation and function of triacylglycerol lipases in cellular metabolism. *Biochemical Journal*. 414 (3), pp. 313–325.

Wei, M., Fabrizio, P., Madia, F., Hu, J., Ge, H., Li, L.M. & Longo, V.D. (2009) Tor1/Sch9-Regulated Carbon Source Substitution Is as Effective as Calorie Restriction in Life Span Extension Stuart K Kim (ed.). *PLoS Genetics*. 5 (5), pp. e1000467.

Wei, W., McCusker, J.H., Hyman, R.W., Jones, T., Ning, Y., Cao, Z., Gu, Z., Bruno, D., Miranda, M., Nguyen, M., Wilhelmy, J., Komp, C., Tamse, R., Wang, X., et al. (2007) Genome sequencing and comparative analysis of Saccharomyces cerevisiae strain YJM789. *Proceedings of the National Academy of Sciences*. 104 (31), pp. 12825–12830.

Weinberger, M., Feng, L., Paul, A., Smith, D.L., Hontz, R.D., Smith, J.S., Vujcic, M., Singh, K.K., Huberman, J.A. & Burhans, W.C. (2007) DNA Replication Stress Is a Determinant of Chronological Lifespan in Budding Yeast. *PLoS ONE*. 2 (8), pp. e748.

Weindruch, R. & Walford, R.L. (1988) T*he Retardation of Aging and Disease by Dietary Restriction*. Charles C Thomas Pub Limited. 436pp. -.

Welch, A.Z. & Koshland, D.E. (2013) A simple colony-formation assay in liquid medium, termed 'tadpoling', provides a sensitive measure of Saccharomyces cerevisiae culture viability. *Yeast*. 30 (12), pp. 501–509.

Welte, M.A. (2015) Expanding roles for lipid droplets. *Current Biology*. 25 (11), pp. R470–R481.

Werner-Washburne, M., Braun, E.L., Crawford, M.E. & Peck, V.M. (1996) Stationary phase in Saccharomyces cerevisiae. *Molecular Microbiology*. 19 (6), pp. 1159–1166.

Werner-Washburne, M., Roy, S. & Davidson, G.S. (2012) Aging and the survival of quiescent and non-quiescent cells in yeast stationary-phase cultures. *Sub-Cellular Biochemistry*. 57 (Chap 6), pp. 123–143.

Wesseling, C., van Wendel de Joode, B., Ruepert, C., Leon, C., Monge, P., Hermosillo, H. & Partanen, T.J. (2001) Paraquat in developing countries. *International Journal of Occupational and Environmental Health*. 7 (4), pp. 275–286.

Wilfling, F., Wang, H., Haas, J.T., Krahmer, N., Gould, T.J., Uchida, A., Cheng, J.-X., Graham, M., Christiano, R., Fröhlich, F., Liu, X., Buhman, K.K., Coleman, R.A., Bewersdorf, J., et al. (2013) Triacylglycerol synthesis enzymes mediate lipid droplet growth by relocalizing from the ER to lipid droplets. *Developmental Cell*. 24 (4), pp. 384–399.

Wolinski, H., Kolb, D., Hermann, S., Koning, R.I. & Kohlwein, S.D. (2011) A role for seipin in lipid droplet dynamics and inheritance in yeast. *Journal of Cell Science*. 124 (Pt 22), pp. 3894–3904.

Yang, L., Ding, Y., Chen, Y., Zhang, S., Huo, C., Wang, Y., Yu, J., Zhang, P., Na, H., Zhang, H., Ma, Y. & Liu, P. (2012) Thematic Review Series: Lipid Droplet Synthesis and Metabolism: from Yeast to Man: The proteomics of lipid droplets: structure, dynamics, and functions of the organelle conserved from bacteria to humans. *Journal of Lipid Research*. 53 (7), pp. 1245–1253.

Yen, C.-L.E., Stone, S.J., Koliwad, S., Harris, C. & Farese, R.V. (2008) Thematic review series: glycerolipids. DGAT enzymes and triacylglycerol biosynthesis. *The Journal of Lipid Research*. 49 (11), pp. 2283–2301.

Yi, X. & Maeda, N. (2005) Endogenous production of lipoic acid is essential for mouse development. *Molecular and Cellular Biology*. 25 (18), pp. 8387–8392.

Yoon, K., Han, D., Li, Y., Sommerfeld, M. & Hu, Q. (2012) Phospholipid:diacylglycerol acyltransferase is a multifunctional enzyme involved in membrane lipid turnover and degradation while synthesizing triacylglycerol in the unicellular green microalga Chlamydomonas reinhardtii. *The Plant Cell*. 24 (9), pp. 3708–3724.

Younce, C. & Kolattukudy, P. (2012) MCP-1 induced protein promotes adipogenesis via oxidative stress, endoplasmic reticulum stress and autophagy. *Cellular Physiology and Biochemistry: International Journal of Experimental Cellular Physiology, Biochemistry, and Pharmacology*. 30 (2), pp. 307–320.

Yu, Y.H. & Ginsberg, H.N. (2005) Adipocyte signaling and lipid homeostasis: Sequelae of insulin-resistant adipose tissue. *Circulation Research*. 96 (10), pp. 1042–1052.

Zambrano, M.M. & Kolter, R. (1996) GASPing for life in stationary phase. *Cell*. 86 (2), pp. 181–184.

Zasedatelev, B. (1988) A habit that takes away health. *Meditsinskaia sestra*. 47 (8), pp. 10–13.

Ždralević, M., Guaragnella, N., Antonacci, L., Marra, E. & Giannattasio, S. (2012) Yeast as a Tool to Study Signaling Pathways in Mitochondrial Stress Response and Cytoprotection. *The Scientific World Journal*. 2012 (4), pp. 1–10.

Zhang, M., Fan, J., Taylor, D.C. & Ohlrogge, J.B. (2009) DGAT1 and PDAT1 acyltransferases have overlapping functions in Arabidopsis triacylglycerol biosynthesis and are essential for normal pollen and seed development. *The Plant Cell*. 21 (12), pp. 3885–3901.

Zhang, Q., Chieu, H.K., Low, C.P., Zhang, S., Heng, C.K. & Yang, H. (2003) Schizosaccharomyces pombe cells deficient in triacylglycerols synthesis undergo apoptosis upon entry into the stationary phase. *Journal of Biological Chemistry*. 278 (47), pp. 47145–47155.

Ziegler, D.V., Wiley, C.D. & Velarde, M.C. (2015) Mitochondrial effectors of cellular senescence: beyond the free radical theory of aging. *Aging Cell*. 14 (1), pp. 1–7.

Zimmermann, R., Strauss, J.G., Haemmerle, G., Schoiswohl, G., Birner-Gruenberger, R., Riederer, M., Lass, A., Neuberger, G., Eisenhaber, F., Hermetter, A. & Zechner, R. (2004) Fat mobilization in adipose tissue is promoted by adipose triglyceride lipase. *Science*. 306 (5700), pp. 1383–1386.

Zinser, E., Sperka-Gottlieb, C.D., Fasch, E.V., Kohlwein, S.D., Paltauf, F. & Daum, G. (1991) Phospholipid synthesis and lipid composition of subcellular membranes in the unicellular eukaryote Saccharomyces cerevisiae. *Journal of Bacteriology*. 173 (6), pp. 2026–2034.